

Thermal Limits and Thresholds of Red Sea Biota

Dissertation by

Veronica Chaidez

In Partial Fulfillment of the Requirements

For the Degree of

Doctor of Philosophy

King Abdullah University of Science and Technology

Thuwal, Kingdom of Saudi Arabia

May 2018

EXAMINATION COMMITTEE APPROVALS FORM

The dissertation of Veronica Chaidez is approved by the examination committee.

Committee Chairperson: Prof. Carlos M. Duarte

Committee Members: Prof. Susana Agusti, Prof. Ibrahim Hoteit, Prof. Nuria Marba

ABSTRACT

Thermal Limits and Thresholds of Red Sea Biota

Veronica Chaidez

As ocean temperatures continue to rise, the effect of temperature on marine organisms becomes highly relevant. The Red Sea is the warmest sea and is rapidly warming with current surface temperatures (28 – 34 °C) already exceeding those of most tropical systems. This has major consequences for organisms that may already find themselves at their thermal limits. The aim of this project was to define the thermal limits and thresholds of certain Red Sea species. Firstly, to better understand the thermal regimes of the Red Sea, we looked at decadal trends in maximum sea surface temperature across the basin. Then, we tested the thermal capacities of Red Sea mangroves and zooplankton, two key ecological groups, by performing thermal stress experiments in the laboratory. We found that the Red Sea basin is warming faster than the global average (0.17 °C decade⁻¹), the thermal limit of mangrove propagules is between 33 and 35 °C, and the limits among the most common zooplankton groups range from 30 to 36 °C. This project gives us a better understanding of how organisms respond to extreme temperatures and how they may be affected in a future, warmer, ocean.

ACKNOWLEDGEMENTS

I would like to thank my advisor Carlos Duarte, for giving me the opportunity to study warming in the Red Sea, and in turn contribute my small piece to the global conversation on climate change. I thank Susana Agusti for co-supervising my PhD and for my participation in her laboratory, undertaking phytoplankton, thermal response experiments, which unfortunately, due to time constraints, were not included in this dissertation. I am grateful also to Ibrahim Hoteit for standing on my committee and his participation in my first chapter.

The work presented here could not have been undertaken without the talents of many people. I thank Denis Dreano for his invaluable contribution to the first chapter. I thank Katherine Rowe and Erika Nishitani for their efforts in the field and laboratory during the mangrove experiments. A warm thank you to Mohammed Aljahdali, Ghazi Nami, and Waleed for all the times at sea. A deep gratitude to my collaborators of the zooplankton chapter: Drs. Stamatina Isari, Gauri Mahadik, Sathianeson Satheesh, Gopikrishna Mantha, Reny Devassy, and Mohsen El-Shirbiny.

This experience has taught me that while the effects of warming are real, so are our innate abilities to adapt. For this realization, I am forever grateful to the Kingdom of Saudi Arabia, King Abdullah, and Carlos M. Duarte.

Shukran.

TABLE OF CONTENTS

EXAMINATION COMMITTEE APPROVALS FORM	2
COPYRIGHT PAGE	3
ABSTRACT	4
ACKNOWLEDGEMENTS	5
TABLE OF CONTENTS	6
LIST OF FIGURES	8
LIST OF TABLES	11
1. INTRODUCTION	13
1.1 Global change	13
1.2 Ocean warming and climate change	13
1.3 Thermal thresholds and the Arrhenius equation	15
1.4 Metabolism and thermal limits	16
1.5 Shifting isotherms	18
1.6 The Red Sea	19
1.7 References	20
2. OBJECTIVES	24
CHAPTER I	25
3. Decadal trends in Red Sea maximum surface temperature	25
3.1 Abstract	26
3.2 Introduction	26
3.3 Material and Methods	29
3.3.1 The dataset	29
3.3.2 Calculating decadal trends	30
3.3.3 Calculating heat anomalies	30
3.4 Results	31
3.4.1 Warming rates and timing	31
3.4.2 Heat anomalies	37

3.5	Discussion	39
3.5.1	Conclusions	43
3.6	References	43
3.7	Supplementary Materials	47
CHAPTER II		50
4.	Thermal resistance of <i>Avicennia marina</i> seedlings and effects on early growth in the Red Sea	50
4.1	Abstract	51
4.2	Introduction	51
4.3	Material and Methods	54
4.3.1	Collection	54
4.3.2	Experiment	56
4.3.3	Harvesting	57
4.3.4	Analysis	58
4.4	Results	61
4.5	Discussion	71
4.5.1	Conclusions	75
4.6	References	76
CHAPTER III		81
5.	Thermal thresholds of Red Sea zooplankton	81
5.1	Abstract	82
5.2	Introduction	82
5.3	Material and Methods	84
5.3.1	Collection	84
5.3.2	Experiment	87
5.3.3	Analysis	89
5.4	Results	90
5.5	Discussion	104
5.6	References	110
6.	SYNTHESIS	115
6.1	References	118

LIST OF FIGURES

Figure 1.1. The unimodal thermal response of radial growth rate of sac fungi ($m / (\text{colony} * s)$). Green and brown curves are linear least squares regressions to the Boltzmann-Arrhenius model for the subset of data that are the rise and fall components, respectively.	16
Figure 3.1. Distribution of mean (from 1982 to 2015) maximum annual temperature (T_{max}) across the Red Sea. Insert shows the latitudinal changes in mean (from 1982 to 2015) T_{max} . Values based on daily temperature data. Image created using R (v3.3.1, www.R-project.org) including packages: ggplot2 (Wickham 2009) and rasterVis (Lamigueiro and Hijmans 2016), RStudio (v1.0.143, www.rstudio.com), and InkScape (v0.91, www.inkscape.org).	32
Figure 3.2. Average yearly timing of maximum annual temperature (T_{max}) across the Red Sea. Insert shows the latitudinal trend in the average timing of T_{max} . Image created using R (v3.3.1, www.R-project.org) including packages: ggplot2 (Wickham 2009) and rasterVis (Lamigueiro and Hijmans 2016), RStudio (v1.0.143, www.rstudio.com), and InkScape (v0.91, www.inkscape.org).	33
Figure 3.3. (a) Decadal rates of warming ($^{\circ}\text{C decade}^{-1}$) and (b) change in timing (days decade^{-1}) of mean maximum annual temperature (T_{max}) across the Red Sea. Image created using R (v3.3.1, www.R-project.org) including packages: ggplot2 (Wickham 2009) and rasterVis (Lamigueiro and Hijmans 2016), RStudio (v1.0.143, www.rstudio.com), and InkScape (v0.91, www.inkscape.org).	34
Figure 3.4. Distribution of the frequency, as number of years, across the Red Sea when maximum annual temperature (T_{max}) reached 1.0 $^{\circ}\text{C}$ higher than the mean T_{max} for 1982-2015. Image created using R (v3.3.1, www.R-project.org) including packages: ggplot2 (Wickham 2009) and rasterVis (Lamigueiro and Hijmans 2016), RStudio (v1.0.143, www.rstudio.com), and InkScape (v0.91, www.inkscape.org). .	36
Figure 3.5. Probability, as the frequency of occurrence between 1982-2015, of maximum annual temperature (T_{max}) anomalies of different magnitudes. A Kruskal-Wallis test and post-hoc Dunn's tests found significantly different frequencies among and between all anomalies (Kruskal-Wallis, $p < 2.2e^{-16}$, chi-squared = 2674, $df = 4$; all Dunn's tests, $p < 0.05$, Z range = [4:44]).	38
Figure 3.6. Percent of Red Sea area exhibiting maximum annual temperature (T_{max}) anomalies of different magnitudes between 1982 and 2015. Red indicators signal the occurrence of El Niño events.	39
Figure 3.7. Distribution of mean (from 1982 to 2015) minimum annual temperature (T_{min}) across the Red Sea. Values based on daily temperature data. Image created using R (v3.3.1, www.R-project.org) including packages: ggplot2 and rasterVis, RStudio (v1.0.143, www.rstudio.com).	48
Figure 3.8. Distribution of mean (from 1982 to 2015) average annual temperature across the Red Sea. Values based on daily temperature data. Image created using R (v3.3.1, www.R-project.org) including packages: ggplot2 and rasterVis, RStudio (v1.0.143, www.rstudio.com).	49
Figure 4.1. Percentage of successful seedlings that rooted and remained viable to the end of experiment under different temperature treatments. HM = historical	

mean air temperature of Thuwal, Saudi Arabia, i.e. HM+0 = 29 °C on March 1, 2016. HM+0 (N=43), HM+2 (N=42), and HM+4 (N=42) lasted 51 days while HM+6 (N=24) and HM+8 (N=24) lasted 31 days. T_{max} denotes the HM+x of each treatment during the first half of March. Only treatments HM+6 and HM+8 are statistically different from all others. (Chi-square test: $X^2 = 131.84$, $df = 4$, $p\text{-value} < 2.2 \cdot 10^{-16}$, followed by Bonferroni adjusted post-hoc comparisons where HM+6 and HM+8 had $p = 0.0000$.)

.....	61
Figure 4.2. Germination rates as the percentage of propagules that germinated day ⁻¹ , across treatments that germinated. Least squares linear regressions were run on the natural logarithm of propagules germinated to give the following rates and R ² values: HM+0: 11.7 % (R ² =0.90), HM+2: 10.2% (R ² =0.86), and HM+4: 11.6% (R ² =0.94) [propagules germinated day ⁻¹].	66
Figure 4.3. Germination success [%] across propagule weight classes. Exact ranges of fresh weight [g]: A = 10.0-11.9, B = 8.0-9.9, C = 6.0-7.9, D = 4.0-5.9, E = 2.0-3.9. X-axis shows the mid-point of the weight ranges.	67
Figure 4.4. Time at which 40% of propagules reached germination (T ₄₀). Solid line refers to treatments HM+0 and HM+2 (day 38), dashed line refers to HM+4 (day 40).	68
Figure 4.5. Total length of seedling parts in temperature treatments where seedling development was achieved. Error bars refer to standard deviation. One-way ANOVA's were performed on each parameter group and found no significant differences among the three treatments. Results of ANOVA's are as follows: Stem: $p = 0.08$, $F = 2.7$, $df = 2$. Leaf (L): $p = 0.27$, $F = 1.3$, $df = 2$. Leaf (W): $p = 0.13$, $F = 2.1$, $df = 2$. (L) = length, (W) = width.	69
Figure 5.1. The percentage of mortality over time in temperatures <i>in situ</i> and above (32 to 38 °C) for the zooplankton taxa tested without food. Lines indicate least squares linear regression analysis and are color-coded to correspond to each taxonomic group (symbol and color designated in each legend).	91
Figure 5.2. The percentage of mortality over time in temperatures below <i>in situ</i> (24 to 30 °C) for the zooplankton taxa tested without food. Lines indicate least squares linear regression analysis and are color-coded to correspond to each taxonomic group (symbol and color designated in each legend).	92
Figure 5.3. The percentage of mortality over time in temperatures <i>in situ</i> and above (32 to 38 °C) with and without food for large and small-size <i>Acartia</i> sp., <i>Centropages</i> sp., and <i>Undinula</i> sp. Lines indicate least squares linear regression analysis.	94
Figure 5.4. The percentage of mortality over time in temperatures below <i>in situ</i> (24 to 30 °C) with and without food for large and small-size <i>Acartia</i> sp., <i>Centropages</i> sp., and <i>Undinula</i> sp. Lines indicate least squares linear regression analysis.	95
Figure 5.5. Reduction in mortality due to the presence of food [% ± SE hr ⁻¹] as calculated using an analysis of covariance. Red asterisks signify a statistically significant effect of food at that temperature.	100
Figure 5.6. Temperature curves as mortality rates [% h ⁻¹ ± SE] across all temperatures tested [°C] for common groups of Central Red Sea zooplankton. Black dots signify mortality rates for no food treatments and green dots signify mortality	

rates for food addition treatments in: <i>Acartia</i> large and small sp., <i>Centropages</i> sp., and <i>Undinula</i> sp.	101
Figure 5.7. Plot comparing activation energies (Ae) of the two regimes found in each temperature curve with activation energies [eV] of temperatures above T_{opt} over activation energies [eV] of temperatures below T_{opt}	104

LIST OF TABLES

Table 4.1. Number of propagules in each weight class (A – E) per treatment [total number percentage] in each experiment (HM+x = historical mean temperature + x °C of warming).	55
Table 4.2. Temperature regimes followed throughout experiment. Weekly maximum and minimum air temperatures [°C] for each experimental treatment along with the range of maximum temperature (Ti – Tf) applied during the experiment. HM = historical mean air temperature of Thuwal, Saudi Arabia taken from AccuWeather.com < http://www.accuweather.com/en/sa/thuwal/1684791/month/1684791?monyr=3/01/2014# > accessed on January 12, 2016 and February 1, 2017. N/A means “not applicable” because either the experiment had not yet commenced (HM+2 and HM+4) or the propagules had perished by then (HM+6 and HM+8).	60
Table 4.3. Early development of <i>Avicennia marina</i> seedlings grown at different temperatures. Values are means of 42 – 43 replicates ± S.E. *HM+6 and HM+8 had 24 replicates and shedding of the pericarp did not occur naturally. Results of Kruskal-Wallis tests for differences among treatments are reported.	63
Table 4.4. Results of analysis of germination success and rate. An exact binomial test was performed using Clopper-Pearson 95% confidence intervals. (Lconf. = lower 95% confidence interval, Prob. = probability, Uconf. = upper 95% confidence interval; all as [%].) Rates were calculated using linear regression analysis on log-transformed number of propagules germinated per treatment.	65
Table 4.5. Biomass production of <i>Avicennia marina</i> seedlings grown at different temperatures. Values are means of 42 - 43 replicates ± S.E. P-values in bold are less than 0.05.	70
Table 5.1. Zooplankton species, and developmental stages, tested in experiments conducted in 2016 and 2017. Asterisks denote experiments where survival responses to temperature were observed both in the presence and absence of food supply versus no asterisks denoting experiments where survival was tested in the absence of food alone.	86
Table 5.2. The mean ± SE mortality rates (along with the t-value, and P value) of different zooplankton taxa under a range of temperature, in experiments conducted without food supply. The N value is the number of individuals in the treatment, and NA denotes “not applicable”.	96
Table 5.3. The mean ± SE mortality rates (along with the t-value, and P value) of different zooplankton taxa under a range of temperature, in experiments conducted with food supply. The N value is the number of individuals in the treatment. Significant effect of food to buffer mortality was calculated using an analysis of covariance. NA denotes “not applicable”.	99
Table 5.4. Optimal temperatures (T_{opt} , °C) and activation energies (A_e , [eV]) based on the Arrhenius model using linear regression of the natural logarithm of living animals as a function of $1/kT$. “ A_e for $T < T_{opt}$ ” refers to the thermal window up to T_{opt} , and “ A_e for $T > T_{opt}$ ” refers to the rate of thermal collapse at $T > T_{opt}$. “F”	

designates experiment with food added and "NF" designates experiments where no food was added. "NA" means "not applicable". 102

1. INTRODUCTION

1.1 Global change

Anthropogenic global change has been defined as: “*the global-scale changes resulting from the impact of human activity on the major processes that regulate the functioning of the biosphere*” (Duarte 2014). Anthropogenic climate change is one of the most important components of global change. Since 1951, greenhouse gases have contributed a mean surface warming of 0.5 – 1.3 °C (IPCC 2013). Mean global temperatures have risen 0.85 (0.65 – 1.06) °C over the last century with increases estimated between 1.5 to 4.0 °C by the end of the 21st century (IPCC 2013).

1.2 Ocean warming and climate change

Ocean warming is a major consequence of climate change, as the oceans are the main reservoir for heat in the biosphere. The upper 75 meters have been warming by 0.11 °C decade⁻¹ (0.09 – 0.13 °C between 1971 – 2010) and are estimated to continue to warm by an additional 0.6 – 2.0 °C before the end of the 21st century (IPCC 2013). Warming will also affect the deep sea with a mean rise of temperature from 0.3 – 0.6 °C (IPCC 2013). Sea level has risen by 0.19 (0.17 – 0.21) m since the mid-19th century (IPCC 2013), 30 – 55% of which is accounted for by thermal expansion. The ocean has also absorbed about 30% of anthropogenic carbon dioxide emissions since 1971, which is contributing to a decrease in ocean pH by 0.06 – 0.32 by the end of the 21st century (IPCC 2013).

Climate change has caused isotherms to shift throughout the world. With rising temperatures, the most common isotherm trajectories are toward the poles although the trajectories of shifting isotherms can be locally complex (Burrows et al.

2014). Still, efforts have been made to calculate “climate velocities”, as the rate (km decade⁻¹) of isotherm migration with warming, which can then be used to predict future expansion and trajectories of biogeographic ranges in a warming ocean (Loarie et al. 2009; Burrows et al. 2011; Burrows et al. 2014). Terrestrial biogeographical shifts are moving at about 5 – 20 kilometers decade⁻¹ (Parmesan and Yohe 2003), while those of marine organisms are shifting at faster rates of 50 – 70 kilometers decade⁻¹ (Helmuth et al. 2006). The disparity between marine and terrestrial biogeographical shifts is due to the connectivity of the ocean and the dispersal strategies of many marine organisms (Poloczanska et al. 2013). However, not all oceans are equal. Those where poleward range migration is precluded by the presence of land masses, such as the Northern Indian Ocean and semi-enclosed seas like the Mediterranean and Red Sea, may see local extinctions of species that are unable to migrate with the shifting climate envelopes (Cheung et al. 2009; Burrows et al. 2011). The phenological mismatches brought about by shifting isotherms may also have significant consequences to biological processes and the delivery of ecosystem services (Thackeray et al. 2010), by uncoupling ecosystem and biological processes or interactions between species (Edwards and Richardson 2004). In turn, the timing of biological events and the delineation of biogeographic ranges will be affected.

The warming of the ocean will directly affect organisms’ physiologies. Ectotherms have thermal ranges where their life processes optimally function and in order to remain in their optimal bioclimate envelopes, it will be necessary to migrate or adapt (Dell et al. 2011). In response to warmer temperatures, marine organisms

may shift their latitudinal and/or depth range or adjust their phenological responses (Perry et al. 2005; Parmesan 2006; Dulvy et al. 2008). For example, phytoplankton blooms, which can respond quickly to environmental conditions, have already advanced 6.3 days decade⁻¹ (Poloczanska et al. 2013). Vulnerability of extinction will depend on organisms' capacities to adapt or migrate. Polar organisms, adapted to a narrow temperature range, cannot escape by migrating to higher latitudes and organisms in the tropics may already be at or near their thermal limits.

1.3 Thermal thresholds and the Arrhenius equation

Independent research lines are converging in establishing temperature thresholds nearing 30°C for many organisms in the temperate and tropical regions of the world ocean (Cantin et al. 2010; Jones et al. 2010; Olsen et al. 2012; Thomas et al. 2012; Boyd et al. 2013; Duarte 2014). A threshold is the changing point between two different regimes (Anderson et al. 2008), and a temperature threshold is the temperature beyond which a sharp decline in performance occurs (Dell et al. 2011). The Arrhenius equation has become a useful tool in understanding these thresholds and regimes. The Arrhenius equation was originally formulated to model the temperature dependence of chemical reaction rates (Laidler 1984), but it has since been found to be applicable to other processes, including ecological ones (Dell et al. 2011). This temperature dependence however is not monotonous and actually has different regimes. Most organisms exhibit at least two regimes in their metabolic and physiological response to temperature effects, one above their optimal performance temperature (rise), and one below their optimum (fall) (Dell et al.

2011) as illustrated in Figure 1.1 (Dell et al. 2011). The figure reproduced from Dell et al. (2011) (Figure 1.1) shows the Boltzmann – Arrhenius model, which involves calculating activation energies from the temperature dependence of reaction rates. Activation energy is the minimum energy required for reactants in a system to react. The range of the rise component is where organisms normally operate (Dell et al. 2011). The fall regimes of biological traits are usually steeper and typically indicate biological collapse, highlighting the importance of understanding the thresholds of organisms (Dell et al. 2011).

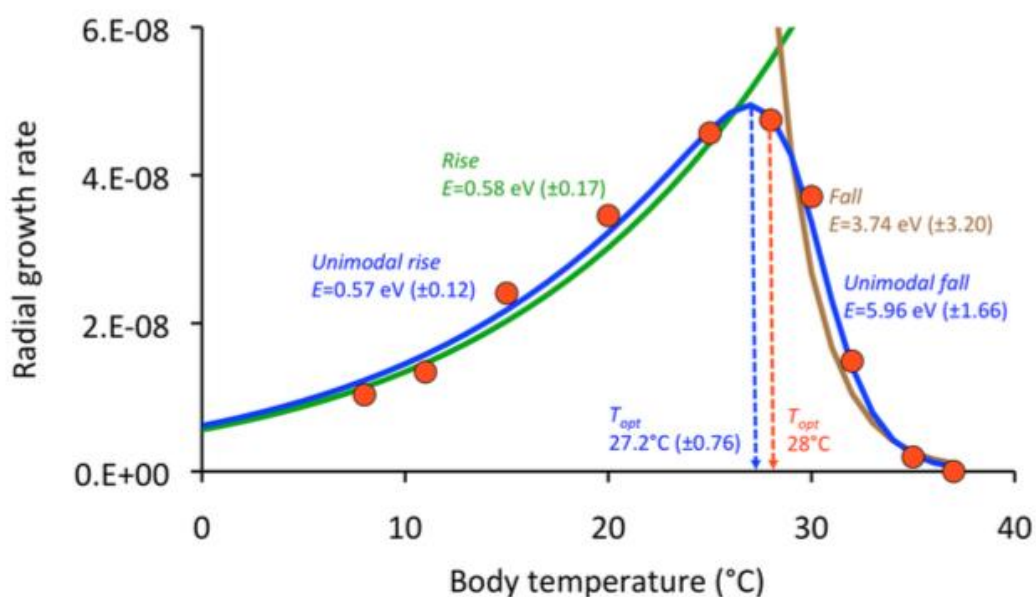


Figure 1.1. The unimodal thermal response of radial growth rate of sac fungi ($m / (\text{colony} \cdot s)$). Green and brown curves are linear least squares regressions to the Boltzmann-Arrhenius model for the subset of data that are the rise and fall components, respectively. Figure from the supplementary material of Dell et al. 2011.

1.4 Metabolism and thermal limits

Temperature is a key driver of metabolic processes. According to the metabolic theory of ecology, metabolic rates vary with body size and temperature and may be

used to help determine the responses of life histories, community and population dynamics, and ecosystem processes to temperature changes (Brown et al. 2004; Dell et al. 2011; Boyd et al. 2013; Holding et al. 2013). There is evidence that with rising global temperatures, many physiological processes will accelerate, such as increased phytoplankton and bacterial growth, egg development, larval dispersal, and mortality (O'Connor et al. 2007; Dell et al. 2011; Regaudie-de-Gioux and Duarte 2012). Although metabolic rates increase with temperature, there are thermal limits to the physiological capacities of organisms (Olsen et al. 2012; Thomas et al. 2012; Boyd et al. 2013). In particular, most organisms are characterized by thermal optima close to the upper range of their thermal niche, with an abrupt decline in performance at warmer temperatures (Olsen et al. 2012; Boyd et al. 2013). Hence, the transition between optimal temperature and lethal and sublethal temperature is relatively abrupt.

Boyd et al. (2013) compiled temperature experiments run at multiple research institutions to measure the growth rates of 25 strains of phytoplankton. Among genera, optimal growth temperatures and other reaction norms differed while similarities within a species were common, pointing toward an evolutionary history of selection (Boyd et al. 2013). In a study by Thomas et al. (2012), the optimal growth rates of multiple strains of phytoplankton were compared to the mean temperatures of their environment. Phytoplankton from polar and temperate waters had higher optimum temperatures than the mean annual temperature of their respective ocean basins, while tropical strains closely matched the mean temperatures of their habitat (Thomas et al. 2012). This could be an indicator that

phytoplankton in the tropics are already approaching their thermal limits. Phytoplankton show higher variability at the ceilings of their thermal niches and more uniformity in their optimal temperatures signifying a potential for genetic plasticity at their thermal limits (Boyd et al. 2013). Thomas et al. (2012) also looked at past and potential biodiversity patterns based on changing temperature regimes noting that extinction rates might increase at the lower latitudes. A 2 °C (0.6 – 2.0 °C) rise in the first 100 meters of the ocean has been predicted by climate change scenarios (IPCC 2013). With a rise of 2 °C, one-third of tropical phytoplankton species are at risk of becoming extinct as many exhibit declines in growth rate at temperatures exceeding their optimum (Thomas et al. 2012). Characterizing reaction norms also allows for the inference of biogeographical ranges and biodiversity changes (Boyd et al. 2013). For example, as annual temperatures rise above the thermal limits of N₂ fixing microbes (diazotrophs), they are likely to be replaced by more thermally tolerant microbes (Breitbarth et al. 2007), leading to the loss of a fundamental ecosystem function.

1.5 Shifting isotherms

Ocean warming will see the disappearance of isotherms near the poles and the creation of new ones in the tropics (Williams et al. 2007). As isotherms migrate, so too must the organisms optimally adapted to those climate envelopes (Burrows et al. 2011; Poloczanska et al. 2013). However, no organism is yet adapted to isotherms that appear for the first time over millennia and therefore, organisms in the tropical ocean in conjunction with those at the poles, are at greatest risk with warming. Another factor to consider is how quickly these isotherms are shifting and

whether this is ample time for organisms to either migrate or adapt. Due to the homogenous nature of the ocean environment, the velocity of climate change is less patchy than on land (Burrows et al. 2011). In the last fifty years, isotherms at the sea surface have traveled at an equal or faster rate than isotherms on land (about 1.5 to 5 times faster) (Sorte et al. 2010; Burrows et al. 2011). Whether organisms and ecological communities are capable of migrating with them is of important consequence to predict the impacts of ocean warming on biota. A high extinction rate is predicted for phytoplankton in the tropics (Thomas et al. 2012), which is also predicted to experience a drop of 40 – 60% in fisheries yield by 2055, further exacerbating food insecurity in the region (IPPC 2014).

We seek to find the upper limits of Red Sea biota and measure the effect of temperature on their growth, fecundity, and survival, as these are important factors for understanding adaptation and resiliency to current and future thermal pressure. The Red Sea is an ideal candidate for such an undertaking as it is one of the warmest seas. What is more, articles on the thermal limits of its organisms are highly lacking, although it is one of most extreme environments on earth in terms of temperature and salinity.

1.6 The Red Sea

The Red Sea is a semi-enclosed, extremely warm sea basin, experiencing rapid warming (Fishelson 1971; Belkin 2009; Raitzos et al. 2011; Raitzos et al. 2013). Between 1982 and 2006, the average annual temperature of the Red Sea increased by 0.74 °C (Belkin 2009), which is on par with the global average (0.85 °C) (IPPC, 2013). Raitzos et al. (2011) report an intense warming after 1994 with a difference

of 0.7 °C following the shift. Average temperatures in the Red Sea exceed those of other tropical regions (Kleypas et al. 2008; Cantin et al. 2010) with recorded temperatures already exceeding the known thresholds of many marine organisms (up to 33 °C in the Southern Red Sea, Sawall et al. 2014). Although it is considered a fast warming, large marine ecosystem, its thermal regimes and evolution remain largely understudied (Belkin 2009). We have at present, limited understanding of how organisms cope with its warm environment or how they will cope in a future, warmer, Red Sea.

1.7 References

- Anderson T, Carstensen J, Hernandez-Garcia E, Duarte CM (2009) Ecological thresholds and regime shifts: approaches to identification. *Trends Ecol Evol* 24:49-57
- Belkin IM (2009) Rapid warming of large marine ecosystems. *Prog Oceanogr* 81:207-213
- Boyd PW, Rynearson TA, Armstrong EA, Fu F, Hayashi K, Hu Z, Hutchins DA, Kudela RM, Litchman E, Mulholland MR, Passow U, Strzepek RF, Whittaker KA, Yu E, Thomas MK (2013) Marine phytoplankton temperature versus growth responses from polar to tropical waters – outcome of a scientific community-wide study. *PLoS ONE* 85:e63091
- Breitbarth E, Oschlies A, LaRoche J (2007) Physiological constraints on the global distribution of *Trichodesmium* – effect of temperature on diazotrophy. *Biogeosciences* 4:53-61
- Brown JH, Gillooly JF, Allen AP, Savage VM, West GB (2004) Toward a metabolic theory of ecology. *Ecology* 85:1771-1789
- Burrows MT, Schoeman DS, Buckley LB, Moore P, Poloczanska ES, Brander KM, Brown C, Bruno JF, Duarte CM, Halpern BS, Holding J, Kappel CV, Kiessling W, O'Connor MI, Pandolfi JM, Parmesan C, Schwing FB, Sydeman WJ, Richardson AJ (2011) The pace of shifting climate in marine and terrestrial ecosystems. *Science* 334:652-655

- Burrows MT, Schoeman DS, Richardson AJ, Molinos JG, Hoffmann A, Buckley LB, Moore PJ, Brown CJ, Bruno JF, Duarte CM, Halpern BS, Hoegh-Guldberg O, Kappel CV, Kiessling W, O'Connor MI, Pandolfi JM, Parmesan C, Sydeman WJ, Ferrier S, Williams KJ, Poloczanska ES (2014) Geographical limits to species – range shifts are suggested by climate velocity. *Nature* doi:10.1038/nature12976
- Cantin NE, Cohen AL, Karnauskas KB, Tarrant AM, McCorkle DC (2010) Ocean warming slows coral growth in the Central Red Sea. *Science* 329:322-325
- Cheung WWL, Lam VWY, Sarmiento JL, Kearney K, Watson R, Pauly D (2009) Projecting global marine biodiversity impacts under climate change scenarios. *Fish Fish* 10:235-251
- Dell AI, Pawar S, Savage VM (2011) Systematic variation in the temperature dependence of physiological and ecological traits. *P Natl Acad Sci* 108(26):10591-10596
- Duarte CM (2014) Global change and the future ocean: a grand challenge for marine sciences. *Front Mar Sci* 1:63
- Dulvy NK, Rogers SI, Jennings S, Stelzenmuller V, Dye SR, Skjoldal HR (2008) Climate change and deepening of the North Sea fish assemblage: a biotic indicator of warming seas. *J Appl Ecol* 45:1029-1039
- Edwards M, Richardson AJ (2004) Impact of climate change on marine pelagic phenology and trophic mismatch. *Nature* 430:881-884
- Fishelson L (1971) Ecology and distribution of the benthic fauna in the shallow waters of the Red Sea. *Mar Biol* 10:113-133
- Helmuth B, Mieszkowska N, Moore P, Hawkins SJ (2006) Living on the edge of two changing worlds: forecasting the responses of rocky intertidal ecosystems to climate change. *Annu Rev Ecol Evol Syst* 37:373-404
- Holding JM, Duarte CM, Arrieta JM, Vaquer-Suyner R, Coello-Camba A, Wassmann P, Agusti S (2013) Experimentally determined temperature thresholds for Arctic plankton community metabolism. *Biogeosciences* 10:357-370
- Intergovernmental Panel on Climate Change Fifth Assessment Report Climate Change 2013: the Physical Science Basis (eds Stocker, T.F., Qin, D., Plattner, G., Tignor, M.M.B., Allen, S.K., Boschung, J., Nauels, A., Xia, Y., Bex, V., Midgley, P.M.) Cambridge Univ. Press Cambridge, 2013
- Intergovernmental Panel on Climate Change Fifth Assessment Report Climate Change 2014: Impacts, Adaptation, and Vulnerability, Part A: Global and

Sectoral Aspects (eds Field, C.B., Barros, V.R., Dokken, D.J., Mach, K.J., Mastrandrea, M.D., Bilir, T.E., Chatterjee, M., Ebi, K.L., Estrada, Y.O., Genova, R.C., Girma, B., Kissel, E.S., Levy, A.N., MacCracken, S., Mastrandrea, P.R., White, L.L.) Cambridge Univ. Press Cambridge, 2014

Jones SJ, Lima FP, Wetthey DS (2010) Rising environmental temperatures and biogeography: poleward range contraction of the blue mussel, *Mytilus edulis* L., in the western Atlantic. *J. Biogeogr* 37:2243-2259

Kleypas JA, Danabasoglu G, Lough JM (2008) Potential role of the ocean thermostat in determining regional differences in coral reef bleaching events. *Geophys Res Lett* 35:L03613

Laidler KJ (1984) The development of the Arrhenius equation *J Chem Educ* 61:494

Loarie SR, Duffy PB, Hamilton H, Asner GP, Field CB, Ackerly DD (2009) The velocity of climate change. *Nature* 462:1052-1057

O'Connor MI, Bruno JF, Gaines SD, Halpern BS, Lester SE, Kinlan BP, Weiss JM (2007) Temperature control of larval dispersal and the implications for marine ecology, evolution, and conservation. *P Natl Acad Sci* 104(4):1266-1271

Olsen YS, Sanchez-Camacho M, Marba N, Duarte CM (2012) Mediterranean seagrass growth and demography responses to experimental warming. *Estuar Coast* doi: 10.1007

Parmesan C, Yohe G (2003) A globally coherent fingerprint of climate change impacts across natural systems. *Nature* 421:37-42

Parmesan C (2006) Ecological and evolutionary responses to recent climate change. *Annu Rev Ecol Evol Syst* 37:637-669

Perry AL, Low PJ, Ellis JR, Reynolds JD (2005) Climate change and distribution shifts in marine fishes. *Science* 308:1912-1915

Poloczanska ES, Brown CJ, Sydeman WJ, Kiessling W, Shoeman DS, Moore PJ, Brander K, Bruno JF, Buckley LB, Burrows MT, Duarte CM, Halpern BS, Holding J, Kappel CV, O'Connor MI, Pandolfi JM, Parmesan C, Schwing F, Thompson SA, Richardson AJ (2014) Global imprint of climate change on marine life. *Nat Clim Chang* doi: 10.1038/nclimate1958

Raitsos DE, Hoteit I, Prihartato PK, Chronis T, Triantafyllou G, Abualnaja Y (2011) Abrupt warming of the Red Sea. *Geophys Res Lett* 38:L14601.

- Raitsos DE, Pradhan Y, Brewin RJW, Stenchikov G, Hoteit I (2013) Remote sensing the phytoplankton seasonal succession of the Red Sea. *PloS ONE* 8(6): e64909
- Regaudie-de-Gioux A, Duarte CM (2012) Temperature dependence of planktonic metabolism in the ocean. *Global Biogeochem Cy* 26: GB1015 doi: 10.1029/2010GB003907
- Sawall Y, Al-Sofyani A, Banguera-Hinestroza E, Voolstra CR (2014) Spatio-temporal analyses of *Symbiodinium* physiology of the coral *Pocillopora verrucosa* along large-scale nutrient and temperature gradients in the Red Sea. *PloS ONE* 9: e103179
- Sorte CJB, Williams SL, Carlton JT (2010) Marine range shifts and species introductions: comparative spread rates and community impacts. *Global Ecol Biogeogr* 19:303-316
- Thackeray SJ, Sparks TH, Frederiksen M, Burthe S, Bacon PJ, Bell JR, Botham MS, Brereton TM, Bright PW, Carvalho L, Clutton-Brock T, Dawson A, Edwards M, Elliott JM, Harrington R, Johns D, Jones ID, Jones JT, Leech DI, Roy DB, Scott WA, Smith M, Smithers RJ, Winfield IJ, and Wanless S (2010) Trophic level asynchrony in rates of phenological change for marine, freshwater and terrestrial environments. *Global Change Biol* 16:3304-3313
- Thomas MK, Kremer CT, Klausmeier CA, Litchman E (2012) A global pattern of thermal adaptation in marine phytoplankton. *Science* 338:1085-1088
- Williams JW, Jackson ST, Kutzbach JE (2007) Projected distributions of novel and disappearing climates by 2100 AD *P Natl Acad Sci* 104:5738-5742

2. OBJECTIVES

This Ph.D. dissertation aimed to delineate the thermal limits and thresholds of Red Sea organisms, which had been previously lacking in the literature. Three chapters explore the historical decadal trends and current warming of the Red Sea, the thermal tolerance of *Avicennia marina* propagules, and the thermal thresholds of zooplankton in the Red Sea.

CHAPTER I

3. Decadal trends in Red Sea maximum surface temperature

Veronica Chaidez¹, Denis Dreano², Susana Agusti¹, Carlos M. Duarte¹, and Ibrahim Hoteit³

¹King Abdullah University of Science and Technology (KAUST), Red Sea Research Center (RSRC), Thuwal, 23955-6900, Saudi Arabia.

²King Abdullah University of Science and Technology (KAUST), Computer, Electrical and Mathematical Sciences and Engineering Division (CEMSE), Thuwal, 23955-6900, Saudi Arabia.

³King Abdullah University of Science and Technology (KAUST), Physical Sciences and Engineering Division (PSE), Thuwal, 23955-6900, Saudi Arabia.

This manuscript has been published in *Scientific Reports*
(Published, 15 August 2017)

Chaidez V, Dreano D, Agusti S, Duarte CM, Hoteit I (2017) Decadal trends in Red Sea maximum surface temperature. *Sci Rep-UK* 7

3.1. Abstract

Ocean warming is a major consequence of climate change, with the surface of the ocean having warmed by $0.11\text{ }^{\circ}\text{C decade}^{-1}$ over the last 50 years and is estimated to continue to warm by an additional $0.6 - 2.0\text{ }^{\circ}\text{C}$ before the end of the century (Rhein et al. 2013). However, there is considerable variability in the rates experienced by different ocean regions, so understanding regional trends is important to inform on possible stresses for marine organisms, particularly in warm seas where organisms may be already operating in the high end of their thermal tolerance. Although the Red Sea is one of the warmest ecosystems on earth, its historical warming trends and thermal evolution remain largely understudied. We characterized the Red Sea's thermal regimes at the basin scale, with a focus on the spatial distribution and changes over time of sea surface temperature maxima, using remotely sensed sea surface temperature data from 1982 – 2015. The overall rate of warming for the Red Sea is $0.17 \pm 0.07\text{ }^{\circ}\text{C decade}^{-1}$, while the northern Red Sea is warming between 0.40 and $0.45\text{ }^{\circ}\text{C decade}^{-1}$, all exceeding the global rate. Our findings show that the Red Sea is fast warming, which may in the future, challenge its organisms and communities.

3.2. Introduction

Ocean warming with climate change (Rhein et al. 2013) is creating challenges for organisms, which accommodate to warming by shifting their distribution poleward and advancing their phenology (Poloczanska et al. 2013). While parts of the ocean may be warming gradually, others may experience rapid fluctuations, tipping points,

or extreme weather events, such as heat waves, likely inducing greater impacts on biodiversity (Duarte et al. 2012; Rhein et al. 2013), as exemplified by the impacts of heat waves on seagrass (Marba and Duarte 2010; Jorda et al. 2012) and other organisms in the Mediterranean, a rapidly warming sea (Marba et al. 2015). Extreme heat events such as ocean heat waves propagated by El Niño-Southern Oscillation are also major concerns for coral reefs as they may lead to bleaching (Wilkinson 1998; Lasker 2005; Tkachenko 2015). The magnitude and duration of such events is important for organisms experiencing temperature anomalies outside their optimal thermal range and perhaps even above their thermal limits. High temperature anomalies of air and water are also linked to stratification of the water column, potentially diminishing oxygen levels and/or increasing microbial virulence, thus causing mass mortality of organisms and disrupting community structure (Romano et al. 2000; Sparnocchia et al. 2006; Coma et al. 2009).

Impacts of warming are likely to be greatest in semi-enclosed seas, which tend to support warming rates faster than average (Jorda et al. 2012; Lima and Wetthey 2012), and where the capacity of organisms to adapt to warming by shifting their biogeographical range poleward is limited by the presence of continental masses (Burrows et al. 2011), rendering most semi-enclosed seas climatic sink areas for marine organisms (Burrows et al. 2014).

The Red Sea is a semi-enclosed, extremely warm sea basin, experiencing rapid warming (Fishelson 1971; Belkin 2009; Raitzos et al. 2011; Raitzos et al. 2013). Between 1982 and 2006, the average annual temperature of the Red Sea increased by 0.74 °C (Belkin 2009), comparable to the global average of 0.85 °C (Rhein et al.

2013). An intense warming event occurred in 1994 leading to a 0.7 °C increase in mean annual SST (sea surface temperature) (Raitsos et al. 2011). Modern average temperatures in the Red Sea already exceed those of other tropical regions (Kleypas et al. 2008; Cantin et al. 2010). Although it is considered a fast warming, large marine ecosystem, its thermal regimes and evolution remain largely unresolved (Belkin 2009; Sherman et al. 2009). Yet, the Red Sea hosts one of the largest reef systems in the world, where organisms may be already close to their thermal limits.

Whereas most analyses focus on mean seawater temperature, maximum temperature may be a more relevant property in relation to some specific questions. For instance, thermal collapse is determined by temperature exceeding the thermal capacity of organisms (Stillman 2003), which is, therefore, dependent on the maximum, rather than the mean temperature the organisms experience. This may be particularly important in the Red Sea where maximum seawater temperatures are already extremely high. Yet, available analyses of thermal regimes in the Red Sea focus on annual mean values (Raitsos et al. 2011; Raitsos et al. 2013; Sawall et al. 2014; Roik et al. 2016), rather than the dynamics of maximum temperature. Here we characterize the variability in temperature maxima across the Red Sea and over time (1982 to 2015), based on daily values, identifying rates of change in annual maximum sea surface temperature, hereafter T_{\max} , as well as the distribution of anomalies, relative to T_{\max} over time.

3.3. Materials and Methods

3.3.1. Dataset

We used remotely sensed sea surface temperature (SST, °C) data to examine maximum temperatures on a basin-wide scale across the Red Sea. The AVHRR – OI (Advanced Very High Resolution Radiometer – Optimum Interpolation) Pathfinder sensor currently provides the longest continuous daily dataset of infrared SST from 1981 to present (Reynolds et al. 2007), allowing the assessment of decadal trends of temperatures. Whereas other sensors provide higher resolution, in terms of pixel size, they encompass a period too short to be climatically-relevant as yet (ERS-1/ATSR-1 and Acqua/AMSR-E) (Brasnett 2008) and do not allow us to identify, with confidence, the maximum temperature achieved over time. A daily Level-4, gap-free dataset merging day and night analysis AVHRR SST was obtained from NASA's (National Aeronautics and Space Administration) National Climatic Data Center* at podaac.jpl.nasa.gov accessed on January 5, 2016 encompassing 34 years over the period 1982 to 2015. This dataset has been optimally interpolated and mapped on a 0.25° x 0.25° grid. The values in the dataset were corrected with *in situ* measurements from buoys and ships (Reynolds et al. 2007). Daily fluctuations in daily SST time series may significantly affect the measurement of maximum SST phenology and magnitude, because the recurrence of the passage of AVHRR Pathfinder is 2 to 3 days and, the time of passage may not match the time of T_{\max} , typically found in the late afternoon with a daily range in T_{\max} , derived from moorings in the central Red Sea, of up to 3 °C. Moreover, the individual estimates

may be affected by dust, which is prevalent in the region at the time of T_{\max} , and cloud cover. Whereas the data we used is interpolated, the individual daily values may be affected by the sources of error above, leading to underestimates of the actual T_{\max} . To attenuate this source of error, we extracted the maximum daily T value within sets of interpolated daily values over 8-day periods, and then selected, for each of the 669 pixels, the highest T observed in any one year as that providing the best estimate of T_{\max} for that pixel and year. The dataset can be downloaded from the Pangea open-access data repository (Chaidez et al. 2017).

3.3.2. Calculating decadal trends

The decadal trends of maximum temperatures and time of occurrence were estimated by fitting a linear regression relating T_{\max} to year for each of the pixel's yearly time series. The slopes of the fitted linear regressions provide an estimate of the rates of change for each pixel in the Red Sea (units: $^{\circ}\text{C decade}^{-1}$, and days decade^{-1} , respectively). We tested the possible occurrence of autocorrelation in T_{\max} among years, and found, for a sample of pixels, no evidence of autocorrelation, i.e. the T_{\max} in any one year is independent of T_{\max} in preceding year(s).

3.3.3. Calculating heat anomalies

For each pixel, a reference maximum temperature was computed by taking the mean of the highest temperatures per year over the study period. A heat wave event was defined as a yearly maximum temperature above the reference maximum temperature by a given threshold chosen at 0.5 $^{\circ}\text{C}$ intervals between 0.5 and 1.5 $^{\circ}\text{C}$. The number of heat wave events over the 34 years was counted for each pixel, as well as the area of the Red Sea experiencing heat waves of various magnitudes in a

given year. A Kruskal-Wallis test followed by Dunn's test for multiple comparisons, was used to compare the frequencies of occurrence for all magnitudes of heat anomalies in Figure 3.5. The percentage of area in Figure 3.6 was calculated as the percentage of pixels. We are aware that the area of each pixel depends on latitude, as the length of a degree longitude varies with latitude. However, for the narrow range of latitude covered by the Red Sea, the difference is minimal, so percent of pixels and area are essentially equivalent.

All data manipulation and analyses were conducted using R (v3.3.1, www.R-project.org).

3.4. Results

3.4.1. Warming rates and timing.

The Red Sea displays a latitudinal gradient of increasing T_{\max} from north to south with the southern Red Sea exhibiting the highest T_{\max} (33 °C) until the southernmost Bab-el-Mandeb Strait (Figure 3.1). The Gulf of Suez and the Gulf of Aqaba both exhibit lower temperatures than the open Red Sea (Figure 3.1).

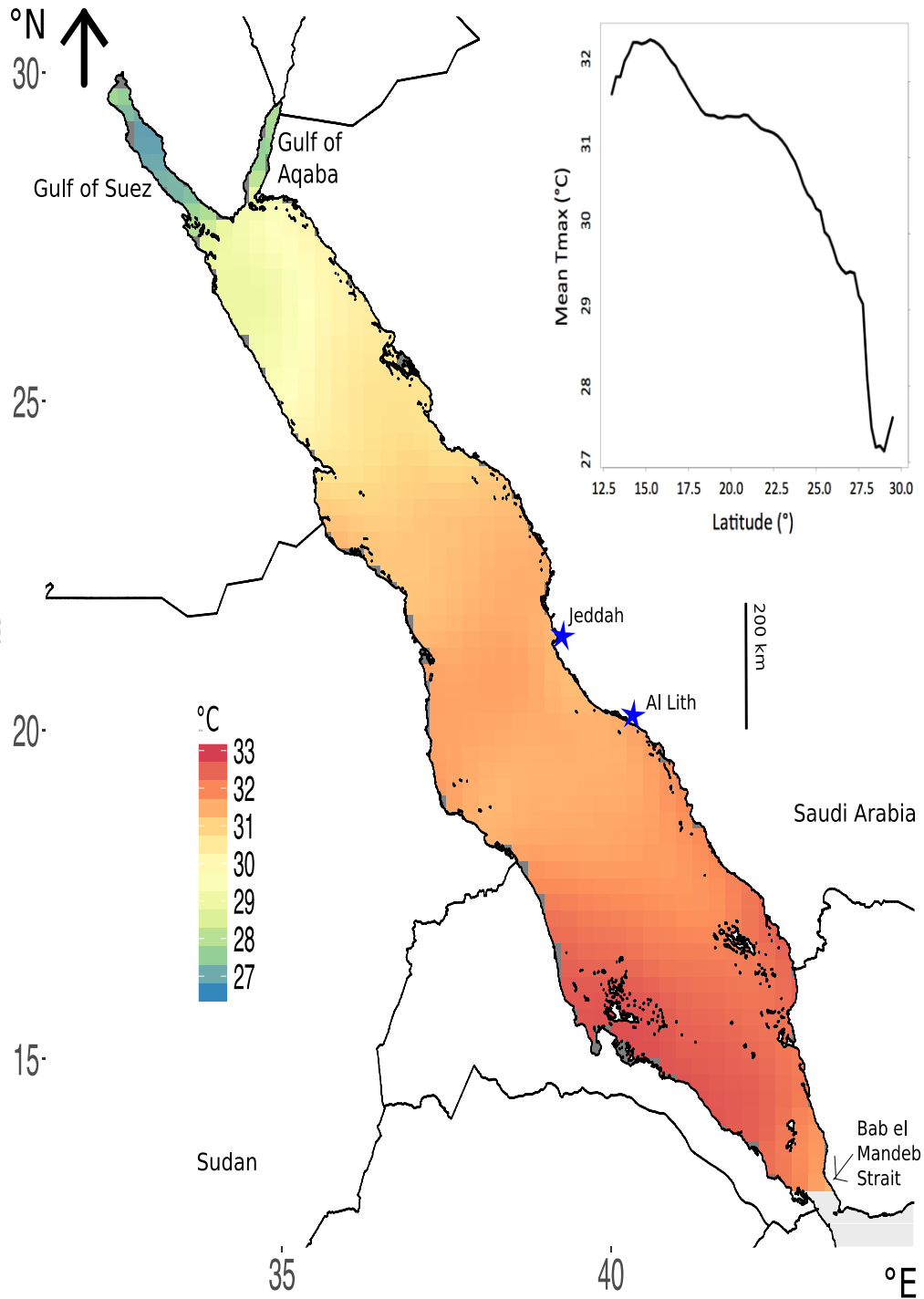


Figure 3.1. Distribution of mean (from 1982 to 2015) maximum annual temperature (T_{max}) across the Red Sea. Insert shows the latitudinal changes in mean (from 1982 to 2015) T_{max} . Values based on daily temperature data. Image created using R (v3.3.1, www.R-project.org) including packages: ggplot2 (Wickham 2009) and rasterVis (Lamigueiro and Hijmans 2016), RStudio (v1.0.143, www.rstudio.com), and Inkscape (v0.91, www.inkscape.org).

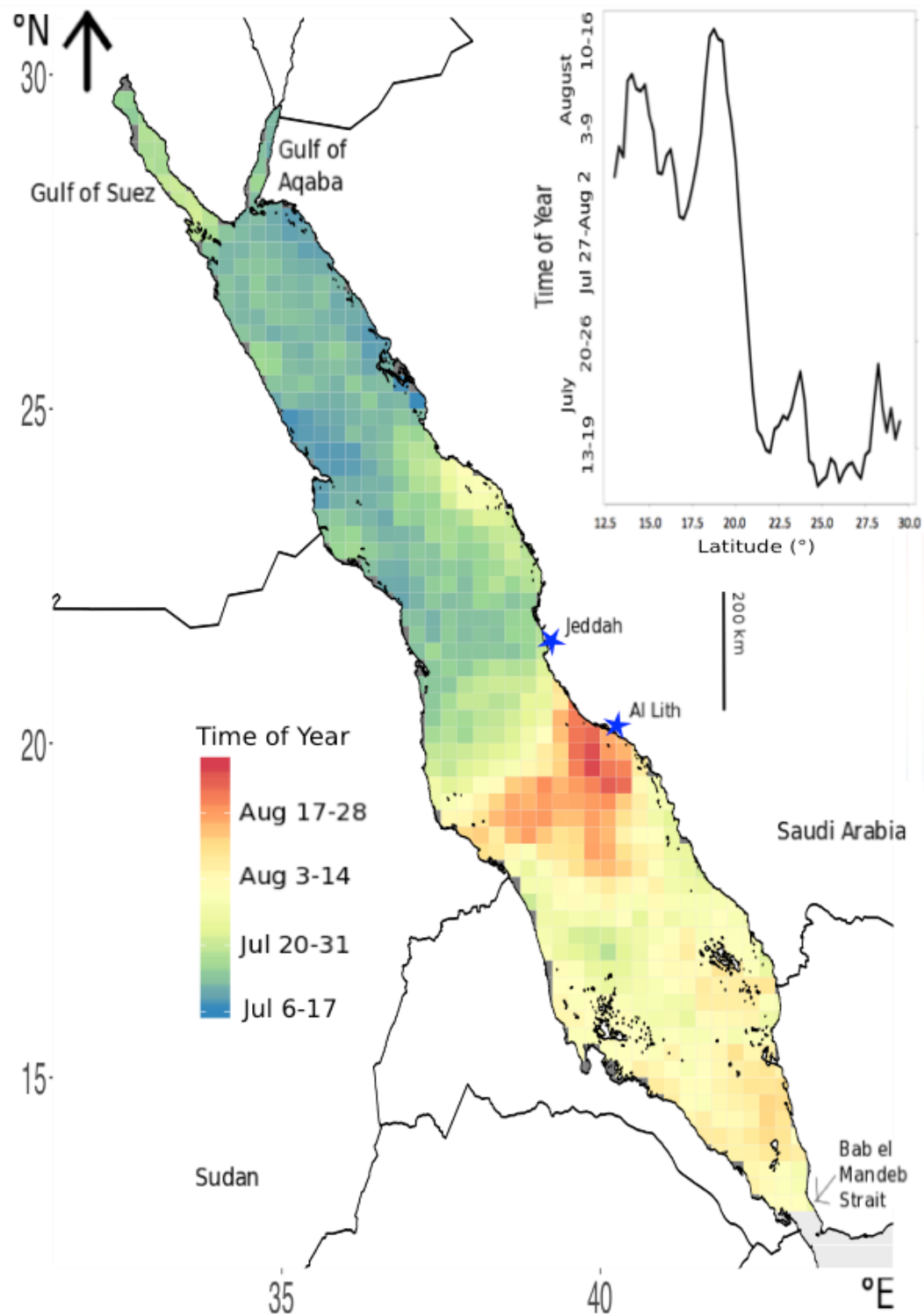


Figure 3.2. Average yearly timing of maximum annual temperature (T_{max}) across the Red Sea. Insert shows the latitudinal trend in the average timing of T_{max} . Image created using R (v3.3.1, www.R-project.org) including packages: ggplot2 (Wickham 2009) and rasterVis (Lamigueiro and Hijmans 2016), RStudio (v1.0.143, www.rstudio.com), and InkScape (v0.91, www.inkscape.org).

The northern Red Sea experiences T_{\max} throughout July while T_{\max} is reached between late July and mid–August in the southern Red Sea (Figure. 3.2). The area off of Al Lith, Saudi Arabia, prominently exhibits delayed T_{\max} from approximately mid August to early September (red area in Figure. 3.2).

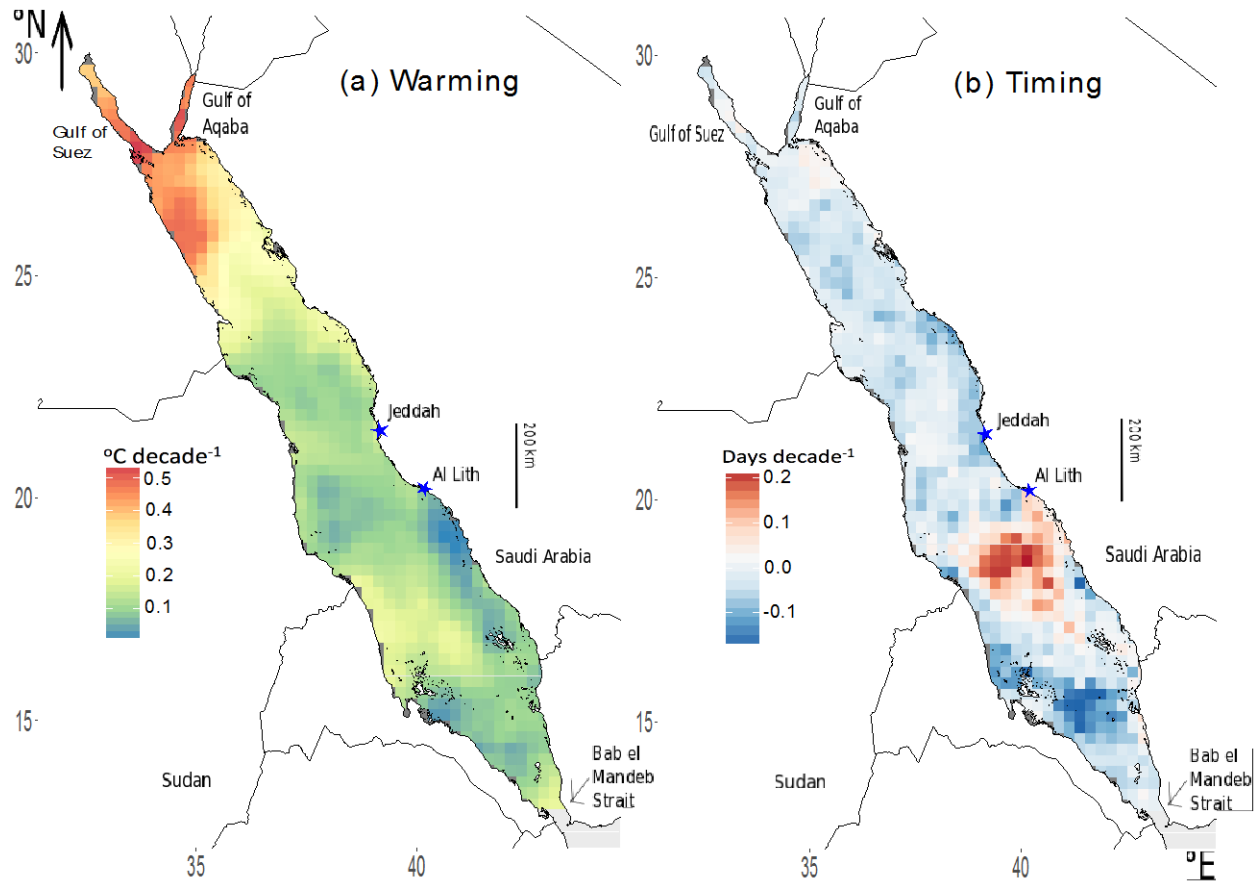


Figure 3.3. (a) Decadal rates of warming ($^{\circ}\text{C decade}^{-1}$) and (b) change in timing (days decade^{-1}) of mean maximum annual temperature (T_{\max}) across the Red Sea. Image created using R (v3.3.1, www.R-project.org) including packages: ggplot2 (Wickham 2009) and rasterVis (Lamigueiro and Hijmans 2016), RStudio (v1.0.143, www.rstudio.com), and Inkscape (v0.91, www.inkscape.org).

We assessed the rate of change in the magnitude and timing of T_{\max} across the Red Sea. We observed a significant trend toward increased T_{\max} across the Red Sea, at an

average rate of 0.17 ± 0.07 °C decade⁻¹ ($p = 0.02$, $df = 32$, $t = 2.437$). Rates of change in T_{\max} varied across the Red Sea, with highest rates found in the colder areas of the Red Sea, including the northern Red Sea with rates for the Gulf of Suez and Gulf of Aqaba at $0.40 - 0.45$ °C decade⁻¹ (Figure 3.3a). The region experiencing the lowest rate of warming is, again, that exhibiting a delayed T_{\max} off the coast of Al Lith, Saudi Arabia (blue area in Figure 3.3a).

In addition to a general pattern toward increasing T_{\max} , maximum temperatures in the Red Sea are also being reached earlier, with an average rate of change in the timing of T_{\max} of 0.19 ± 0.30 days earlier decade⁻¹ (Figure 3.3b). Most of the Red Sea experienced progressively earlier T_{\max} by 0.1 to 2 days earlier decade⁻¹, but a region in the southern Red Sea showed a delay in T_{\max} by 1 to 2 days decade⁻¹. This is the same region that exhibits anomalous trends in the annual timing of T_{\max} (Figure 3.2).

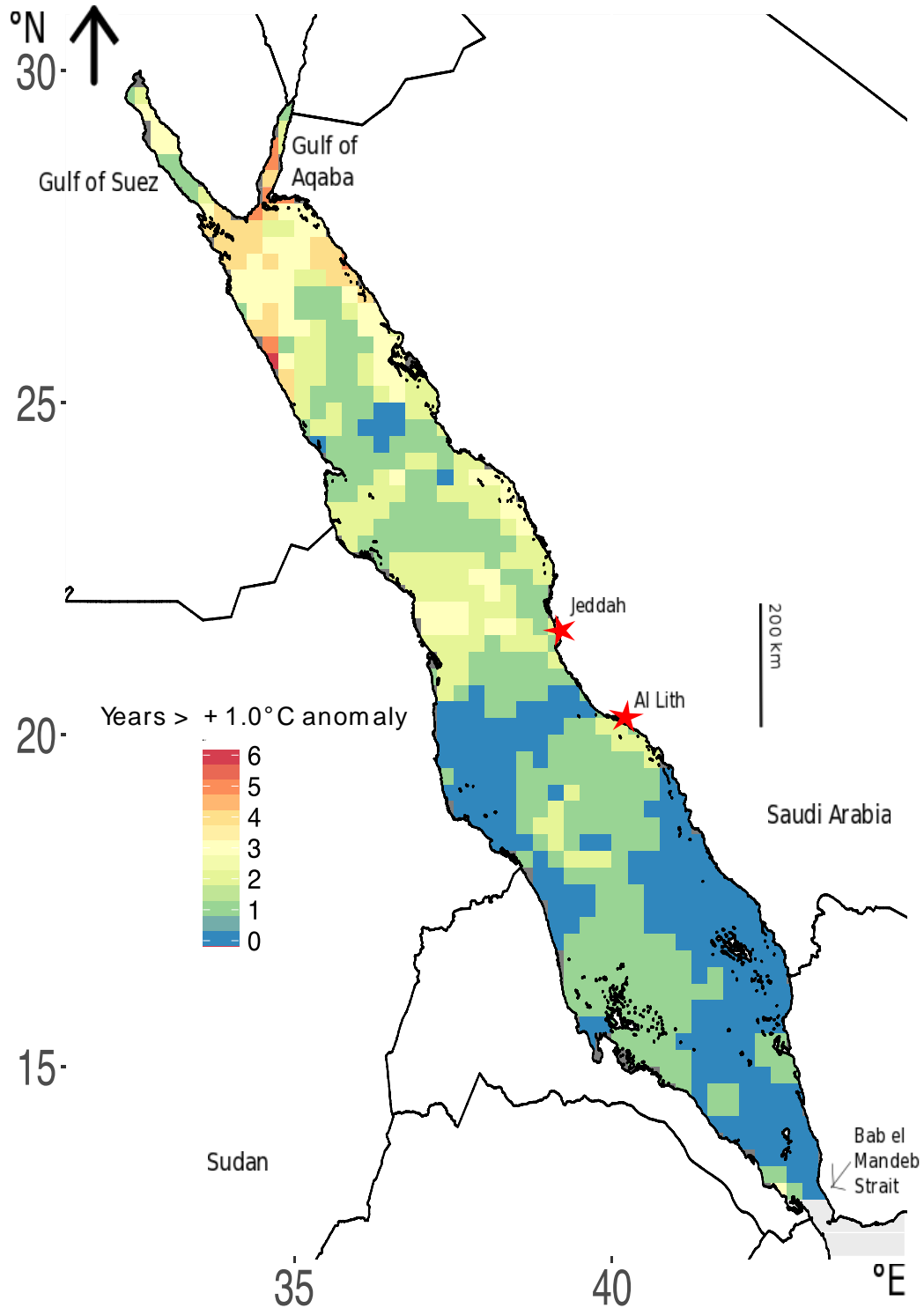


Figure 3.4. Distribution of the frequency, as number of years, across the Red Sea when maximum annual temperature (T_{max}) reached 1.0 °C higher than the mean T_{max} for 1982-2015. Image created using R (v3.3.1, www.R-project.org) including packages: ggplot2 (Wickham 2009) and rasterVis (Lamigueiro and Hijmans 2016), RStudio (v1.0.143, www.rstudio.com), and InkScape (v0.91, www.inkscape.org).

3.4.2. Heat anomalies.

Heat waves representing anomalies of 1.0 °C above the average T_{\max} were observed more frequently in the northern half of the Red Sea over the last 34 years. The majority of the basin experienced such anomalies during at least one year and up to 6 years (which may or may not have been successive years). Some areas in the northern Red Sea, including the Gulf of Aqaba, experienced 1.0 °C magnitude heat waves as often as 5 or 6 years over the 34 year period examined here (Figure 3.4).

T_{\max} values 0.5 °C above the mean (1982 – 2015) values occurred 15 to 24% of the years, whereas thermal anomalies involving T_{\max} values 0.75 °C above the mean values occurred 6 to 12% of the years, and years with T_{\max} values of 1.0 °C above the mean values occurred with a probability < 6% (Figure 3.5). The decline in the frequency of T_{\max} anomalies with increasing magnitude of anomalies was significant (Kruskal-Wallis, $p < 2.2e^{-16}$, chi-squared = 2674, df = 4, Figure 3.5) and significant differences were found among all groups (Dunn's, $p < 0.05$, Z range = [4:44]).

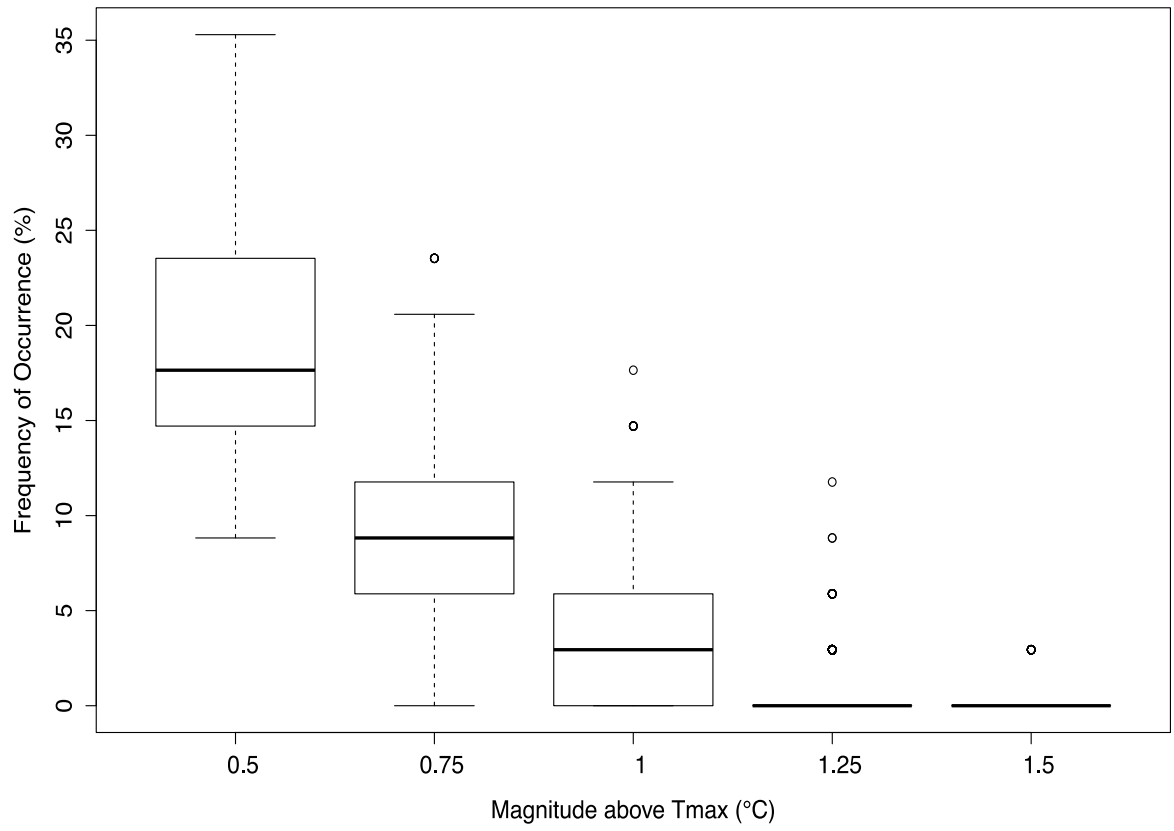


Figure 3.5. Probability, as the frequency of occurrence between 1982-2015, of maximum annual temperature (T_{\max}) anomalies of different magnitudes. A Kruskal-Wallis test and post-hoc Dunn's tests found significantly different frequencies among and between all anomalies (Kruskal-Wallis, $p < 2.2e^{-16}$, chi-squared = 2674, $df = 4$; all Dunn's tests, $p < 0.05$, Z range = [4:44]).

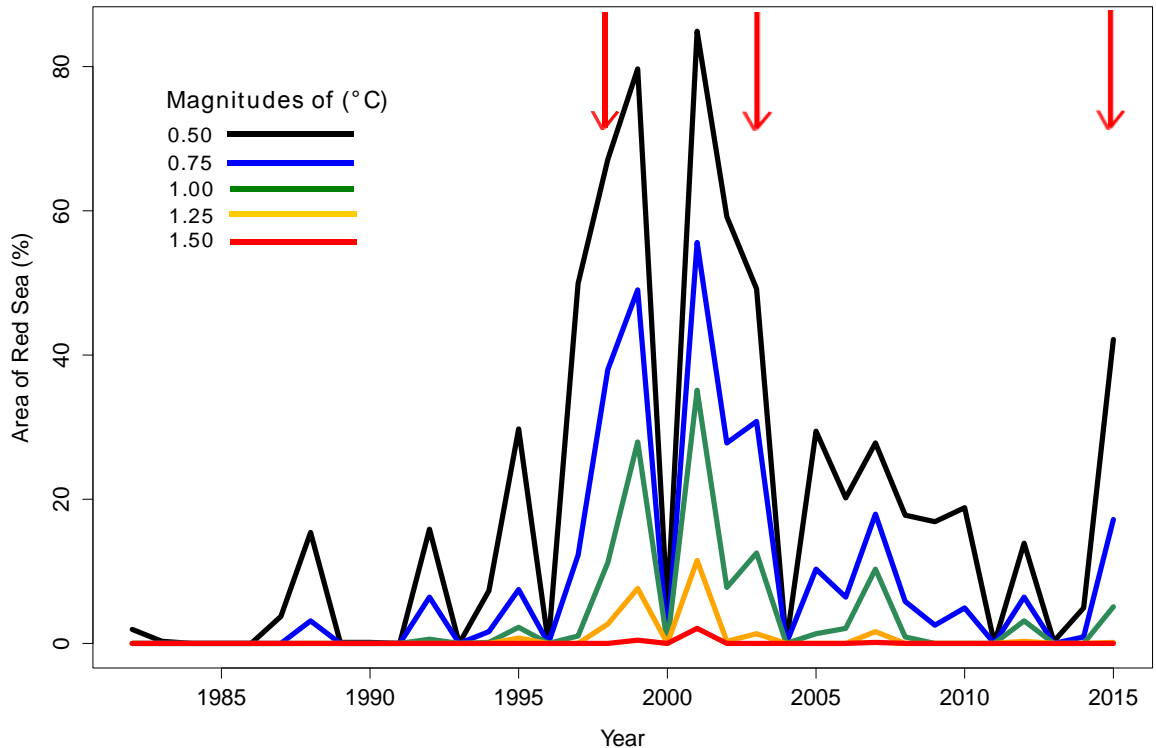


Figure 3.6. Percent of Red Sea area exhibiting maximum annual temperature (T_{\max}) anomalies of different magnitudes between 1982 and 2015. Red indicators signal the occurrence of El Niño events.

3.5. Discussion

The latitudinal gradient of increasing T_{\max} from north to south in the Red Sea is largely a consequence of the variation in solar radiation associated with these latitudinal differences, and is consistent with previous studies reporting the same trend based on mean temperatures, with the warmest thermal regime in the southern region¹⁹. The Gulf of Suez and the Gulf of Aqaba have colder thermal regimes. Previous studies reported that, in the summer, the surface water entering the Gulf of Aqaba from the Red Sea is about 2 °C warmer than the water inside the Gulf (Manasrah et al. 2006).

The Red Sea basin presents a discontinuity in terms of the timing of T_{\max} , associated with an abrupt transition between 20 and 22 °N. The timing of T_{\max} occurs two months earlier south of this boundary compared to the timing north of this boundary. The distinct break between North and South (Figure 3.2), may be evidence for the strong coupling of wind and sea surface temperatures over the basin as in other ocean systems (Hayes et al. 1989; Chelton et al. 2004; Chelton et al. 2007). During winter (October – April), the basin experiences opposing southward and northward winds, converging at about the same belt between 19 – 20 °N (Raitsos et al. 2013) where the divide in timing of T_{\max} is observed. From May to September, the major wind vector is from north to south (Raitsos et al. 2013).

The warming rate of the Red Sea, 0.17 ± 0.07 °C decade⁻¹, is higher than the global ocean rate of 0.11 °C decade⁻¹ (Rhein et al. 2013). The northern Red Sea is warming faster with the Gulf of Suez and Gulf of Aqaba ($0.40 - 0.45$ °C decade⁻¹) (Figure 3.3a) warming four times faster than the mean global ocean warming rate. The semi-enclosed nature of the two gulfs as well as that of the Red Sea as a whole may account for the intense warming (Fishelson 1980; Belkin 2009; Nykjaer 2009), while the slower rate of increase in the southern Red Sea may be buffered by its closer connection to the Indian Ocean. Although the northern Red Sea is warming faster, it remains the coolest region in the basin throughout the year.

Increased T_{\max} will have effects on marine biota, which are particularly vulnerable to heat waves, when their thermal limits may be approached or exceeded (Stillman 2003; Thomas et al. 2012). The occurrence of heat anomalies, which are also likely to increase in the future¹, are greatly relevant to the physiology of organisms,

particularly for those inhabiting already warm environments, like the Red Sea, where temperature anomalies may lead to thermal collapse (Jones et al. 1998; Thomas et al. 2012; Maor-Landaw et al. 2014; Sawall et al. 2014). The years 1999 and 2001 experienced the largest anomalies across the basin (Figure 3.6). During the years 1997 – 1998, one of the strongest El Niño events occurred, while 2000 – 2001 was considered a weak La Niña event (Hjelle and Glass 2000). The years 2003 and 2015, also El Niño years, showed the second greatest percentage of area covered by T_{\max} anomalies, although of a relatively small, 0.5 °C, magnitude (Figure 3.6).

Systematic monitoring efforts are required to detect the effect of heat anomalies on marine organisms, such as bleaching and mass mortality events (Caputi et al. 2014). Unfortunately, there is no systematic monitoring of biological events in the Red Sea, such as bleaching events, which may be affected by thermal anomalies such as those reported here. Extensive bleaching was reported in the southern half of the Red Sea in 2015, one of the years with extensive, but relatively moderate, thermal anomalies in our analysis (Figure 3.6). Whether bleaching events also occurred in other years with extensive T_{\max} anomalies is unknown due to lack of long-term monitoring.

The distribution of T_{\max} in the Red Sea conforms to the four provinces, described by Raitzos *et al.* (2013) based on phytoplankton biomass. The warmer T_{\max} regime in the South is associated with higher phytoplankton biomass, while the lowest T_{\max} in the northern Red Sea is associated with the lowest phytoplankton biomass. However, this pattern may be a result of the decrease in nutrient concentrations from south to north along the Red Sea (Souvermezoglou et al. 1989), rather than its

thermal regime. A region in the central Red Sea emerges as deviating from the general pattern with a slower rate of warming and T_{\max} reached later in the year over time.

That T_{\max} is rapidly increasing in the Red Sea, which is already one of the warmest seas, anticipates challenges to biota. Whereas T_{\max} is increasing more rapidly in the North than in the South, the warmer thermal regime in the South may already be near the thermal limits of organisms and, therefore, even a modest increase in T_{\max} may suffice to exceed their thermal tolerance, although experimental work is necessary to test this suggestion. Unfortunately, although the Red Sea ranks as the warmest sea on the planet, aside from one study examining the effect of temperature on grazing rates of Red Sea parrotfish (Afeworki et al. 2013), there is, at present, no quantitative information on the thermal limits of Red Sea biota. However, reports of a decline in coral growth and calcification across the thermal range of Red Sea corals (Sawall et al. 2015), together with widespread bleaching in the southern half of the Red Sea during 2015, as well as lower growth rates reported for brown macroalgae (Ateweberhan et al. 2005), suggests that warm Red Sea temperatures already challenge the capacities of organisms. In addition to increasing T_{\max} , the general tendency towards an earlier occurrence indicates that phenology patterns of organisms might need to adjust to this shift. Marine organisms generally cope with warming by shifting their biogeographical range poleward tracking the migration of isotherms (Burrows et al. 2011; Poloczanska et al. 2013). However, this strategy is not possible in semi-enclosed seas, such as the Red Sea (Burrows et al. 2011; Burrows et al. 2014), rendering its large pool of

endemic species at risk of extinction unless they become Lessepsian migrants and colonize the Mediterranean Sea as a hundred Red Sea species have done (Raitsos et al. 2010). Altogether, higher and earlier T_{max} may challenge the capacities of Red Sea biota to cope.

Results presented here provide a context for experimental analyses examining thermal limits, by defining the regimes and trends in T_{max} across the Red Sea, as well as the likelihood of observing anomalies of different magnitudes. In addition, these results may help understand biodiversity patterns and losses across natural gradients in the Red Sea by matching the distribution of communities and habitats with the distribution of T_{max} . This will provide an underpinning to the assessment thermal maxima play in explaining patterns of biodiversity across the Red Sea.

3.5.1. Conclusions

In conclusion, Red Sea biota are exposed to increased ocean warming, particularly in the northern Red Sea, which may affect their future persistence, especially if unable to migrate into the Mediterranean. The results on Red Sea warming presented here, coupled with experimental evidence on the thermal limits of Red Sea organisms, yet to be resolved, would provide a powerful tool to predict the future of marine biodiversity in this biodiversity hotspot containing a high degree of endemism.

3.6. References

- Afeworki Y, Zekeria ZA, Videler JJ, Bruggemann JH (2013) Food intake by the parrotfish *Scarus ferrugineus* varies seasonally and is determined by temperature, size and territoriality. *Marine Ecology Progress Series* 489:213-224
- Ateweberhan M, Bruggemann JH, Breeman AM (2005) Seasonal dynamics of *Sargassum ilicifolium* (Phaeophyta) on a shallow reef flat in the southern Red Sea (Eritrea). *Marine Ecology Progress Series* 292:159-171

- Belkin IM (2009) Rapid warming of large marine ecosystems. *Progress in Oceanography* 81:207-213
- Brasnett B (2008) The impact of satellite retrievals in a global sea-surface-temperature analysis. *Quarterly Journal of the Royal Meteorological Society* 134:1745-1760
- Burrows MT, Schoeman DS, Buckley LB, Moore P, Poloczanska ES, Brander KM, Brown C, Bruno JF, Duarte CM, Halpern BS, Holding J, Kappel CV, Kiessling W, O'Connor MI, Pandolfi JM, Parmesan C, Schwing FB, Sydeman WJ, Richardson AJ (2011) The pace of shifting climate in marine and terrestrial ecosystems. *Science* 334:652-655
- Burrows MT, Schoeman DS, Richardson AJ, Molinos JG, Hoffmann A, Buckley LB, Moore PJ, Brown CJ, Bruno JF, Duarte CM, Halpern BS, Hoegh-Guldberg O, Kappel CV, Kiessling W, O'Connor MI, Pandolfi JM, Parmesan C, Sydeman WJ, Ferrier S, Williams KJ, Poloczanska ES (2014) Geographical limits to species – range shifts are suggested by climate velocity. *Nature* doi:10.1038/nature12976
- Cantin NE, Cohen AL, Karnauskas KB, Tarrant AM, McCorkle DC (2010) Ocean warming slows coral growth in the Central Red Sea. *Science* 329:322-325
- Caputi N, Jackson G, Pearce AF (2014) The marine heat wave off Western Australia during the summer of 2010/11 – 2 years on. Fisheries Research Report No. 250. Department of Fisheries, Western Australia 40pp
- Chaidez V, Dreano D, Agusti S, Duarte CM, Hoteit I (2017) Annual maximum sea surface temperature across the Red Sea (1982-2015). PANGAEA, Dataset #877876 (<https://doi.pangaea.de/10.1594/PANGAEA.877876>)
- Chelton DB, Schlax MG, Freilich MH, Milliff RF (2004) Satellite measurements reveal persistent small-scale features in ocean winds. *Science* 303:978-983
- Chelton DB, Schlax MG, Samelson RM (2007) Summertime coupling between sea surface temperature and wind stress in the California Current System. *Journal of Physical Oceanography* 37:495-517
- Coma R, Ribes M, Serrano E, Jimenez E, Salat J, Pascual J (2009) Global warming-enhanced stratification and mass mortality events in the Mediterranean. *Proceedings of the National Academy of Sciences of the United States of America* 106:6176-6181
- Duarte CM, Lenton TM, Wadhams P, Wassmann P (2012) Abrupt climate change in the Arctic. *Nature Climate Change* 2:60-62

- Fishelson L (1971) Ecology and distribution of the benthic fauna in the shallow waters of the Red Sea. *Marine Biology* 10:113-133
- Fishelson L (1980) Marine reserves along the Sinai Peninsula (northern Red Sea). *Helgoländer Meeresun* 33:624-640
- Hayes SP, McPhaden MJ, Wallace JM (1989) The influence of sea-surface temperature on surface wind in the eastern equatorial Pacific: Weekly to monthly variability. *Journal of Climate* 2:1500-1506
- Hjelle B, Glass GE (2000) Outbreak of hantavirus infection in the four corners region of the United States in the wake of the 1997-1998 El Niño-Southern Oscillation. *The Journal of Infectious Diseases* 181:1569-1573
- Jones RJ, Hoegh-Guldberg O, Larkum AWD, Schreiber U (1998) Temperature-induced bleaching of corals begins with impairment of the CO₂ fixation mechanism in zooxanthellae. *Plant, Cell and Environment* 21:1219-1230
- Jordà G, Marbà N, Duarte CM (2012) Mediterranean seagrass vulnerable to regional climate warming. *Nature Climate Change* 2:821-824
- Kleypas JA, Danabasoglu G, Lough JM (2008) Potential role of the ocean thermostat in determining regional differences in coral reef bleaching events. *Geophysical Research Letters* 35
- Oscar Perpignan Lamigueiro and Robert Hijmans (2016), *meteoForecast*. R package version 0.40
- Lasker HR (2005) Gorgonian mortality during a thermal event in the Bahamas. *Bulletin of Marine Science* 76:155-162
- Lima FP, Wetthey DS (2012) Three decades of high-resolution coastal sea surface temperatures reveal more than warming. *Nature Communications* 3
- Manasrah R, Raheed M, Badran MI (2006) Relationships between water temperature, nutrients and dissolved oxygen in the northern Gulf of Aqaba, Red Sea. *Oceanologia* 48:237-253
- Maor-Landaw K, Karako-Lampert S, Ben-Asher HW, Goffredo S, Falini G, Dubinsky Z, Levy O (2014) Gene expression profiles during short-term heat stress in the red sea coral *Stylophora pistillata*. *Global Change Biology* 20:3026-3035
- Marbà N, Duarte CM (2010) Mediterranean warming triggers seagrass (*Posidonia oceanica*) shoot mortality. *Global Change Biology* 16:2366-2375

- Marbà N, Jorda G, Agusti S, Girard C, Duarte CM (2015) Footprints of climate change on Mediterranean Sea biota. *Frontiers in Marine Science* 2
- Nykjaer L (2009) Mediterranean Sea surface warming 1985–2006. *Climate Research* 39:11-17
- Poloczanska ES, Brown CJ, Sydeman WJ, Kiessling W, Shoeman DS, Moore PJ, Brander K, Bruno JF, Buckley LB, Burrows MT, Duarte CM, Halpern BS, Holding J, Kappel CV, O'Connor MI, Pandolfi JM, Parmesan C, Schwing F, Thompson SA, Richardson AJ (2014) Global imprint of climate change on marine life. *Nat Clim Chang* doi: 10.1038/nclimate1958
- Raitsos, D. E. *et al.* Global climate change amplifies the entry of tropical species into the Eastern Mediterranean Sea. *Limnology and Oceanography* 55, 1478-1484 (2010)
- Raitsos DE, Hoteit I, Prihartato PK, Chronis T, Triantafyllou G, Abualnaja Y (2011) Abrupt warming of the Red Sea. *Geophysical Research Letters* 38
- Raitsos DE, Pradhan Y, Brewin RJW, Stenchikov G, Hoteit I (2013) Remote sensing the phytoplankton seasonal succession of the Red Sea. *PloS ONE* 8(6): e64909
- Reynolds RW, Smith TM, Liu C, Chelton DB, Casey KS, Schlax MG (2007) Daily high-resolution-blended analyses for sea surface temperature. *Journal of Climate* 20:5473-5496
- Rhein, M., S. R. Rintoul, S. Aoki, E. Campos, D. Chambers, R. A. Feely, S. Gulev, G. C. Johnson, S. A. Josey, A. Kostianoy, C. Mauritzen, D. Roemmich, L. D. Talley, and F. Wang (2013), Observations: ocean. In: *Climate Change 2013: the physical science basis. Contribution of Working Group I to the Fifth Assessment Report of the Intergovernmental Panel on Climate Change* (T. F. Stocker, D. Qin, G.-K. Plattner, M. Tignor, S. K. Allen, J. Boschung, A. Nauels, Y. Xia, V. Bex, and P. M. Midgley, eds.), Cambridge University Press, Cambridge, United Kingdom and New York, NY, USA
- Roik A, Roder C, Rothig T, Voolstra CR (2016) Spatial and seasonal reef calcification in corals and calcareous crusts in the central Red Sea. *Coral Reefs* 35:681-693
- Romano JC, Bensoussan N, Younes WAN, Arlhac D (2000) Thermal anomaly in the waters of the Gulf of Marseilles during summer 1999. A partial explanation of the mortality of certain fixed invertebrates?. *Comptes rendus de l'Academie des sciences. Serie III, Sciences de la vie* 323:415-427

- Sawall Y, Al-Sofyani A, Banguera-Hinestroza E, Voolstra CR (2014) Spatio-temporal analyses of *Symbiodinium* physiology of the coral *Pocillopora verrucosa* along large-scale nutrient and temperature gradients in the Red Sea. *PloS one* 9
- Sawall Y, Al-Sofyani A, Hohn S, Banguera-Hinestroza E, Voolstra CR, Wahl M (2015) Extensive phenotypic plasticity of a Red Sea coral over a strong latitudinal temperature gradient suggests limited acclimatization potential to warming. *Scientific Reports* 5
- Sherman K, Belkin I, Friedland KD, O'Reilly J, Hyde K (2009) Accelerated warming and emergent trends in fisheries biomass yields of the world's large marine ecosystems. *AMBIO* 38:215-224
- Souvermezoglou E, Metzl N, Poisson A (1989) Red Sea budgets of salinity, nutrients and carbon calculated in the Strait of Bab-El-Mandab during the summer and winter seasons. *Journal of Marine Research* 47:441-456
- Sparnocchia S, Schiano ME, Picco P, Bozzano R, Cappelletti A (2006) The anomalous warming of summer 2003 in the surface layer of the Central Ligurian Sea (Western Mediterranean). *Annales Geophysicae* 24:443-452
- Stillman JH (2003) Acclimation capacity underlies susceptibility to climate change. *Science* 301:65-65
- Thomas MK, Kremer CT, Klausmeier CA, Litchman E (2012) A global pattern of thermal adaptation in marine phytoplankton. *Science* 338:1085-1088
- Tkachenko KS (2015) Impact of repetitive thermal anomalies on survival and development of mass reef-building corals in the Maldives. *Marine Ecology* 36:292-304
- Wickham H (2009) *ggplot2: Elegant Graphics for Data Analysis*. Springer-Verlag New York
- Wilkinson CP (1998) The 1997-1998 mass bleaching event around the world. Status of Coral Reefs of the World: 1998 Report, Australian Institute of Marine Science, Townsville, Australia 23pp.
- R Core Team (2013) *R: A language and environment for statistical computing*. R Foundation for Statistical Computing, Vienna, Austria. URL www.R-project.org/
- National Climatic Data Center. GHRSSST Level 4 AVHRR_OI Global Blended Sea Surface Temperature Analysis. 1st ed. doi:10.5067/GHAAO-4BC01

3.7. Supplementary Materials

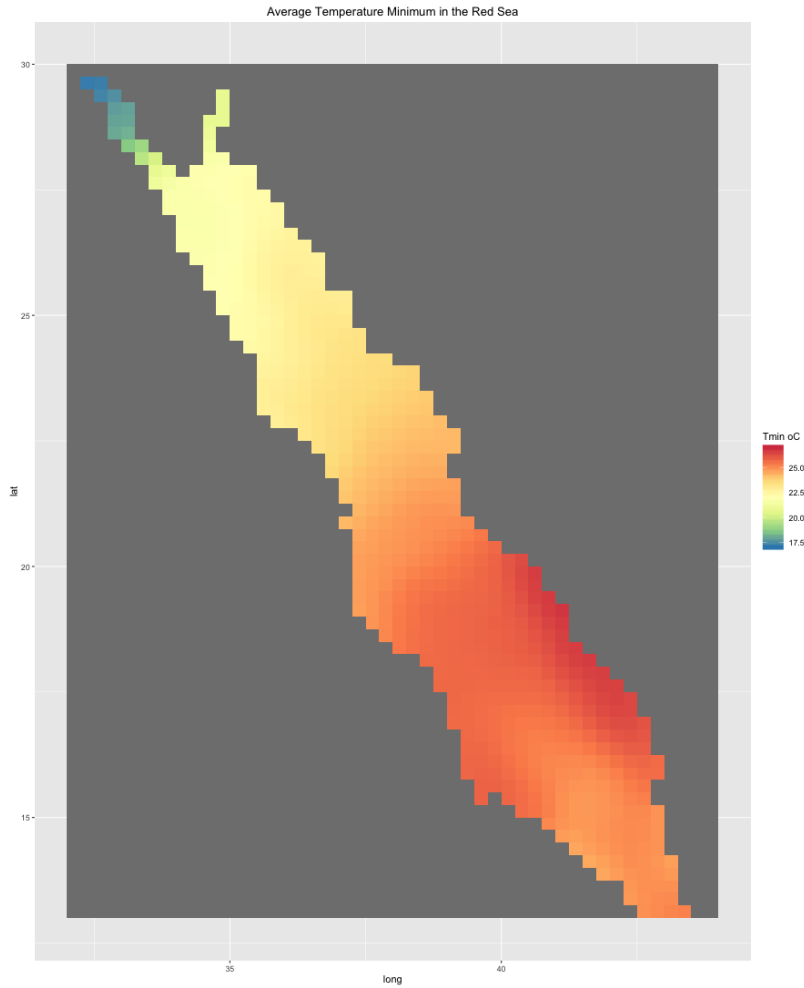


Figure 3.7. Distribution of mean (from 1982 to 2015) minimum annual temperature (T_{\min}) across the Red Sea. Values based on daily temperature data. Image created using R (v3.3.1, www.R-project.org) including packages: ggplot2 and rasterVis, RStudio (v1.0.143, www.rstudio.com).

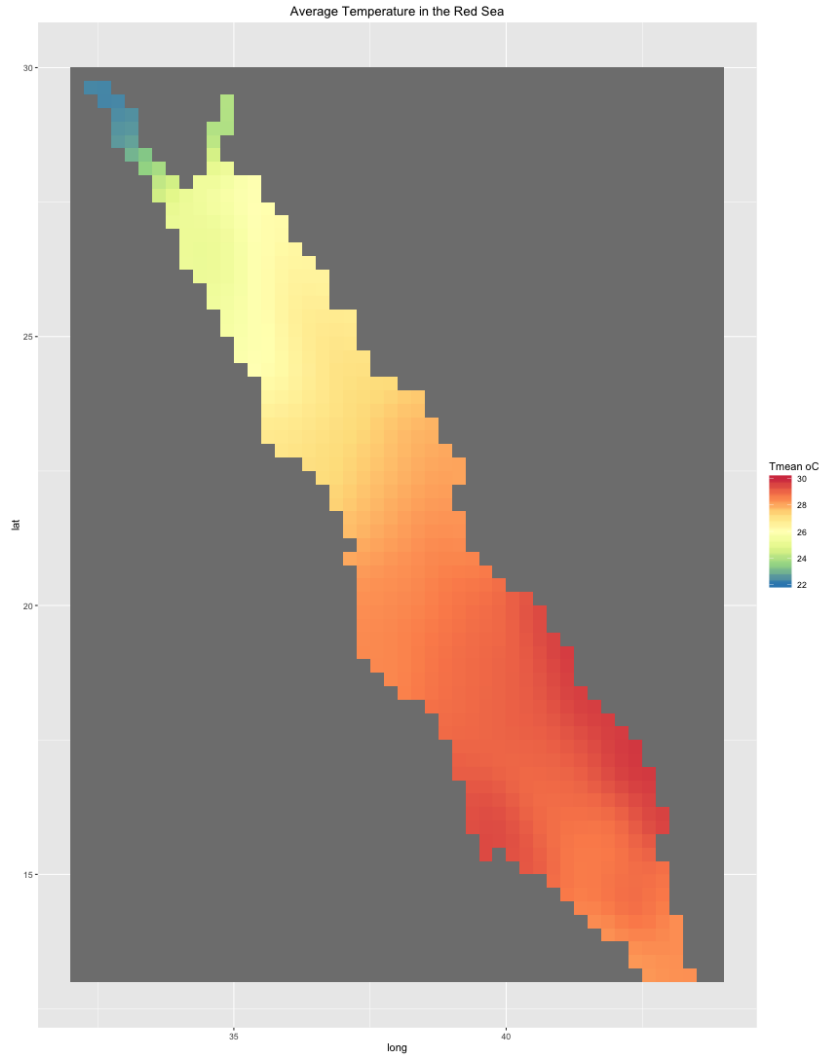


Figure 3.8. Distribution of mean (from 1982 to 2015) average annual temperature across the Red Sea. Values based on daily temperature data. Image created using R (v3.3.1, www.R-project.org) including packages: ggplot2 and rasterVis, RStudio (v1.0.143, www.rstudio.com).

CHAPTER II

4. Thermal resistance of *Avicennia marina* seedlings and effects on early growth in the Red Sea

Veronica Chaidez and Carlos M. Duarte

King Abdullah University of Science and Technology (KAUST), Red Sea Research Center (RSRC), Thuwal, 23955-6900, Saudi Arabia.

This manuscript is prepared for submission to

Estuaries and Coasts

Chaidez V, Duarte CM (in prep) Thermal resistance of *Avicennia marina* seedlings and effects on early growth in the Red Sea

4.1. Abstract

Mangroves are resilient ecosystem engineers, colonizing a variety of tropical coastal regions around the globe. The ubiquitous mangrove species, *Avicennia marina*, is especially tolerant of high temperature and high salinity, characteristics that define the understudied coastal Red Sea, where organisms may be presently living near their upper thermal thresholds and maybe impacted by further warming. The effects of temperature on the early development of *A. marina* was examined by evaluating germination and growth of its propagules and seedlings across a range of experimental temperature regimes encompassing present and future conditions spanning from current mean temperatures to +8 °C above these. The propagules failed to survive at temperatures +6 °C above present values, with the thermal limit of early life stages of *A. marina* identified between 33 and 35 °C. Of the lower temperature treatments that successfully germinated, we found no significant difference among germination rates nor aboveground biomass production, indicating that *A. marina* is expected to be unaffected by a 2 or even 4 °C increment in mean temperature. In order to adapt to higher temperatures, *A. marina*, allocated more energy to develop stronger roots and larger leaves at the expense of a reduction in upward growth. The results presented show that the early life stages of *A. marina* are relatively resistant to forecasted warming within the 21st Century.

4.2. Introduction

Mangrove ecosystems are ubiquitous throughout tropical and subtropical coastal regions; they play a pivotal role as carbon sinks, reservoirs of biodiversity, and in coastal protection (Tomlinson 1986; Mumby et al. 2004; Bouillon et al. 2008; Duarte

et al. 2013). Mangrove trees are well adapted to extreme environments, often encountering high temperatures, high irradiance, anoxia, intense wind, flooding, and hyper-saline conditions (Scholander et al. 1955; Clough 1984; Tomlinson 1986; Bjorkman et al. 1988; Saifullah 1996; Owen and Forbes 1997). However, despite their resistance, they are experiencing world-wide decline (Valiela et al. 2001; Alongi 2002), largely attributable to deforestation (Valiela et al. 2001; Alongi 2002; Carney et al. 2014; Wong 2014). While scientific attention has been given to the threats deforestation and rising sea levels pose to mangrove ecosystems, limited attention has been allocated to assessing the responses of mangroves to rising temperature (Valiela et al. 2001; Alongi 2008). Recently, mangroves were found to deviate from other marine biota in that they do not seem to be extending their range poleward with climate change (Hickey et al. 2017).

Avicennia marina is one of the most widely distributed mangrove species in the world (Tomlinson 1986), and was first reported for western science in the Red Sea, arguably the only mangrove region of the world where mangroves are not declining (Almahasheer et al. 2016a). The Red Sea provides a challenging environment for *Avicennia marina* due to extreme high temperature, high salinity (Mandura et al. 1987; Saifullah 1996), and strong nutrient-limitation due to the absence of nutrient and sediment inputs from rivers to the Red Sea (Almahasheer et al. 2016b). Red Sea mangroves experience very warm regimes (seawater and air temperatures in excess of 35 °C and 40 °C, respectively), with even warmer conditions expected in the future, as the Red Sea is currently warming at a rate of 0.17 °C decade⁻¹, higher than the global ocean (Chaidez et al. 2017). Aside from one study assessing seasonal

growth of *Sargassum ilicifolium* (Ateweberhan et al. 2005), there is, as yet, no present study experimentally testing the thermal limits of marine plants in the Red Sea. Hence, whether current thermal regimes contributed to the low growth and stature reported for *Avicennia marina* in the Red Sea (Almahasheer et al. 2016c), is unknown, although rates of assimilation of CO₂ by mangroves are expected to decline at leaf temperatures in excess of 30 °C (Ball et al. 1988), which are well exceeded in the Red Sea. Whereas mature trees can protect themselves from high temperatures by self-shading and evapotranspirative heat loss (Miller 1972; Ball et al. 1988; Ganguly et al. 2008), seedlings are more exposed and vulnerable. This suggests that, provided the expected future warming, the stability of Red Sea mangrove stands may be dependent on the thermal resistance of its propagules and seedlings.

A. marina has viviparous propagules which upon abscission, are buoyant and ready to germinate (Berjak et al. 1989). Propagules may be carried by currents (Clarke 1993), and while uncertain how far they disperse, it is clear that they restock local populations (Duke 1995). The environmental conditions in which propagules reside and disperse may be important indicators for their successful establishment, making adaptation to these conditions crucial as early life stages of propagules are a bottleneck for population growth and/or persistence.

Here we assess the thermal resistance of *A. marina* propagules and seedlings in the Central Red Sea. We do so on the basis of experiments conducted in 2016 and 2017 testing the performance of *A. marina* propagules and seedlings across a range of present day and future temperature regimes.

4.3. Materials and Methods

4.3.1. Collection

Propagules were collected on March 2, 2016 and February 8, 2017, the time when seeds are ripe (Almahasheer et al. 2016c), from a mangrove stand near Thuwal, Saudi Arabia (22° 16.978 N, 39° 05.067 E). Viable propagules that were completely dry, intact, had fullness of shape and uniformity of color (green or yellow), were selected from those already abscised and lying on the ground. Propagules were transported to the laboratory in dry buckets and kept at room temperature in the laboratory until the start of the experimental treatments 48 hours later. To control for possible effects of initial propagule size on performance, propagules were divided into five weight classes and distributed equally among the treatments (Table 4.1). Propagules were planted in large seed trays that held seawater and sand while still allowing slow drainage of water.

Table 4.1. Number of propagules in each weight class (A – E) per treatment [total number | percentage] in each experiment (HM+x = historical mean temperature + x °C of warming).

Weight class Weight [g]	A 10.0 – 11.9		B 8.0 – 9.9		C 6.0 – 7.9		D 4.0 – 5.9		E 2.0 – 3.9	
	HM+0	2	4.7	3	7.0	10	23.3	22	51.2	6
HM+2	2	4.8	2	4.8	11	26.2	21	50.0	6	14.3
HM+4	1	2.4	3	7.1	10	23.8	22	52.4	6	14.3
HM+6	3	12.5	7	29.2	8	33.3	6	25.0	0	0.0
HM+8	0	0.0	3	12.5	8	33.3	8	33.3	5	20.8

4.3.2. Experiment

Seedlings were grown in temperature-controlled incubators (Percival Scientific Inc., Boone, Iowa 50036) following a daily temperature regime that gradually moved from T (temperature) max to T min, spending 8 hours at T max and 8 hours at T min, with 4 hours of transition time between these extremes. Experimental temperature regimes were designed by adopting the historical mean (HM) air temperatures of Thuwal, Saudi Arabia throughout the dates of February and March, the peak seed abscission season, and adjusting T_{\max} and T_{\min} each week to the corresponding long-term mean temperature values (Table 4.2), retrieved from AccuWeather.com

(<<http://www.accuweather.com/en/sa/thuwal/1684791/month/1684791?monyr=3/01/2014#>>, accessed on January 12, 2016 and February 1, 2017). Treatments were named: HM+0, HM+2, HM+4, HM+6, and HM+8 to reflect the temperature scenarios including 0 to 8 degrees °C above the long-term mean temperature values. A photoperiod of 12h light : 12h dark was used. Light conditions were matched as closely as possible to those of the coastal Central Red Sea during March and April, to the capacity of the incubators, (111.0 – 117.2 $\mu\text{E m}^{-2} \text{s}^{-1}$). Relative humidity was between 65 – 85%. Propagules were watered with raw seawater from Thuwal's coast as frequently as needed to keep sand moist.

Our experiment took place over two consecutive years, HM+0, HM+2, and HM+4 were run in 2016 with the majority of each treatments' seeds and seedlings remaining viable. As our goal was to assess the thermal thresholds of *A. marina*, we

conducted a second experiment in 2017 including the treatments HM+0, HM+6, and HM+8. HM+0 was our control treatment and all propagules remained viable. Experimental variables remained the same over the two years including potting materials and sources of sand and water.

Throughout the experiment, the propagules and seedlings were inspected every two days, recording the date of pericarp shedding, root initiation, exposure of apical leaves, and unfurling of apical leaves (germination). Once the first node had extended past the cotyledon, stem height from the first node to the base of the shoot apex was measured concurrently with leaf measurements, also every two days. Germination was determined by observing when the first pair of leaves unfurled beyond the cotyledon (Tuan et al. 1996; Clarke and Johns 2002; Ye et al. 2005; Purnobasuki and Utami 2017).

4.3.3. Harvesting

Experiments in 2016 lasted 51 days while those in 2017 lasted 31 days; experiments were prolonged in 2016 to measure stem growth for at least three weeks and prolonged in 2017 until no observable developmental change occurred for at least two weeks. Propagules were assessed as living or dead at the end of each treatment, when all individuals were harvested and tissue could be closely examined, except for HM+6 and HM+8, which contained individuals with clear signs of necrosis before the termination time and these propagules were removed before they decayed. Harvesting included gently digging out every plant intact, rinsing with distilled water, weighing the whole plant, separating the plant into different parts

(roots, body and stem, and leaves), weighing each part, then placing each part in a drying oven at 60 °C and weighing again after thoroughly drying for several days (Tuan et al. 1996).

4.3.4. Analysis

As the survival data was not normally distributed, a chi-square analysis was performed on the percentage of successful seedlings (those that remained viable until the end of the experiment) to test for differences among the treatments, followed by Bonferroni-adjusted post-hoc comparisons. Seedling development was calculated as the average time since planting to: shedding of the pericarp, root initiation, exposure of apical leaves, and germination. As the developmental data did not conform to normal distribution, a Kruskal-Wallis test was performed on each developmental parameter to determine if there were any significant differences among the treatments. The probability of germination success was calculated as the number of germinated propagules per total number in each treatment. An exact binomial test using Clopper-Pearson 95% confidence intervals of germination percentage was performed (Documenta Geigy 1965; Zpevak et al. 2012). Germination rates were calculated using linear regression analysis of the number of germinated plants over time, since planting. To find differences in biomass production, each plant part (i.e leaves, body and stem, etc.), per treatment, underwent a Shapiro-Wilk test for normality, followed by a Kruskal-Wallis analysis that found significant difference in root biomass, and finally a Dunn's test for root biomass. To find differences in the means of total stem length, leaf length, and leaf width, one way ANOVA's were performed following verification that each group was

normally distributed under Shapiro-Wilk tests and had equal variance according to the Levene's test.

4.4. Results

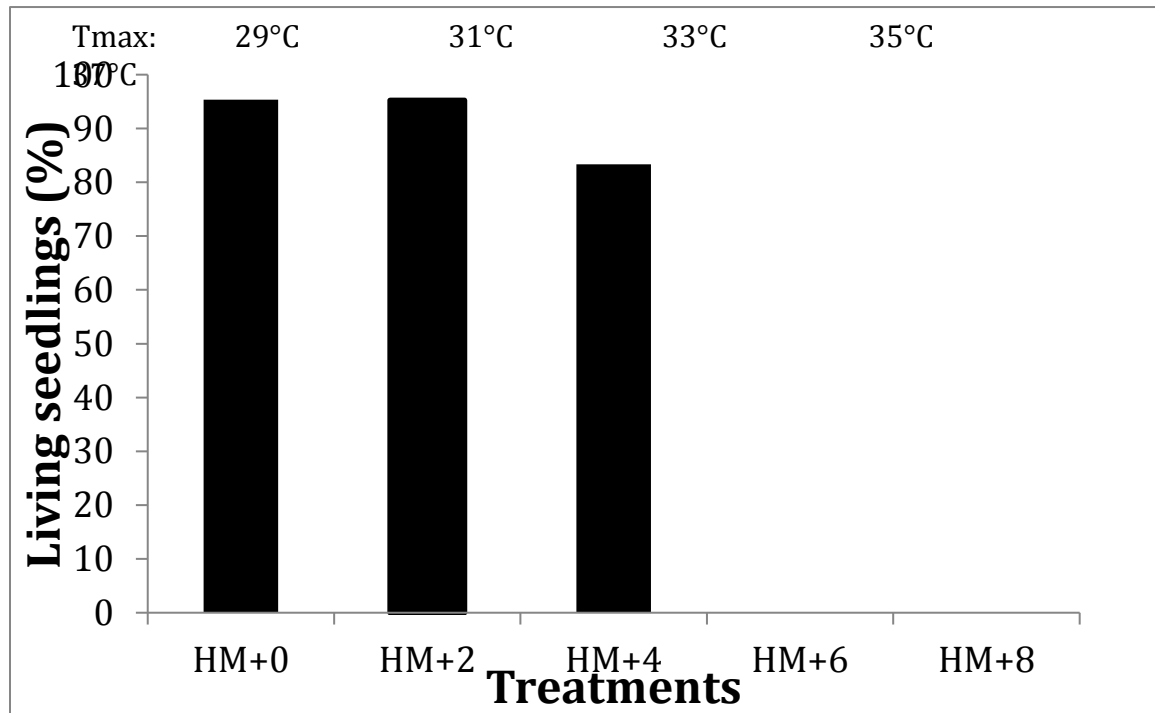


Figure 4.1. Percentage of successful seedlings that rooted and remained viable to the end of experiment under different temperature treatments. HM = historical mean air temperature of Thuwal, Saudi Arabia, i.e. HM+0 = 29 °C on March 1, 2016. HM+0 (N=43), HM+2 (N=42), and HM+4 (N=42) lasted 51 days while HM+6 (N=24) and HM+8 (N=24) lasted 31 days. T_{max} denotes the HM+x of each treatment during the first half of March. Only treatments HM+6 and HM+8 are statistically different from all others. (Chi-square test: $X^2 = 131.84$, $df = 4$, $p\text{-value} < 2.2 \cdot 10^{-16}$, followed by Bonferroni adjusted post-hoc comparisons where HM+6 and HM+8 had $p = 0.0000$.)

The HM+0 treatment, which mimics present day (1985 – 2005) temperature conditions, had 95.34% of its individuals still alive and growing until the termination of the experiment (Figure 4.1). This is equal to the percentage of success of HM+2, two degrees Celsius above the historical mean, of 95.24% (Figure 4.1). The percentage of successful seedlings declined to 83.33% when the temperature was increased 4 °C over current mean values (Figure 4.1), and all

propagules failed when temperature was increased more than 4 °C over current mean values (Figure 4.1).

Table 4.3. Early development of *Avicennia marina* seedlings grown at different temperatures. Values are means of 42 – 43 replicates \pm S.E. *HM+6 and HM+8 had 24 replicates and shedding of the pericarp did not occur naturally. Results of Kruskal-Wallis tests for differences among treatments are reported.

Treatment	Time since planting [days]			
	Pericarp shed	Root initiation	Exposure of apical leaves	Germination (unfurling of leaves)
HM+0	5.1 \pm 0.6	14.0 \pm 1.5	29.9 \pm 1.3	38.8 \pm 1.3
HM+2	5.7 \pm 0.6	13.0 \pm 1.2	31.6 \pm 1.6	37.1 \pm 1.3
HM+4	6.0 \pm 0.6	14.0 \pm 1.5	28.2 \pm 2.0	34.7 \pm 1.6
HM+6*	N/A	12.4 \pm 1.4	N/A	N/A
HM+8*	N/A	12.4 \pm 1.5	N/A	N/A
Kruskal-Wallis [chi-sq, df, p]	2.1938, 2, 0.33	0.4327, 4, 0.98	2.9504, 2, 0.23	3.5972, 2, 0.17

All pericarps were naturally shed within one week of commencing the experiment with ample moisture in the incubators (Table 4.3). Root initiation (first signs of a basal knob elongating) occurred soonest in HM+6 and HM+8 after 12.4 ± 1.4 days (Table 4.3). The other treatments initiated roots between 13.0 ± 1.2 and 14.0 ± 1.5 days (Table 4.3). Exposure of the apical leaves occurred soonest in HM+4 after 28.2 ± 2.0 days, then in HM+0 after 29.9 ± 1.3 days, and in HM+2 after 31.6 ± 1.6 days (Table 4.3).

A. marina propagules did not root or initiated rooting, but then shortly died in the hottest treatments, HM+6 and HM+8, with high mean temperatures of 35 °C and 37 °C, respectively (Figure 4.1, Table 4.3). This is in sharp contrast to observations at temperatures up to +4 °C above the current mean air temperature, where almost all propagules remained viable.

Germination occurred soonest in HM+4 after 34.7 ± 1.6 days, then in HM+2 after 37.1 ± 1.3 days, and took longest for HM+0 after 38.8 ± 1.3 days (Table 4.3). The probability of germination success decreased with warming, being highest at present temperature conditions, with 60.47% compared to 42.86% at +4 °C above the current mean air temperature, with germination failing at warmer temperatures (Table 4.4). The germination rate was fairly uniform among the treatments at temperatures up to +4 °C above the current mean air temperature, between 10 to 12% propagules germinated d^{-1} (Figure 4.2, Table 4.4).

Table 4.4. Results of analysis of germination success and rate. An exact binomial test was performed using Clopper-Pearson 95% confidence intervals. (Lconf. = lower 95% confidence interval, Prob. = probability, Uconf. = upper 95% confidence interval; all as [%].) Rates were calculated using linear regression analysis on log-transformed number of propagules germinated per treatment.

Treatment	Tmax [°C] (Mar)	Germination [%]				Germination rate [ln propagules d ⁻¹] Regression			
		Lconf.	Prob.	Uconf.	P-value	slope	SE slope	Intercept	R ²
HM+0	29	60.03	60.47	61.22	2.20E-16	0.117	0.01	-2.14	0.90
HM+2	31	56.73	57.14	57.86	2.20E-16	0.102	0.02	-1.50	0.86
HM+4	33	42.58	42.86	43.45	4.22E-13	0.116	0.01	-2.01	0.94
HM+6	35	0	0	0.14	6.31E-01	N/A	N/A	N/A	N/A
HM+8	37	0	0	0.14	6.31E-01	N/A	N/A	N/A	N/A

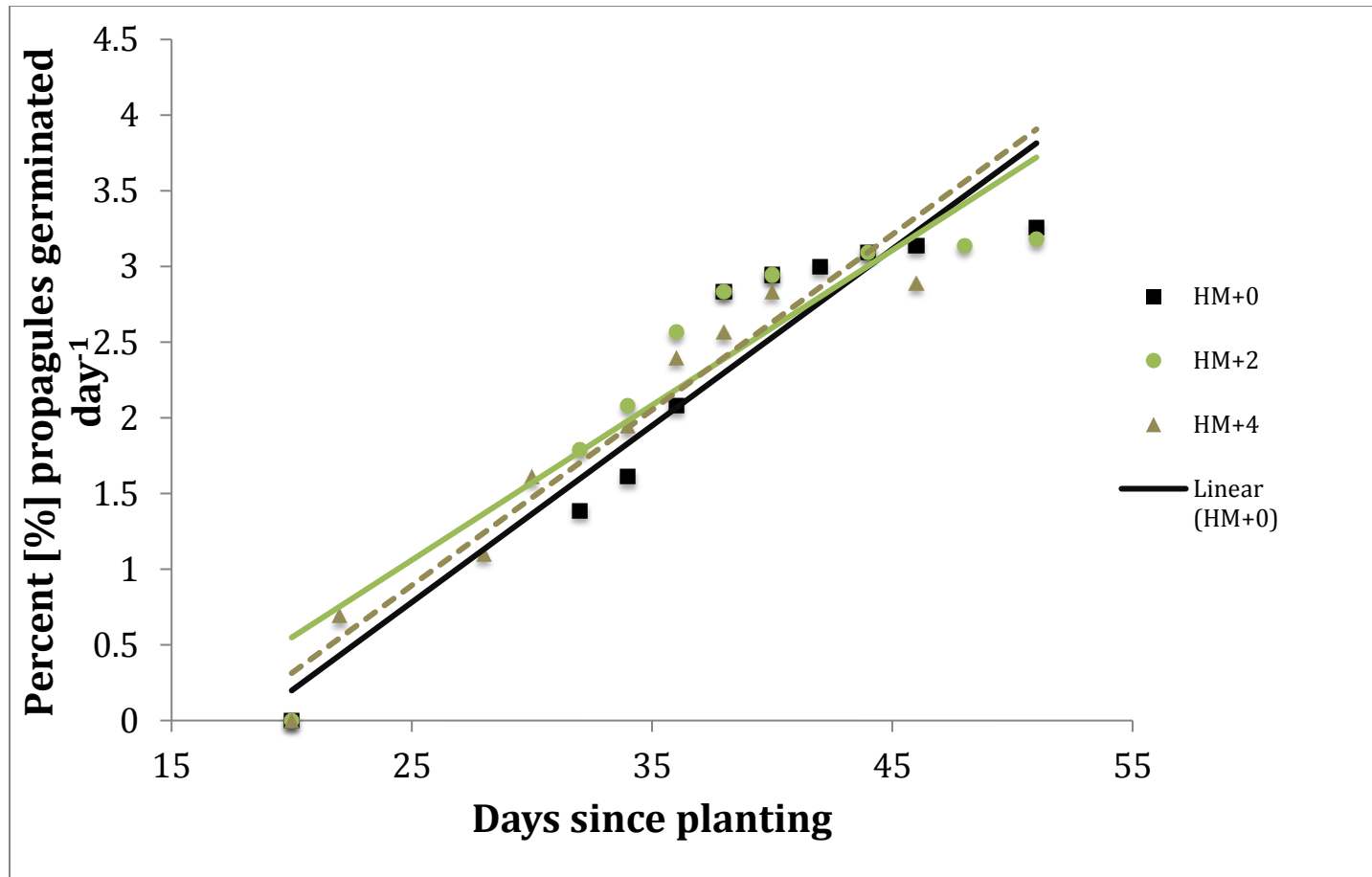


Figure 4.2. Germination rates as the percentage of propagules that germinated day⁻¹, across treatments that germinated. Least squares linear regressions were run on the natural logarithm of propagules germinated to give the following rates and R² values: HM+0: 11.7 % (R²=0.90), HM+2: 10.2% (R²=0.86), and HM+4: 11.6% (R²=0.94) [propagules germinated day⁻¹].

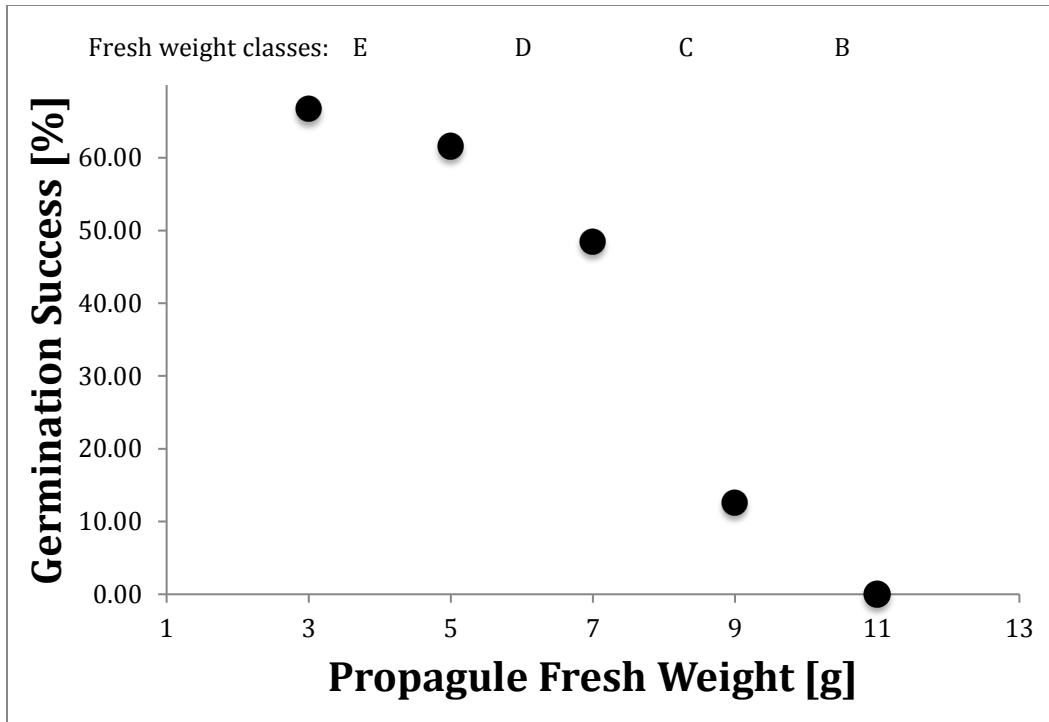


Figure 4.3. Germination success [%] across propagule weight classes. Exact ranges of fresh weight [g]: A = 10.0-11.9, B = 8.0-9.9, C = 6.0-7.9, D = 4.0-5.9, E = 2.0-3.9. X-axis shows the mid-point of the weight ranges.

Among the pooled treatments, exclusive of +6 and +8 °C above current temperatures, germination success decreased with increasing propagule size, with the highest success (66.67%) among the smallest propagules weighing 2.0 – 3.9 g (Figure 4.3). The next smallest weight class [D], weighing 4.0 – 5.9 g had a 61.54% success and class [C], weighing 6.0 – 7.9 g had 48.39% success (Figure 4.3). The largest propagules in weight classes [A] (10.0-11.9 g) and [B] (8.0-9.9 g), had a 0 and 12.50 % germination success respectively (Figure 4.3).

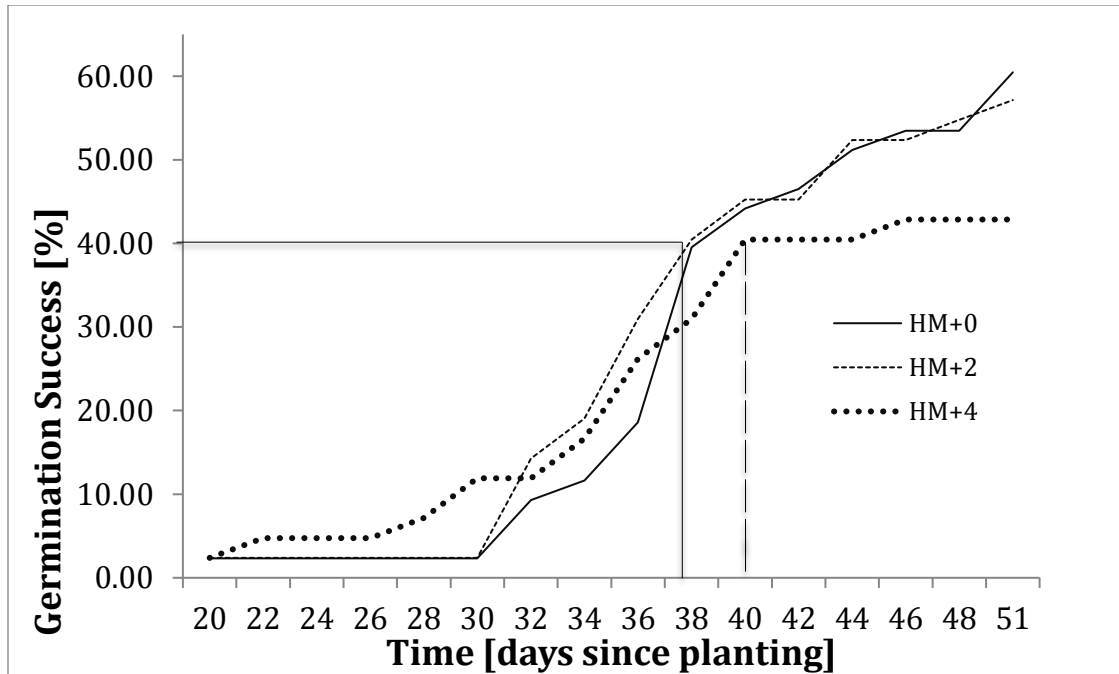


Figure 4.4. Time at which 40% of propagules reached germination (T_{40}). Solid line refers to treatments HM+0 and HM+2 (day 38), dashed line refers to HM+4 (day 40).

The number of days for 50% of the population to germinate (T_{50}) is another measure of germination success (Soltani et al. 2015). However, only the plants grown under the current thermal regime and 2 °C above the current mean air temperature reached T_{50} , thus we used T_{40} instead, as a comparative measure. Treatments, HM+0 and HM+2 reached T_{40} on day 38 while plants exposed to 4 °C above present temperature reached T_{40} on day 40 (Figure 4.4), and those exposed to warmer temperatures died before germinating.

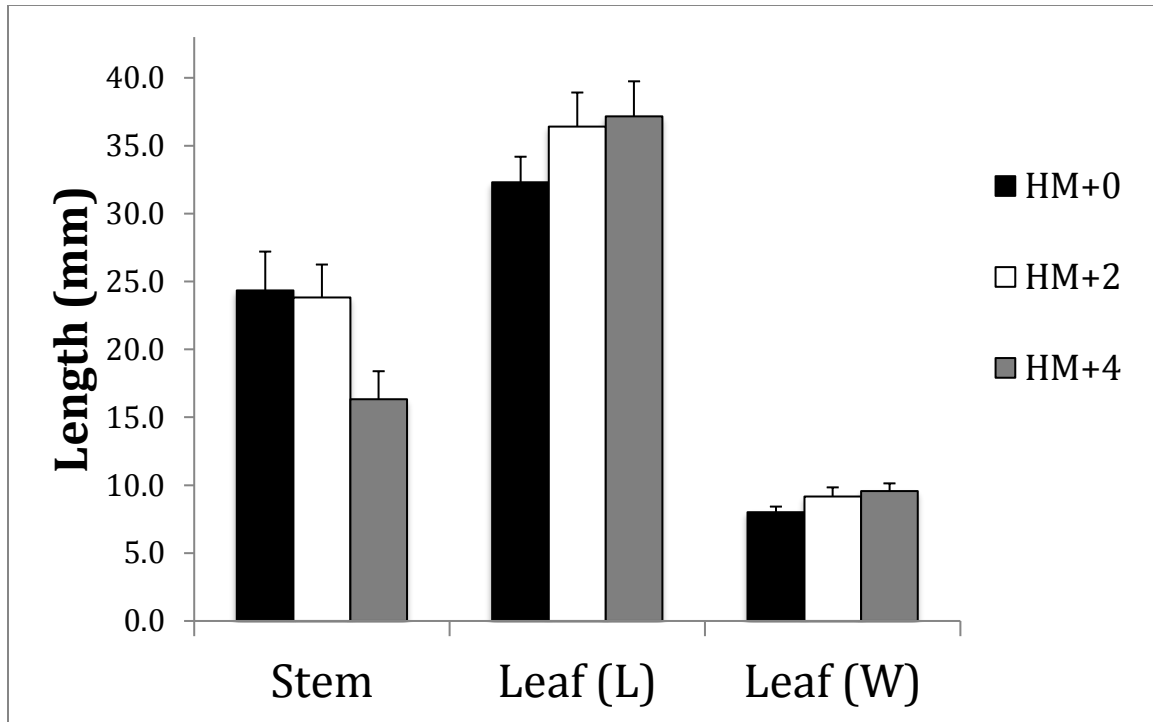


Figure 4.5. Total length of seedling parts in temperature treatments where seedling development was achieved. Error bars refer to standard deviation. One-way ANOVA's were performed on each parameter group and found no significant differences among the three treatments. Results of ANOVA's are as follows: Stem: $p = 0.08$, $F = 2.7$, $df = 2$. Leaf (L): $p = 0.27$, $F = 1.3$, $df = 2$. Leaf (W): $p = 0.13$, $F = 2.1$, $df = 2$. (L) = length, (W) = width.

Seedlings at lower temperatures grew taller than those grown at +4 °C above current temperature while leaf area remained similar across temperature treatments, except for a weak tendency for plants grown at +4 °C above current temperature to develop wider leaves than those at current temperature. Biomass production of *A. marina* seedlings was fairly uniform across all treatments, with roots becoming larger at warmer thermal regimes ($2\text{ °C} < T < 6\text{ °C}$) than currently experienced by the plants (Dunn's $p < 0.05$, Table 4.5).

Table 4.5. Biomass production of *Avicennia marina* seedlings grown at different temperatures. Values are means of 42 - 43 replicates \pm S.E. P-values in bold are less than 0.05.

Treatment	Dry weight [g]			Kruskal-Wallis rank sum test			Dunn's Test for		
	HM+0	HM+2	HM+4	chi-square	df	p-value	Comparison	Z	p-value
Leaves	0.08 \pm 0.01	0.12 \pm 0.01	0.09 \pm 0.01	1.9854	2	0.3706	HM0 - HM2	-3.15	0.005
Body and stem	1.86 \pm 0.11	1.96 \pm 0.13	1.79 \pm 0.13	1.0107	2	0.6033	HM0 - HM4	-2.56	0.021
Roots	0.16 \pm 0.01	0.22 \pm 0.01	0.21 \pm 0.01	11.34	2	0.0034	HM2 - HM4	0.50	0.620
Whole	2.09 \pm 0.12	2.28 \pm 0.13	2.07 \pm 0.13	2.2136	2	0.3306			

4.5. Discussion

The results presented show that the thermal limit of *A. marina* propagules in the Central Red Sea is between 33 and 35 °C (Figure 4.1), with a high likelihood of mortality before initiating roots at warmer temperatures. *A. marina* propagules are metabolically active upon shedding of their pericarp to proceed rapidly to germination (Pammenter et al. 1984; Farrant et al. 1993). Due to this heightened metabolic activity, their carbon and water requirements increase, which may be compromised under excess temperature (Pammenter et al. 1984). This is likely due to the inhibition of normally regulated mechanisms controlling oxygen radicals produced during oxidative metabolism and respiration (Leprince et al. 1999; Greggains et al. 2001). It is unclear from our study, whether the thermal limit is due solely to temperature or if elevated temperature also caused desiccation. That *A. marina* propagules were resistant to warming up to 4 °C above current values in the Central Red Sea, is consistent with the extensive distribution of *A. marina* at warmer regimes experienced in the Southern Red Sea (Almahasheer et al. 2016a). For instance, the average T_{max} in Jizan, in the Southern Red Sea, during the time of *A. marina* germination, is 33 °C, which is 4 °C above the T_{max} in Thuwal and corresponds, therefore, to the HM+4 treatment in our experiment. However, thermal regimes 6 °C above those in the Central Red Sea are not experienced in the Red Sea and, if reached with further warming, would lead to catastrophic mortality of early stages of *A. marina*, conducive to a population bottleneck.

The timing of early developmental stages is likely important not only for the mangroves themselves but for the rest of the organisms and processes that depend

on them. Whereas the propagules were relatively resilient to warming up to 4 °C above current values, subtle effects still emerged in the timing of some early development stages within that temperature range (Table 4.3). Warming up to 4 °C above current values temperatures caused pericarps to shed slightly later (Table 4.3). This could be because hotter treatments might have experienced slightly drier conditions. Germination was observed earlier in the hottest successful treatment (HM+4) (Table 4.3). Metabolic and developmental processes are accelerated with increased temperature (Brown et al. 2004). Also, some propagules in the hottest treatments (HM+6 and HM+8) initiated roots before perishing and they did so in 12.4 ± 1.4 days, earlier than observed in treatments with cooler thermal regimes (> 13 days, Table 4.3). Again, early propagule development is accelerated with warming, but young roots are unable to survive past this stage at temperatures > 4 °C above current values, indicating that failure of root initiation under excessive temperature might be the critical bottleneck stage of *A. marina* leading to failure under excessive temperature and setting its thermal limits. Indeed, the phase between shedding of the pericarp and root initiation is also the obligate phase of dispersal as well as a particularly vulnerable time, as the embryo is completely exposed (Clarke 1993).

Germination rates were similar across treatments with moderate warming up to 4 °C above current values (Figure 4.2, Table 4.4) with 43 to 61% of the plants germinating. While propagules and seedlings are able to tolerate high temperatures, as evidenced by their successful germination, present day mean temperatures seem more favorable to overall success. This is consistent with the expectation that

organisms should be adapted to the long-term thermal regimes where they occur (e.g. Compton et al. 2007). Although our results show that the propagules will be resistant to warming up to 4 °C above current values, which encompasses the scenarios envisaged for the 21st century (Rhein et al. 2013), rapid warming in the Red Sea region, occurring faster than the global average (Chaidez et al. 2017), will challenge the plants. The thermal limits for *A. marina* propagule development may be met in the Southern Red Sea, where temperatures are already warmer, perhaps representing a bottle neck for the future stability of *A. marina* populations therein. Conversely, warming may allow expansion of *A. marina* north of its current distributional limit, at 28.21° North, in the Northern Red Sea (Galal 2007; Hickey et al. 2017), although current assessments concluded that there is no evidence that mangroves, unlike other marine biota, have experienced a poleward displacement of their latitudinal limits (Hickey et al. 2017). In the warmer, southern range of *A. marina*, adaptation to warming may provide a stronger selection pressure for more heat tolerant phenotypes. Our experimental work suggests that the more heat-tolerant phenotype may be a plant producing small and lightweight propagules, as these had the highest germination success (Figure 4.3).

We observed a general trend of larger leaves accompanying shorter stems with increasing temperature (Figure 4.5). This might be due to stress and a consequent reallocation of resources. As the organism is under more thermal stress, the photosynthetic product may be allocated to support metabolic processes conferring resistance to warming, thereby being driven to maintain homeostasis rather than allocating extra energy and materials to support upward growth. This is consistent

with observations that extreme temperature, beyond the optimum for plant development, typically results in suppressed growth (Niu et al. 2014; Hatfield and Prueguer 2015), including direct effects on plant performance, and indirect effects through impacts to the soil microbiota and associated processes (Yang et al. 2009). While leaf area was similar across treatments, the shorter stem length observed under warming by 4 °C above current values, may indicate at thermal stress, contributing to stunted growth (Figure 4.5). Dwarf stature of 2 – 3 meters, is already a characteristic of *A. marina* in the Central Red Sea, and has been attributed to nutrient limitation and lack of alluvial soils (Mandura et al. 1987; Almahasheer et al. 2016b). The stark contrast to its counterparts in the warmer, Southern Red Sea, which can grow higher than 14 meters, indicates that temperature alone, does not account for less growth, but may still add stress. Our results also suggest that seedlings shift their allocation for growth to invest more in their root systems under thermal stress (Table 4.5). This plasticity in growth and phenotype will likely continue to allow *A. marina* to cope with warming in the future, until the critical warming of > 4 °C above present values may be reached.

There is no long-term record on the flowering and fruiting seasons of *A. marina* on the Saudi Arabian Red Sea coast. According to a publication that surveyed the Central Red Sea in the 1980's, young fruit appeared on adult *A. marina* trees in March and flowers bloomed throughout June, July, and August (Mandura et al. 1987). Since then, a 16 month study from 2014 to 2015, quantitatively measured that the peak abscission season was during January and February and observed a clear annual reproductive cycle of 12 months (Almahasheer et al. 2016c). In the two

years our study was undertaken (2016 and 2017), mature propagules had fallen from trees also during January and February. It is important to consider the effects of mother plant status and the influence of higher temperatures on flowering and bud development, which in the Central Red Sea has been observed to occur July through September (Almahasheer et al. 2016c). Almahasheer et al. (2016c) also showed that as the temperature increases during the summer, so does flower and bud production, which suggests future shifts in phenology patterns with warming; although it is likely that photoperiod, and not temperature conditions, may trigger flowering, as suggested by the variation of mangrove reproductive cycles across latitudes (Duke et al. 1984; Duke 1990; Wang'ondou et al. 2010).

While it may be unlikely that future warming will reach as high as 6 °C above present temperatures, such extreme temperatures may occur during heat waves. If such high temperatures occur at the time of propagule abscission, and are maintained for several weeks, even with high humidity, the propagules may experience necrosis. Heat anomalies and the annual timing of temperature maxima is also important for population recruitment as, unlike terrestrial plants, *A. marina* propagules have no dormant stage and are prepared to germinate upon abscission (Clarke 1993). Higher temperature also increases salinity in coastal areas due to higher evaporation rates, with higher salinity stunting mangrove growth and decreasing germination (Ye et al. 2005).

4.5.1 Conclusions

A. marina propagules in the Central Red Sea have a high thermal capacity as evidenced by their successful establishment at 4 °C above present day conditions.

Increased temperature will accelerate all metabolic processes including germination and growth up to a certain threshold whereupon elevated temperature may be detrimental to seedling establishment. Their experimentally-determined thermal limit lies between 33 to 35 °C, > 4 °C above present temperatures at the time of propagule germination, and seem to affect the critical root initiation and dispersal phase. As global temperatures continue to rise, *A. marina* will likely be under selection for smaller propagules at the initial life stage and show phenotypic plasticity in stunted growth. Still, from the stressors that currently plague mangroves, and of those that are coming, *A. marina* seems to emerge as an ideal forerunner in the grand trial of adaptation to a warmer Red Sea.

4.6. References

- Almahasheer H, Aljowair A, Duarte CM, Irigoien X (2016a) Decadal stability of Red Sea mangroves. *Estuarine, Coastal and Shelf Science* 169:164–172
- Almahasheer H, Duarte CM, Irigoien X (2016b) Nutrient limitation in Central Red Sea mangroves. *Frontiers in Marine Science* 3:271
- Almahasheer H, Duarte CM, Irigoien X (2016c) Phenology and growth dynamics of *Avicennia marina* in the Central Red Sea. *Scientific Reports* 6:37785
- Alongi DM (2002) Present state and future of the world's mangrove forests. *Environmental conservation* 29:331-349
- Alongi DM (2008) Mangrove forests: resilience, protection from tsunamis, and responses to global climate change. *Estuarine, Coastal and Shelf Science* 76:1-13
- Ateweberhan MJ, Bruggemann H, Breeman AM (2005) Seasonal dynamics of *Sargassum ilicifolium* (Phaeophyta) on a shallow reef flat in the southern Red Sea (Eritrea). *Marine Ecology Progress Series* 292:159-171
- Ball M, Cowan IR, Farquhar GD (1988) Maintenance of leaf temperature and the optimisation of carbon gain in relation to water loss in a tropical mangrove forest. *Functional Plant Biology* 15:263-276

- Berjak P, Farrant JM, Pammenter NW (1989) The basis of recalcitrant seed behaviour: cell biology of the homoiohydrous seed condition. In: Recent advances in the development and germination of seeds. (eds Taylorson RB), pp. 89-108. New York, London, Plenum Press
- Bjorkman O, Demmig B, Andrews TJ (1988) Mangrove photosynthesis: response to high-irradiance stress. *Functional Plant Biology* 15:43-61
- Bouillon S, Borges AV, Castaneda-Moya E, Diele K, Dittmar T, Duke NC, Kristensen E, Lee SY, Marchand C, Middelburg JJ, Rivera-Monroy VH (2008) Mangrove production and carbon sinks: A revision of global budget estimates, *Global Biogeochem. Cycles*, 22:GB2013, doi:10.1029/2007GB003052
- Brown JH, Gillooly JF, Allen AP, Savage VM, West GB (2004) Toward a metabolic theory of ecology. *Ecology* 85(7):1771-1789
- Carney J, Gillespie TW, Rosomoff, R (2014) Assessing forest change in a priority West African mangrove ecosystem: 1986-2010. *Geoforum* 53:126-135
- Chaidez V, Dreano D, Agusti S, Duarte CM, Hoteit I (2017) Decadal trends in Red Sea maximum surface temperature. *Scientific Reports* 7:8144
- Clarke PJ (1993) Dispersal of grey mangrove (*Avicennia marina*) propagules in southeastern Australia. *Aquatic Botany* 45:195-204
- Clarke A, Johns L (2002) Mangrove nurseries: Construction, propagation and planting. Queensland Department of Primary Industries
- Clough BF (1984) Growth and salt balance of the mangroves *Avicennia marina* (Forsk.) Vierh. and *Rhizophora stylosa* Griff. in relation to salinity. *Functional Plant Biology* 11:419-430
- Compton TJ, Rijkenberg MJA, Drent J, Piersma T (2007) Thermal tolerance ranges and climate variability: A comparison between bivalves from differing climates. *Journal of Experimental Marine Biology and Ecology* 352:200-211
- Documenta Geigy. (1965) *Tablas Cientificas*. Geigy S.A., Basel.
- Duarte CM, Losada IJ, Hendriks IE, Mazarrasa I, Marba N (2013) The role of coastal plant communities for climate change mitigation and adaptation. *Nature Climate Change* 3:961-968
- Duke N, Bunt J, Williams W (1984) Observations on the floral and vegetative phenologies of north-eastern Australian mangroves. *Australian Journal of Botany* 32:87-99

- Duke N (1990) Phenological trends with latitude in the mangrove tree *Avicennia marina*. *The Journal of Ecology* 113–133
- Duke NC (1995) Genetic diversity, distributional barriers and rafting continents—more thoughts on the evolution of mangroves. *Asia-Pacific Symposium on Mangrove Ecosystems*, Springer Netherlands
- Galal N (2007) National Action Plan for the Conservation of Mangroves in Egypt. Ministry of Agriculture and Land Reclamation, Egyptian Government, Egypt. p 469
- Hatfield JL, Prueger JH (2015) Temperature extremes: effect on plant growth and development. *Weather and Climate Extremes* 10:4-10
- Hickey SM, Phinn SR, Callow NJ, Van Niel KP, Hansen JE, Duarte CM (2017) Is climate change shifting the poleward limit of mangroves? *Estuaries and Coasts* 40:1215–1226
- Farrant JM, Pammenter NW, Berjak P (1993) Seed development in relation to desiccation tolerance: A comparison between desiccation-sensitive (recalcitrant) seeds of *Avicennia marina* and desiccation-tolerant types. *Seed Science Research* 3:1-13
- Ganguly D, Dey M, Mandal SK, De TK, Jana TK (2008) Energy dynamics and its implication to biosphere–atmosphere exchange of CO₂, H₂O and CH₄ in a tropical mangrove forest canopy. *Atmospheric Environment* 42:4172-4184
- Greggains V, Finch-Savage WE, Atherton NM, Berjak P (2001) Viability loss and free radical processes during desiccation of recalcitrant *Avicennia marina* seeds. *Seed Science Research* 11:235-242
- Leprince O, Buitink J, Hoekstra FA (1999) Axes and cotyledons of recalcitrant seeds of *Castanea sativa* Mill. exhibit contrasting responses of respiration to drying in relation to desiccation sensitivity. *Journal of Experimental Botany* 50:1515-1524
- Mandura AS, Saifullah SM, Khafaji AK (1987) Mangrove ecosystem of southern Red Sea coast of Saudi Arabia. *Proceedings of the Saudi Biological Society* 10:165-193
- Miller PC (1972) Bioclimate, leaf temperature, and primary production in red mangrove canopies in South Florida. *Ecology* 53:22–45

- Mumby PJ, Edwards AJ, Arias-Gonzalez JE, Lindeman KC, Blackwell PG, Gall A, Gorczynska MI, Harborne AR, Pescod CL, Renken H, Wabnitz CC (2004) Mangroves enhance the biomass of coral reef fish communities in the Caribbean. *Nature* 427:533-536
- Niu S, Luo Y, Li D, Cao S, Xia J, Li J, Smith MD (2014) Plant growth and mortality under climatic extremes: an overview. *Environmental and Experimental Botany* 98:13-19
- Owen RK, Forbes AT (1997) Salinity, floods and the infaunal macrobenthic community of the St. Lucia estuary, KwaZulu-Natal, South Africa. *Southern African Journal of Aquatic Science* 23:14-30
- Pammenter NW, Farrant JM, Berjak P (1984) Recalcitrant seeds: short-term storage effects in *Avicennia marina* (Forsk.) Vierh. may be germination-associated. *Annals of Botany* 54:843-846
- Purnobasuki H, Utami ESW (2017) Seed germination of *Avicennia marina* (Forsk.) Vierh. by pericarp removal treatment. *BIOTROPIA-The Southeast Asian Journal of Tropical Biology* 23:75-84
- Ranal MA, Garcia de Santana D (2006) How and why to measure the germination process? *Brazilian Journal of Botany* 29:1-11
- Rhein, M., S. R. Rintoul, S. Aoki, E. Campos, D. Chambers, R. A. Feely, S. Gulev, G. C. Johnson, S. A. Josey, A. Kostianoy, C. Mauritzen, D. Roemmich, L. D. Talley, and F. Wang (2013), Observations: ocean. In: *Climate Change 2013: the physical science basis. Contribution of Working Group I to the Fifth Assessment Report of the Intergovernmental Panel on Climate Change* (T. F. Stocker, D. Qin, G.-K. Plattner, M. Tignor, S. K. Allen, J. Boschung, A. Nauels, Y. Xia, V. Bex, and P. M. Midgley, eds.), Cambridge University Press, Cambridge, United Kingdom and New York, NY, USA.
- Saifullah SM (1996) Mangrove ecosystem of Saudi Arabian Red Sea coast – an overview. *Marine Sciences-Ceased Issuerg* 17:1-2
- Scholander PF, Van Dam L, Scholander SI (1955) Gas exchange in the roots of mangroves. *American Journal of Botany* 42:92-98
- Soltani E, Ghaderi-Far F, Baskin CC, Baskin JM (2015) Problems with using mean germination time to calculate rate of seed germination. *Australian Journal of Botany* 63:631-635

- Tomlinson PB (1986) The botany of mangroves. Cambridge tropical biology series.
- Valiela I, Bowen JL, York JK (2001) Mangrove forests: one of the world's threatened major tropical environments. *Bioscience* 51:807-815
- Tuan MS, Ninomiya I, Ogino K (1996) Effect of different levels of external salinity on germination, growth and photosynthesis in a mangrove, *Avicennia marina*. *Tropics* 6:39-50
- Wang'ondu, VW, Kairo JG, Kinyamario JI, Mwaura FB, Bosire JO, Dahdouh-Guebas F, Koedam N (2010) Phenology of *Avicennia marina* (Forsk.) Vierh. in a disjunctly-zoned mangrove stand in Kenya. *Western Indian Ocean Journal of Marine Science* 9:135-144
- Wong PP, Losada IJ, Gattuso JP, Hinkel J, Khattabi A, McInnes KL, Saito Y, Sallenger A, (2014) Coastal systems and low-lying areas. In: *Climate Change 2014: Impacts, Adaptation, and Vulnerability. Part A: Global and Sectoral Aspects. Contribution of Working Group II to the Fifth Assessment Report of the Intergovernmental Panel on Climate Change* [Field, C.B., V.R. Barros, D.J. Dokken, K.J. Mach, M.D. Mastrandrea, T.E. Bilir, M. Chatterjee, K.L. Ebi, Y.O. Estrada, R.C. Genova, B. Girma, E.S. Kissel, A.N. Levy, S. MacCracken, P.R. Mastrandrea, and L.L.White (eds.)]. Cambridge University Press, Cambridge, United Kingdom and New York, NY, USA, pp. 361-409
- Yang J, Kloepper JW, Ryu C (2009) Rhizosphere bacteria help plants tolerate abiotic stress. *Trends in Plant Science* 14:1-4
- Ye Y, Tam NF, Lu CY, Wong YS (2005) Effects of salinity on germination, seedling growth and physiology of three salt-secreting mangrove species. *Aquatic Botany* 83:193-205
- Zpevak FA, Güaltieri de Perez SCJ, Buckeridge MS. (2012) Isothermal seed germination of *Adenanthera pavonina*. *Brazilian Journal of Botany* 35:401-408

CHAPTER III

5. Thermal thresholds of Central Red Sea zooplankton

Veronica Chaidez¹, Stamatina Isari¹, Gauri A. Mahadik¹, Mohsen M. O. El-Shirbiny²,
Gopikrishna Mantha², Reny Devassy², Sathianeson Satheesh², Ali M. Al-Aidaros²,
Susana Agusti¹, and Carlos M. Duarte^{1,2}

¹King Abdullah University of Science and Technology (KAUST), Red Sea Research
Center (RSRC), Thuwal, 23955-6900, Saudi Arabia.

²King Abdulaziz University, Faculty of Marine Sciences, Department of Marine
Biology, Jeddah, 21589, Saudi Arabia.

This manuscript is prepared for submission to

PloS one

Chaidez V, Isari S, Mahadik GA, El-Shirbiny MM, Mantha G, Devassy R, Satheesh S, Al-
Aidaros AM, Agusti S, Duarte CM (in prep) Thermal thresholds of Central Red Sea
zooplankton

5.1. Abstract

Zooplankton, which compose a critical group in the oceanic food web, may see changes in its community due to the sensitivity to higher temperature on the individual. Our study experimentally assessed the thermal capacity of the most common groups found in the warm-season, zooplankton community of the Central Red Sea, including several genera of copepods, an ostracod, and two stages of crab development. As stress is reduced with the input of adequate energy, some experiments included algal food as an added variable and we compared the difference that the addition of food made on mortality. Our results delineated thermal limits ranging from 30 to 36 °C, a range of temperature often exhibited in the Central Red Sea. Smaller bodied organisms had higher mortality rates than larger counterparts, and were more sensitive to the addition of food. The effect of food most noticeably buffered mortality at the highest temperatures. These results indicate that the most common groups of Central Red Sea zooplankton may be vulnerable to warming.

5.2. Introduction

Climate change and ocean warming are affecting marine ecosystems through impacts on organismal performance and biogeographical ranges (Poloczanska et al. 2014), with the ocean expected to warm between 1.5 and 4.0 °C by the end of the 21st century (Rhein et al. 2013). These impacts can propagate through food webs through changes in the strength of trophic interactions and the decoupling of prey-predator phenological relationships (Edwards and Richardson 2004; Freitas et al. 2007; Tewksbury et al. 2008). Zooplankton play a key role in marine ecosystems as

a link between primary producers and upper trophic levels (Ikeda 1985; Calbet 2001). Zooplankton also play a major role in the oceanic biological carbon pump, by packaging organic carbon into rapidly-sinking fecal pellets (Fowler and Small 1972; Turner and Ferrante 1979; Turner 2015). Hence, understanding the impacts of ocean warming on zooplankton is particularly relevant to predict the response of oceanic ecosystems to climate change. Specifically, copepods often make up a significant portion of biomass among marine zooplankton (Mauchline 1998; Planque and Batten 2000; Saiz et al. 2013), and as ectotherms, are highly sensitive to changes in temperature (Loosanoff 1958; Hwang et al. 2010). It is therefore, important to assess the effects of warming on copepods as these organisms are often considered sentinels for climate change.

A first step to understanding the direct effects of warming on marine organisms is to experimentally resolve the thermal performance curves and, particularly, the thermal optima and upper thermal limits of species (Frietas et al. 2007; Boyd et al. 2013). While many studies have looked at the effects of warming on zooplankton communities (Ikeda 1985; Müren et al. 2005; Coyle et al. 2008; Alcaraz et al. 2013a; Lewandowska et al. 2014), the upper thermal limits have been resolved for only a few species (Gonzalez 1974; Lee et al. 2003; Willett 2010; Alcaraz et al. 2013b).

The Red Sea, the warmest of all seas, exhibiting maximum surface temperatures up to 35 °C (Bethoux 1988; Raitsos et al. 2013; Sawall et al. 2014; Chaidez et al. 2017), offers a particularly relevant case to understand the upper thermal limits of marine zooplankton species and the upper scope of their resistance to ocean warming. Due to the Red Sea's extreme maximum temperatures, it is likely that zooplankton may

be operating at or above their thermal optima, and perhaps even close to their upper thermal limits (Thomas et al. 2012; Sawall et al. 2014). Yet, no study has yet assessed the upper thermal limits of copepods or other zooplankton of the Red Sea. In addition to extreme temperature, the Red Sea also displays extreme oligotrophy (Raitsos et al. 2013; Kurten et al. 2015); so that zooplankton lack access to the abundant energy sources they require in order to deploy resistance mechanisms against heat stress, such as greater oxygen consumption, synthesis of heat shock proteins, and the upregulation of genes involved in ubiquitination and proteolysis (Schoville et al. 2012; Lehette et al. 2016; Rahlff et al. 2017).

This study aims to elucidate the thermal performance curve, thermal optima, and thermal limits of the common zooplankton taxa in the Central Red Sea. We did so by experimentally resolving, during the warm period of the year, the mortality rates at a range of temperatures of seven copepod genera, one ostracod genus, and two stages of crab development. We also tested the hypothesized role of food supply in affecting the response of zooplankton to thermal stress.

5.3. Materials and Methods

5.3.1. Collection

The experiments were conducted along two consecutive years, including experiments testing zooplankton mortality rates across a range of temperature, and where zooplankton mortality was compared in the presence and absence of food supply (Table 5.1). Live zooplankton specimens used for the experiments were collected from different habitats and times of the day in coastal waters around King Abdullah University of Science and Technology (Table 5.1). Sampling was done by

oblique horizontal tows with a 200 μm net and a large, 20 L, plastic bag at the cod end, to avoid pressure damages on the animals, and towed at about 1 knot. Animals were immediately transferred to buckets and placed in cooling boxes to avoid heat stress while being transported to the laboratory, where sorting began immediately at laboratory temperature (23 $^{\circ}\text{C}$). Upon inspection of the samples, the most abundant species were selected for the experiment, and sorted under stereomicroscopes using Pasteur pipettes. Sorted animals were then placed in filtered (0.2 μm) seawater collected daily from the sampling site.

1 Table 5.1. Zooplankton species, and developmental stages, tested in experiments conducted in 2016 and 2017.
 2 Asterisks denote experiments where survival responses to temperature were observed both in the presence and
 3 absence of food supply versus no asterisks denoting experiments where survival was tested in the absence of food
 4 alone.

Experiment	Depth [m]	Habitat	Max depth [m]	Month and Year	Time of day	Latitude	Longitude
<i>Acartia</i> sp. (2016)	5	Coastal lagoon	7	Aug 2016	Mid-morning	22.38979	39.135547
<i>Acartia</i> large sp.*	20-25	Pelagic	50	May 2017	Mid-morning	22.25285	38.96122
<i>Acartia</i> small sp.*	20-25	Pelagic	50	May 2017	Mid-morning	22.25285	38.96122
<i>Candacia</i> sp.	5	Coastal lagoon	7	May 2017	Sunset	22.38979	39.135547
<i>Centropages</i> sp.*	25	Pelagic	50	Aug 2016	Before sunrise	22.25285	38.96122
<i>Corycaeus</i> sp.	25	Pelagic	50	Aug 2016	Before sunrise	22.25285	38.96122
Crab Megalopa	5	Coastal lagoon	7	May 2017	Sunset	22.38979	39.135547
Crab Zoea	<10	Pelagic	50	Aug 2016	Early morning	22.38979	39.135547
<i>Ostracod</i> sp.	25	Pelagic	50	Aug 2016	Before sunrise	22.25285	38.96122
<i>Paracalanus</i> sp.	<10	Pelagic	50	Aug 2016	Early morning	22.38979	39.135547
<i>Tortanus</i> sp.	5	Coastal lagoon	7	Aug 2016	Mid-morning	22.38979	39.135547
<i>Undinula</i> sp.*	20-25	Pelagic	50	May 2017	Before sunrise	22.25285	38.96122

5

5.3.2. Experiment

Twenty healthy individuals were placed into each of the 278 ml rectangular, plastic culture flasks used for each of the temperature treatments in 2016, except for *Centropages* sp., for which experiments were conducted in three 6-well culture plates (10 ml well⁻¹), containing one individual well⁻¹ for a total of 18 individuals treatment⁻¹. In 2017, four 6-well culture plates were used for each of the treatments, again, with one individual well⁻¹.

Survival was tested under eight temperature treatments, ranging from 24 to 38 °C, increasing at 2 °C intervals. In August 2016, the ambient temperature of the sampling site was 32 °C, and 30 °C in May 2017. To acclimate organisms to temperatures above the ambient temperature (*in situ* temperature), individuals were placed at the corresponding ambient temperature, and temperature was increased at 2 °C steps every hour thereafter until reaching the target experimental temperature. During the acclimation process, organisms were monitored for mortality and when individuals died during the acclimation process, they were replaced from a pool of extra live organisms. As organisms had already become acclimated to lower temperatures from being sorted in the laboratory, organisms were placed directly into treatments 24 to 30 °C. We employed temperature-controlled incubators from Percival Scientific Inc. which allowed us to control temperature and light intensity. Across all temperature treatments, light was adjusted to remain between 32 to 35 $\mu\text{E m}^{-2}\text{s}^{-1}$, matching the natural underwater light at the depth of sampling as closely as possible, with a photoperiod of 12 hours light and 12 hours dark.

Counting of living organisms took place every hour, for the first 3 to 5 hours, in the highest temperature treatments (*in situ* temperature and above) as mortality was expected to be high. After this, and for the rest of the lower temperature treatments, observations for mortality took place every two to three hours. Observations were done by placing the culture bottle or plate under the microscope and lightly tapping (in the case of the bottles) or gently prodding the individual with a small instrument (in the case of the well plates) to determine activity level. At the end of each experimental treatment, the final number of organisms, dead and alive, was counted to confirm recovery and where necessary, the initial number for the treatment (N) was corrected for consistency with the final count.

When food was supplied, we supplied *Tetraselmis* sp. cells, a large and easily grazed phytoplankton genus commonly used as aquaculture feed, to the various zooplankton groups. A stock culture of *Tetraselmis* sp. was maintained in the laboratory and from this, food suspensions were created and added *ad libitum* to each treatment based on estimations of the carbon saturation requirements corresponding to each species' size. Visual observation for the production of fecal pellets took place throughout the experiment to assure that the animals were ingesting the algae. Food was also re-added in the higher temperature treatments due to potentially increased ingestion rates.

To assess whether *Tetraselmis* sp. could survive at the highest temperatures tested here, a short thermal response experiment was conducted. Abundances were measured from *Tetraselmis* sp. cultures incubated at 26, 34, 36, and 38 °C. Each culture had an initial volume of 50 ml (*Tetraselmis* and f/2 media) from which 3 ml

of subsample was extracted under sterile conditions approximately every two hours and fixed with 1% Lugol solution (Sigma-Aldrich® 62650; St. Louis, MO, USA). To acclimate *Tetraselmis* sp., which derived from a stock culture kept at 26 °C, three culture flasks were incubated at 32 °C before being transferred to 34 °C an hour later, then to the corresponding 36 and 38 °C treatments, also every hour, until each flask was maintained at the desired temperature. Cell abundances were counted using a sedgewick rafter. Observation of the living cells under the microscope also occurred every two hours where the cell activity level was noted as either active or inactive. After ten hours, all cultures, under the four elevated temperature treatments, had actively swimming cells, thereby confirming survival of *Tetraselmis* sp. across the experimental treatments.

5.3.3. Analysis

Zooplankton mortality rates were calculated from the slope of a least squares linear regression fitted to the natural log of the number of surviving animals at each observation time vs. time (hours), multiplied by -100 to obtain mortality rates as % hr⁻¹. The optimal temperature (T_{opt} , °C) for each taxonomic group was determined from inspection of mortality vs. temperature curves, as the highest temperature preceding a steep increase in mortality. The temperature-dependence of mortality rates was parameterized as the activation energy, expressed as electronvolts (eV), calculated by fitting a least squares linear regression to the relationship between mortality rates and the product inverse of the absolute temperature (°K) and the Boltzmann's constant, following the Arrhenius model (Brown et al. 2004; Frietas et al. 2007; Dell et al. 2011; Alcaraz et al. 2013a), for experimental temperatures up to

the optimal temperature. Analysis of covariance, using general linear models, was used to determine the effect of food on the various temperature treatments, and resolve whether food had no effect, an additive effect (positive or negative), or a synergistic effect with temperature. Statistical analyses were conducted in JMP v. 13.0 (SAS Institute, 2016) with alpha set at 0.05.

5.4. Results

All taxonomic groups, except crab zoea and megalopa, reached complete population mortality before 20 hours under the warmest treatment (38 °C, Figure 5.1). One hundred percent mortality was also observed at 36 °C before 20 hours for all groups except *Acartia* sp., crab zoea, and crab megalopa (Figure 5.1). Crab megalopa had the lowest mortality throughout the whole experimental period, sustaining 0% mortality in all temperatures, except for 38 °C where mortality occurred (Figures 5.1 and 5.2); followed by crab zoea, where some individuals also survived at 38 °C (Figures 5.1 and 5.2). The larger-sized *Acartia* sp. had the lowest mortality rates across all temperatures, when compared to other *Acartia* species as well as many of the other copepod groups (Figures 5.1 and 5.2, Table 5.2). *Paracalanus* sp. and *Undinula* sp. showed the lowest mortality rates among the other copepod genera at the lowest four temperature treatments (Figures 5.1 and 5.2, Table 5.2). In general, mortality was low and similar among temperatures < 34 °C (Figures 5.1 and 5.2).

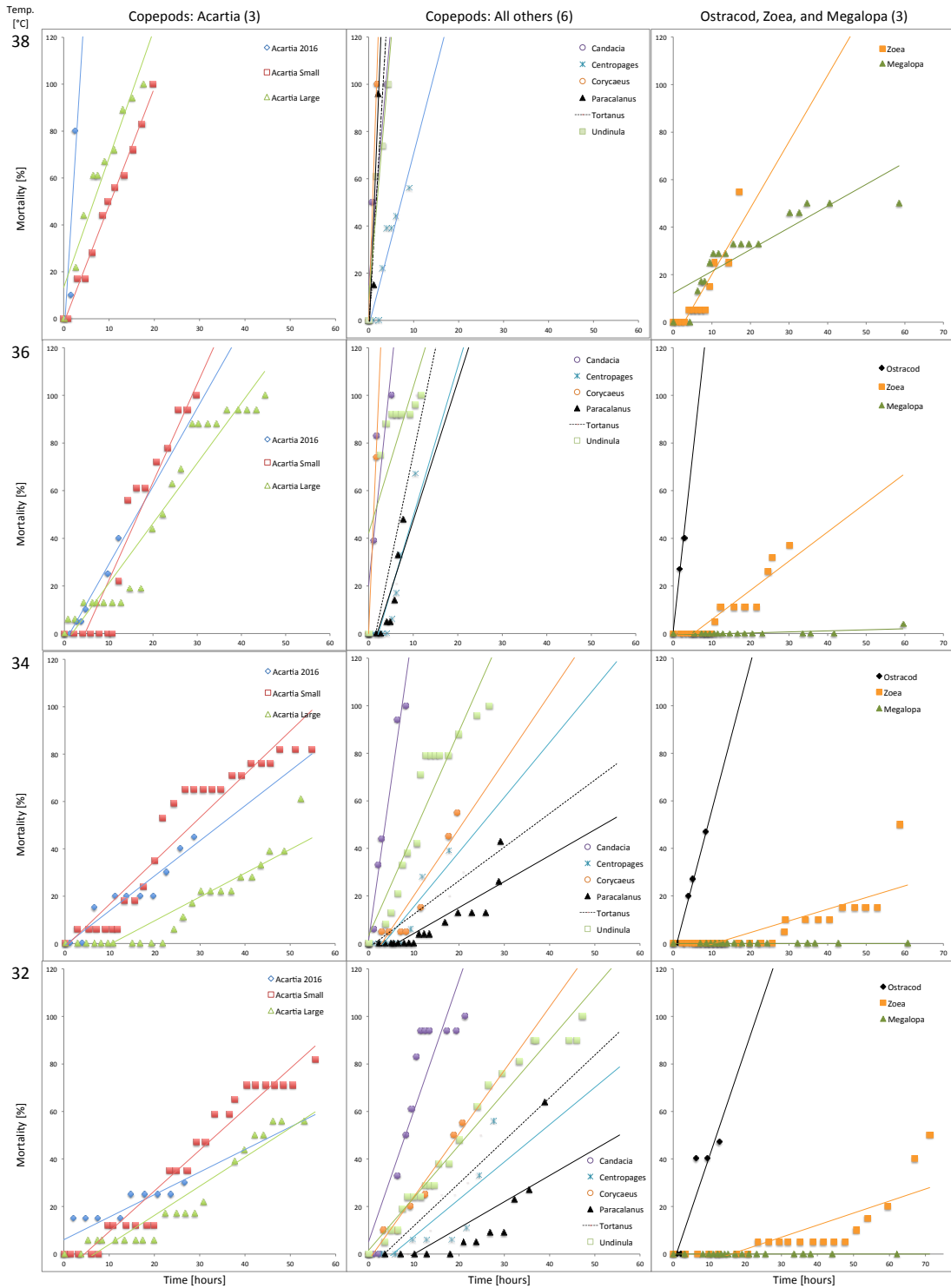


Figure 5.1. The percentage of mortality over time in temperatures *in situ* and above (32 to 38 °C) for the zooplankton taxa tested without food. Lines indicate least squares linear regression analysis and are color-coded to correspond to each taxonomic group (symbol and color designated in each legend).

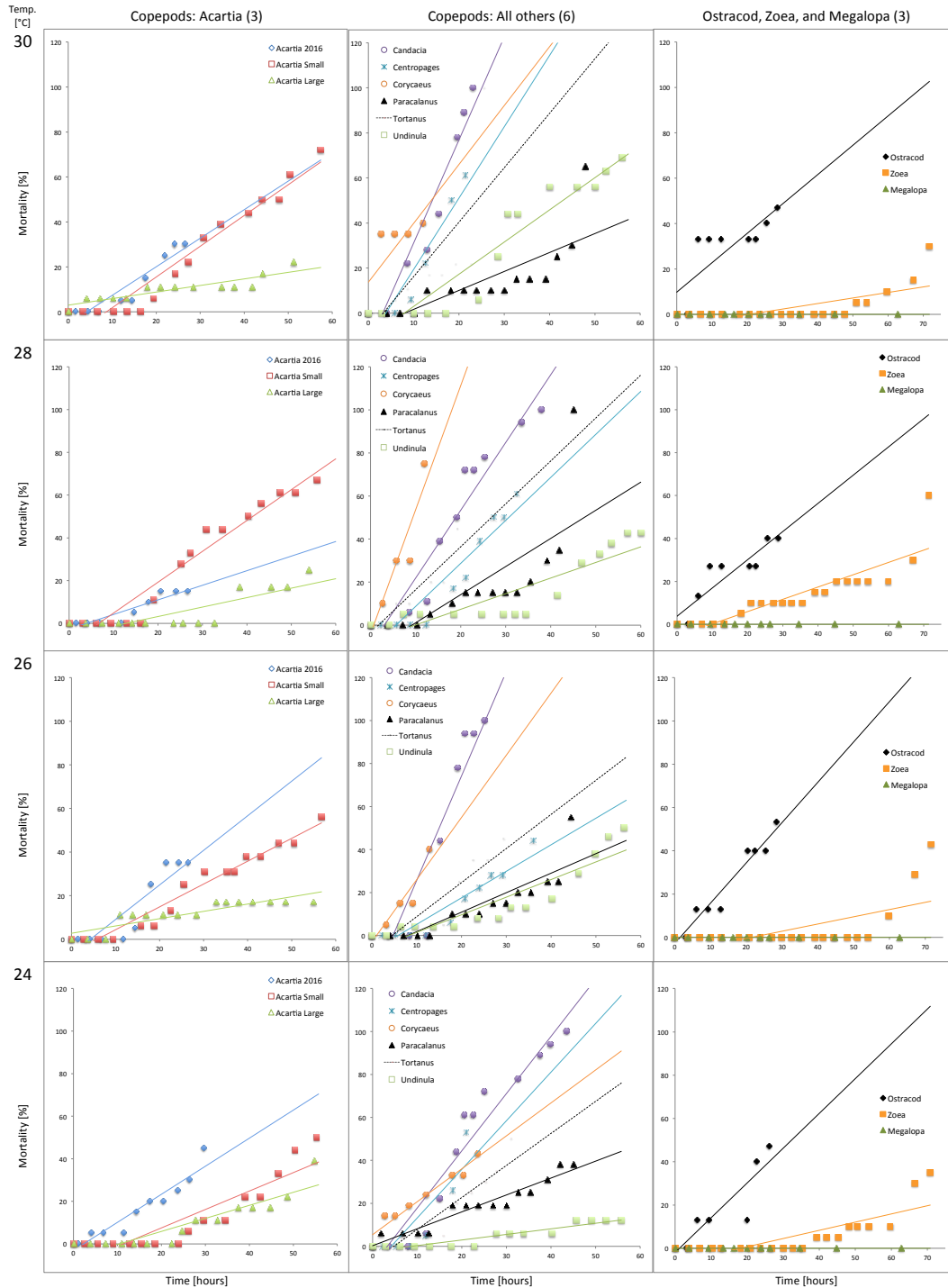


Figure 5.2. The percentage of mortality over time in temperatures below *in situ* (24 to 30 °C) for the zooplankton taxa tested without food. Lines indicate least squares linear regression analysis and are color-coded to correspond to each taxonomic group (symbol and color designated in each legend).

The addition of food led to reduced mortality and higher survivorship compared to the non-food treatments in all of the tested temperatures, except for the large-size *Acartia* sp. at 24 and 28 °C, which experienced similar mortality between food and no-food treatments (Figures 5.3 and 5.4). The steepest mortality was observed at 38 °C for both animals supplied with food, and those that did not receive food, except for the food treatment of the small-size *Acartia* sp., which showed a similar rate to the other food supply treatments at lower temperatures (Figures. 5.3 and 5.4). Across all the temperatures (except 38 °C), for the no-food treatments, small-size *Acartia* sp. had greater mortality rates than its large-size *Acartia* sp. counterpart (Figures 5.1 and 5.2, Table 5.2).

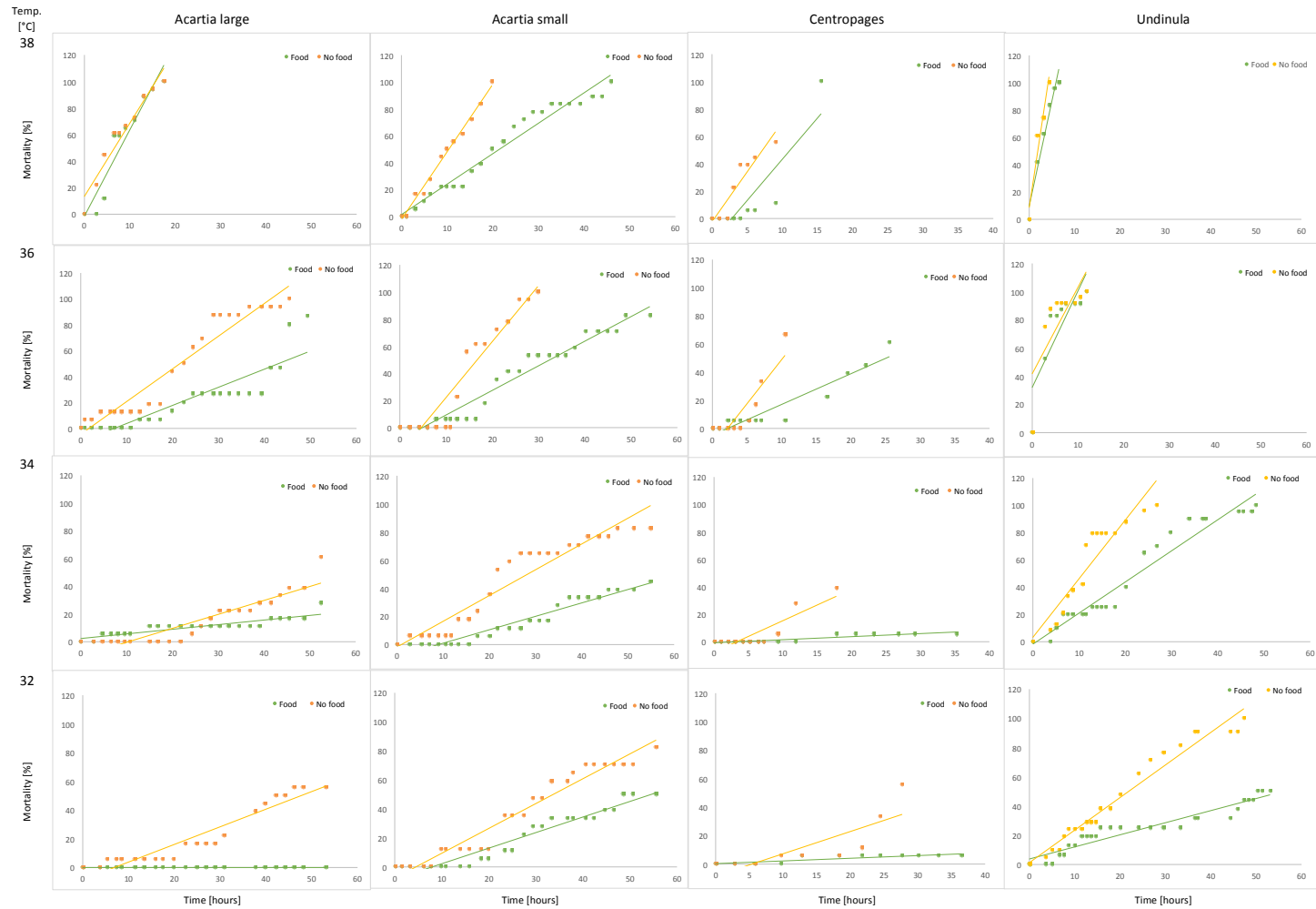


Figure 5.3. The percentage of mortality over time in temperatures *in situ* and above (32 to 38 °C) with and without food for large and small-size *Acartia* sp., *Centropages* sp., and *Undinula* sp. Lines indicate least squares linear regression analysis.

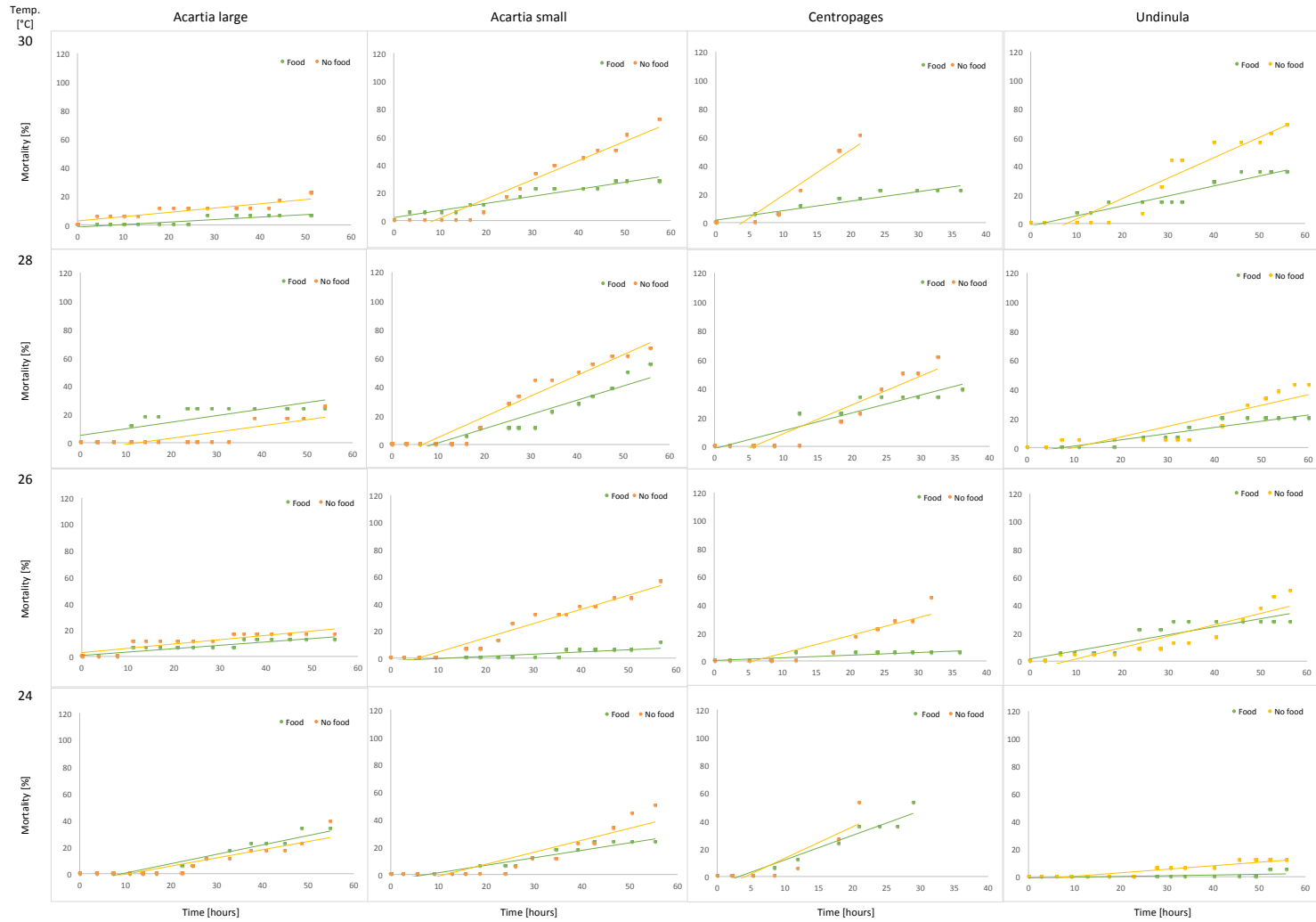


Figure 5.4. The percentage of mortality over time in temperatures below *in situ* (24 to 30 °C) with and without food for large and small-size *Acartia* sp., *Centropages* sp., and *Undinula* sp. Lines indicate least squares linear regression analysis.

1 Table 5.2. The mean \pm SE mortality rates (along with the t-value, and P value)
 2 of different zooplankton taxa under a range of temperature, in experiments
 3 conducted without food supply. The N value is the number of individuals in
 4 the treatment, and NA denotes “not applicable”.

Taxa	Temperature [°C]	Mortality rate \pm SE [% h ⁻¹]	t-value	p-value	N
Acartia 2016	38	61.15 \pm 45.20	-1.35	0.4052	20
Acartia 2016	36	4.10 \pm 0.48	-8.61	0.0003	20
Acartia 2016	34	1.89 \pm 0.21	-9.02	<.0001	20
Acartia 2016	32	1.13 \pm 0.18	-6.4	0.0001	20
Acartia 2016	30	1.49 \pm 0.21	-7.27	<.0001	20
Acartia 2016	28	0.74 \pm 0.11	-6.86	0.0001	20
Acartia 2016	26	1.77 \pm 0.49	-3.61	0.0112	20
Acartia 2016	24	1.74 \pm 0.19	-9	<.0001	20
Acartia large	38	17.82 \pm 2.06	-8.63	<.0001	18
Acartia large	36	7.43 \pm 0.55	-13.41	<.0001	16
Acartia large	34	1.31 \pm 0.15	-8.65	<.0001	18
Acartia large	32	1.77 \pm 0.14	-12.23	<.0001	18
Acartia large	30	0.34 \pm 0.05	-6.85	<.0001	18
Acartia large	28	0.49 \pm 0.09	-5.19	0.0002	12
Acartia large	26	0.36 \pm 0.05	-6.98	<.0001	18
Acartia large	24	0.72 \pm 0.10	-6.85	<.0001	18
Acartia small	38	9.51 \pm 0.81	-11.67	<.0001	18
Acartia small	36	10.58 \pm 1.37	-7.74	<.0001	18
Acartia small	34	3.77 \pm 0.16	-23.01	<.0001	17
Acartia small	32	3.12 \pm 0.17	-18.8	<.0001	17
Acartia small	30	2.11 \pm 0.19	-11.09	<.0001	18
Acartia small	28	2.21 \pm 0.14	-16.22	<.0001	18
Acartia small	26	1.41 \pm 0.10	-14.82	<.0001	16
Acartia small	24	1.12 \pm 0.16	-6.88	<.0001	18
Candacia	38	NA	NA	NA	6
Candacia	36	96.90 \pm 39.94	-2.43	0.2489	18
Candacia	34	48.58 \pm 7.54	-6.44	0.0076	18
Candacia	32	19.36 \pm 2.87	-6.73	<.0001	18
Candacia	30	9.29 \pm 2.37	-3.93	0.0111	18
Candacia	28	8.36 \pm 1.21	-6.92	0.0001	18
Candacia	26	13.32 \pm 3.38	-3.94	0.0076	18
Candacia	24	7.01 \pm 0.74	-9.46	<.0001	18
Centropages	38	10.31 \pm 1.27	-8.1	0.0002	18
Centropages	36	9.63 \pm 2.18	-4.41	0.0031	18
Centropages	34	2.83 \pm 0.51	-5.52	0.0004	18
Centropages	32	2.13 \pm 0.66	-3.21	0.0148	18
Centropages	30	4.70 \pm 0.97	-4.87	0.0082	18

Centropages	28	2.84 ± 0.40	-7.13	<.0001	18
Centropages	26	1.57 ± 0.26	-6.08	0.0002	18
Centropages	24	3.04 ± 0.87	-3.51	0.0171	19
Corycaeus	38	NA	NA	NA	19
Corycaeus	36	NA	NA	NA	19
Corycaeus	34	3.99 ± 0.71	-5.62	0.0014	20
Corycaeus	32	3.87 ± 0.45	-8.53	0.0004	20
Corycaeus	30	3.34 ± 1.57	-2.12	0.1236	20
Corycaeus	28	10.30 ± 3.24	-3.18	0.0501	20
Corycaeus	26	3.66 ± 0.94	-3.91	0.0297	20
Corycaeus	24	2.02 ± 0.17	-11.55	<.0001	21
Megalopa	38	1.35 ± 0.16	-8.67	<.0001	24
Megalopa	36	0.05 ± 0.01	-3.58	0.0028	24
Megalopa	34	0.00 ± 0.00	NA	NA	24
Megalopa	32	0.00 ± 0.00	NA	NA	24
Megalopa	30	0.00 ± 0.00	NA	NA	24
Megalopa	28	0.00 ± 0.00	NA	NA	24
Megalopa	26	0.00 ± 0.00	NA	NA	24
Megalopa	24	0.00 ± 0.00	NA	NA	24
Ostracod	38	NA	NA	NA	9
Ostracod	36	18.63 ± 0.67	-27.87	0.0228	15
Ostracod	34	8.10 ± 0.96	-8.47	0.0011	15
Ostracod	32	5.89 ± 1.04	-5.69	0.0023	15
Ostracod	30	1.70 ± 0.44	-3.91	0.0058	15
Ostracod	28	1.67 ± 0.27	-6.24	0.0004	15
Ostracod	26	2.56 ± 0.26	-9.86	<.0001	15
Ostracod	24	2.12 ± 0.51	-4.18	0.0086	15
Paracalanus	38	164.79 ± 85.89	-1.92	0.3059	27
Paracalanus	36	7.53 ± 2.12	-3.54	0.0122	21
Paracalanus	34	1.32 ± 0.23	-5.85	<.0001	23
Paracalanus	32	1.54 ± 0.49	-3.14	0.0093	22
Paracalanus	30	1.17 ± 0.32	-3.66	0.0026	20
Paracalanus	28	0.92 ± 0.11	-8.61	<.0001	20
Paracalanus	26	1.16 ± 0.24	-4.94	0.0003	20
Paracalanus	24	0.97 ± 0.08	-11.89	<.0001	16
Tortanus	38	NA	NA	NA	16
Tortanus	36	4.46 ± 0.49	-9.2	0.0027	14
Tortanus	34	1.63 ± 0.11	-15.41	<.0001	20
Tortanus	32	2.29 ± 0.36	-6.31	0.0001	20
Tortanus	30	1.29 ± 0.08	-15.4	<.0001	18
Tortanus	28	2.52 ± 0.50	-4.99	0.0025	20
Tortanus	26	2.01 ± 0.29	-6.83	<.0001	20
Tortanus	24	1.90 ± 0.27	-6.95	<.0001	20

Undinula	38	43.95 ± 7.92	-5.55	0.1135	23
Undinula	36	25.60 ± 4.92	-5.2	0.002	24
Undinula	34	13.41 ± 1.15	-11.7	<.0001	24
Undinula	32	6.12 ± 0.33	-18.44	<.0001	21
Undinula	30	2.22 ± 0.21	-10.33	<.0001	16
Undinula	28	0.93 ± 0.14	-6.52	<.0001	21
Undinula	26	1.07 ± 0.15	-6.94	<.0001	24
Undinula	24	0.27 ± 0.03	-9.96	<.0001	17
Zoea	38	3.75 ± 0.68	-5.55	0.0002	20
Zoea	36	1.45 ± 0.17	-8.66	<.0001	19
Zoea	34	0.60 ± 0.11	-5.5	<.0001	20
Zoea	32	0.65 ± 0.13	-5.1	<.0001	20
Zoea	30	0.28 ± 0.07	-4.03	0.0007	20
Zoea	28	0.76 ± 0.13	-5.73	<.0001	20
Zoea	26	0.41 ± 0.12	-3.37	0.0032	21
Zoea	24	0.44 ± 0.08	-5.38	<.0001	20

Table 5.3. The mean \pm SE mortality rates (along with the t-value, and P value) of different zooplankton taxa under a range of temperature, in experiments conducted with food supply. The N value is the number of individuals in the treatment. Significant effect of food to buffer mortality was calculated using an analysis of covariance. NA denotes “not applicable”.

Taxa	Temperature [°C]	Mortality rate \pm SE [% h ⁻¹]	t-value	p-value	N
Acartia large	38	18.81 \pm 0.023 ne	-8.25	<.0001	17
Acartia large	36	2.46 \pm 0.004*	-5.67	<.0001	15
Acartia large	34	0.38 \pm 0.000*	-8.64	<.0001	18
Acartia large	32	0.00 \pm 0.000*			18
Acartia large	30	0.18 \pm 0.000*	-6.19	<.0001	16
Acartia large	28	0.54 \pm 0.001	-5.08	0.0003	17
Acartia large	26	0.28 \pm 0.000	-8.52	<.0001	16
Acartia large	24	0.83 \pm 0.001 ne	-10.68	<.0001	18
Acartia small	38	5.49 \pm 0.002*	-23.73	<.0001	18
Acartia small	36	3.36 \pm 0.002*	-18.4	<.0001	17
Acartia small	34	1.20 \pm 0.001*	-16.6	<.0001	18
Acartia small	32	1.41 \pm 0.001*	-16.19	<.0001	18
Acartia small	30	0.60 \pm 0.000*	-16.17	<.0001	18
Acartia small	28	1.34 \pm 0.002*	-8.84	<.0001	18
Acartia small	26	0.17 \pm 0.000*	-5.42	<.0001	18
Acartia small	24	0.62 \pm 0.001*	-12.34	<.0001	17
Centropages	38	1.38 \pm 0.003*	-5.25	0.0019	18
Centropages	36	3.13 \pm 0.004*	-8.02	<.0001	18
Centropages	34	0.23 \pm 0.000*	-8.21	<.0001	18
Centropages	32	0.19 \pm 0.000*	-4.93	0.0006	18
Centropages	30	0.77 \pm 0.001*	-9.79	<.0001	18
Centropages	28	1.53 \pm 0.002*	-9.22	<.0001	18
Centropages	26	0.20 \pm 0.000*	-4.93	0.0006	18
Centropages	24	2.33 \pm 0.003 ne	-8.48	<.0001	17
Undinula	38	54.52 \pm 0.100 ne	-5.48	0.012	24
Undinula	36	24.03 \pm 0.039 ne	-6.1	0.0009	23
Undinula	34	7.33 \pm 0.004*	-18.27	<.0001	20
Undinula	32	1.15 \pm 0.001*	-16.1	<.0001	16
Undinula	30	0.87 \pm 0.001*	-11.3	<.0001	14
Undinula	28	0.48 \pm 0.000*	-10.68	<.0001	15
Undinula	26	0.69 \pm 0.001*	-8.22	<.0001	18
Undinula	24	0.05 \pm 0.000*	-2.59	0.0226	21

ne=No effect from food.

*=Food buffered mortality at this temperature.

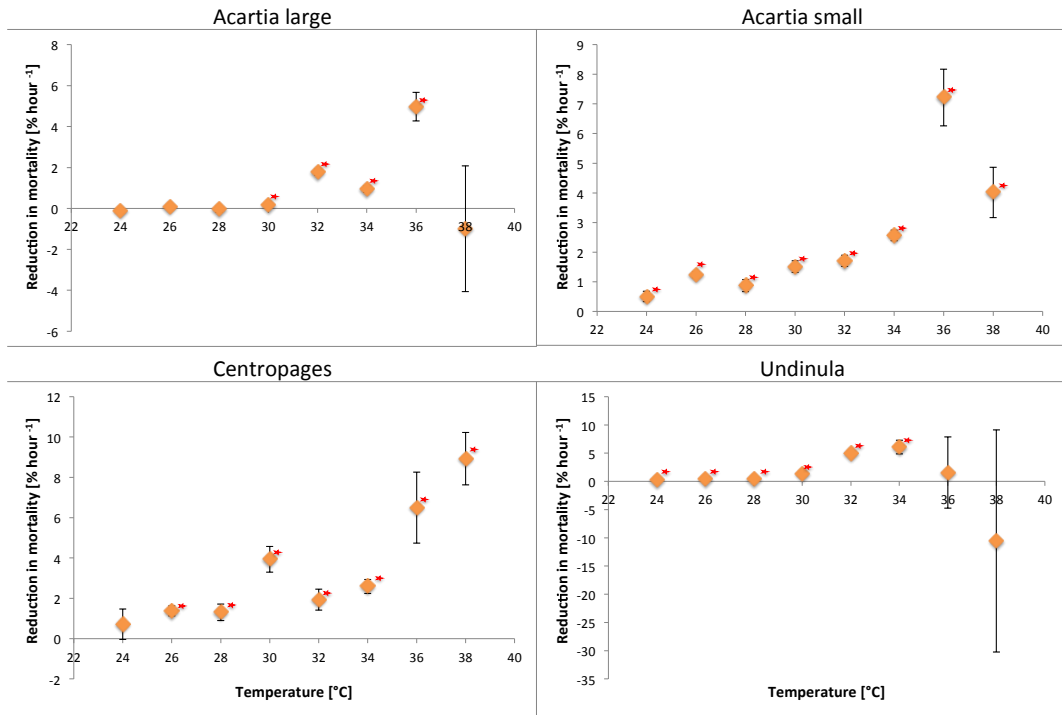


Figure 5.5. Reduction in mortality due to the presence of food [% ± SE hr⁻¹] as calculated using an analysis of covariance. Red asterisks signify a statistically significant effect of food at that temperature.

The provision of food had little effect on mortality rates at temperatures below 30 °C, but buffered mortality significantly at warmer temperatures for the four taxonomic groups tested (Figure 5.5). For the large-size *Acartia* sp., food supply had a significant effect from 30 to 36 °C, with a reduction of mortality rates by 5.0% h⁻¹ at 36 °C (Figure 5.5). For the small-size *Acartia* sp., food supply had a significant effect at all of the temperatures tested, with the greatest effect at 36 °C, reducing mortality rates by 7.2% h⁻¹ (Figure 5.5). *Centropages* sp. also experienced significant reduction in mortality rates with food supply between 26 and 38 °C, with the highest reduction of 8.9% h⁻¹ at 38 °C (Figure 5.5). Food also significantly reduced mortality of *Undinula* sp., with the highest reduction by 6.1% h⁻¹ at 34 °C (Figure

5.5). However, food supply did not alleviate mortality rates when these were very high (e.g. large-size *Acartia* sp. and *Undinula* sp. at 38 °C (Figure 5.5)).

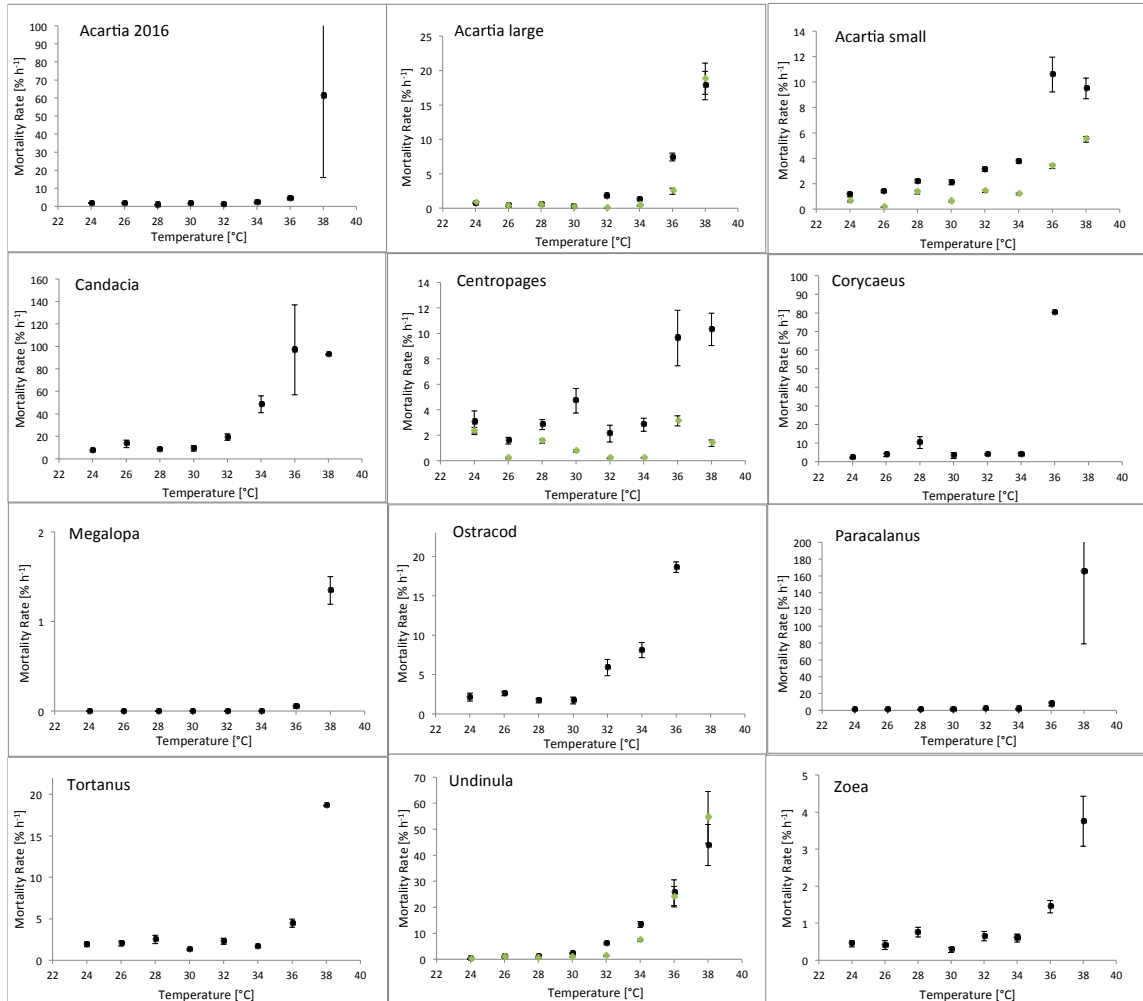


Figure 5.6. Temperature curves as mortality rates [% h⁻¹ ± SE] across all temperatures tested [°C] for common groups of Central Red Sea zooplankton. Black dots signify mortality rates for no food treatments and green dots signify mortality rates for food addition treatments in: *Acartia* large and small sp., *Centropages* sp., and *Undinula* sp.

Table 5.4. Optimal temperatures (T_{opt} , °C) and activation energies (Ae, [eV]) based on the Arrhenius model using linear regression of the natural logarithm of living animals as a function of $1/kT$. “Ae for $T < T_{opt}$ ” refers to the thermal window up to T_{opt} , and “Ae for $T > T_{opt}$ ” refers to the rate of thermal collapse at $T > T_{opt}$. “F” designates experiment with food added and “NF” designates experiments where no food was added. “NA” means “not applicable”.

Taxa	T_{opt} [°C]	Ae for $T < T_{opt}$			Ae for $T > T_{opt}$		
		Ae [eV] \pm SE	t-value	p-value	Ae [eV] \pm SE	t-value	p-value
Acartia (2016) NF	36	1.07 \pm 0.74	-1.45	0.21	236.23	NA	NA
Acartia large F	34	-0.39 \pm 0.23	1.66	0.17	37.85 \pm 17.09	-2.21	0.27
Acartia large NF	34	0.78 \pm 0.47	-1.67	0.17	33.94 \pm 5.20	-6.53	0.10
Acartia small F	34	0.66 \pm 0.41	-1.62	0.18	8.82 \pm 0.00	-3328.00	0.00
Acartia small NF	34	2.05 \pm 0.26	-7.96	0.00	11.84 \pm 9.31	-1.27	0.42
Candacia NF	30	0.76 \pm 5.74	-0.13	0.91	99.01 \pm 18.10	-5.47	0.01
Centropages F	34	-1.27 \pm 0.68	1.88	0.13	2.39 \pm 5.51	-0.43	0.74
Centropages NF	34	0.28 \pm 1.10	-0.26	0.81	15.41 \pm 7.21	-2.14	0.28
Corycaeus NF	34	0.43 \pm 3.05	-0.14	0.90	311.10	NA	NA
Megalopa NF	36	0.02 \pm 0.01	-1.70	0.15	5.38	NA	NA
Ostracod NF	30	-0.83 \pm 0.67	1.25	0.34	21.35 \pm 5.07	-4.21	0.05
Paracalanus NF	36	2.88 \pm 1.49	-1.93	0.11	651.18	NA	NA
Tortanus NF	34	-0.19 \pm 0.46	0.42	0.69	34.92 \pm 13.60	-2.57	0.24
Undinula F	32	0.93 \pm 0.25	-3.73	0.03	72.13 \pm 16.03	-4.50	0.05
Undinula NF	30	2.21 \pm 0.72	-3.07	0.09	41.71 \pm 6.91	-6.03	0.01
Zoea NF	34	0.12 \pm 0.18	-0.66	0.54	6.47 \pm 1.75	-3.71	0.17
Summary Means	33.5	0.59 \pm 1.03			99.36 \pm 8.82		

Optimal temperature, or optimal threshold, was designated as the highest temperature before a steep increase in mortality. *Candacia* sp., *Ostracod* sp., and *Undinula* sp. showed a T_{opt} at 30 °C, when no food was supplied (Figure 5.6, Table 5.4), while the T_{opt} of *Undinula* sp., increased to 32 °C when food was supplied (Figure 5.6, Table 5.4). Most zooplankton species tested exhibited a threshold at 34 °C, and *Acartia* sp. (tested in 2016), crab megalopa, and *Paracalanus* sp. reached a T_{opt} at 36 °C in the absence of food (Figure 5.6, Table 5.4). *Paracalanus* sp., *Corycaeus* sp., *Acartia* sp. of 2016, and *Candacia* sp. experienced the steepest increase in mortality in the absence of food supply at temperatures exceeding their thermal optimum, with exceedingly large activation energies for thermal collapse of 651, 311, 236, and 99 eV, respectively (Table 5.4). All of the activation energies for $T < T_{opt}$ were exceedingly low, with all values (except that of *Paracalanus* sp.), lower than the lowest activation energy for $T > T_{opt}$ ($<2.39 \pm 5.51$ eV, Table 5.4), and some were even negative (Table 5.4), which signifies that mortality declined with increasing temperature up to T_{opt} (Figure 5.6). *Paracalanus* sp. without food supply had the highest activation energies for both $T < T_{opt}$ and $T > T_{opt}$, at 2.88 ± 1.49 and 651.18 eV, respectively (Table 5.4). *Centropages* sp. with food supplied had the lowest activation energy for $T < T_{opt}$ at -1.27 ± 0.68 eV, as well as for $T > T_{opt}$ at 2.39 ± 5.51 eV (Table 5.4), making its threshold for thermal collapse less defined than its threshold for $T > T_{opt}$ in the absence of food, which was 15.41 ± 7.21 eV (Figure 5.6, Table 5.4). In general, activation energies for $T > T_{opt}$ increase greatly with $T > T_{opt}$ (Figure 5.7).

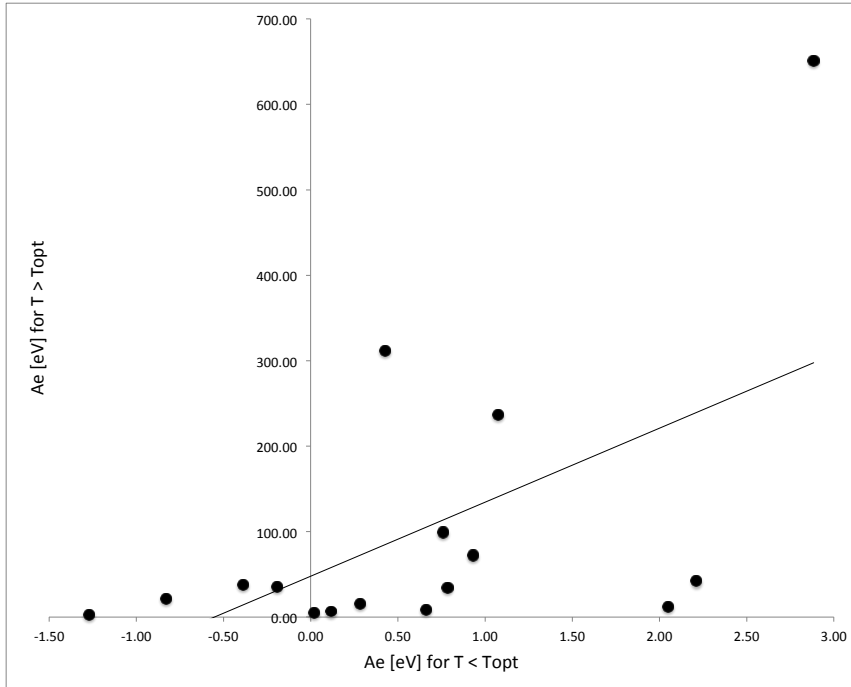


Figure 5.7. Plot comparing activation energies (A_e) of the two regimes found in each temperature curve with activation energies [eV] of temperatures above T_{opt} over activation energies [eV] of temperatures below T_{opt} .

5.5. Discussion

The acclimation process in our experiment involved moving the organisms from *in situ* temperature (32 °C) into 2 °C higher every hour until reaching the target experimental temperature. The organisms tested survived this trajectory, likely due to their ability to cope with large changes in temperature each time they migrate through the water column. Zooplankton may migrate hundreds of meters down to depth and up again to the surface of pelagic waters within 24 hours, making them well adapted to a broad thermal scope. Thus, the 6 °C difference in acclimation from *in situ* to the highest temperature treatment in our experiment, is a regular occurrence for migrating species.

Increasing temperatures led to increased mortality of all major Red Sea zooplankton taxa tested here, with mortality rates increasing greatly at temperature above 34 °C,

which was the modal T_{opt} for the zooplankton taxa tested. All zooplankton taxa experienced a steep increase in mortality rates at 36 and 38 °C, indicating an important thermal threshold for Red Sea zooplankton (Figure 5.1). The rate of increase in mortality rate with temperature, as characterized by the activation energy of mortality rate, increased, on average, by 98.76 eV, or 167 fold once the T_{opt} was exceeded (Table 5.4). Hence, organisms collapsed and died rapidly at these warm temperatures, likely involving the denaturation of enzymes (Gillooly et al. 2001; Tomanek 2010). Furthermore, ectotherms are highly sensitive to temperature as they are governed by the oxygen-limited thermal tolerance hypothesis, which states that performance may be limited to the inability of ventilatory and circulatory systems to meet demands of oxygen at high temperatures (Pörtner 2001).

The availability of food alleviated the effects of temperature on mortality rates and reduced the activation energy for temperature below T_{opt} by, on average, 75 fold, and only increased the activation energy for temperature above T_{opt} slightly by 1.2 fold. However, the large-size *Acartia* sp. showed similar mortality patterns at temperatures 30 °C and below in the presence and absence of food (Figure 5.4), implying that, for this taxa, food did not confer a large advantage and the animals were able to cope at these temperatures even in the absence of food, possibly because their large size allows to accumulate reserves (Lee et al. 1970). Food had a stronger and more significant effect in buffering mortality in the small-size *Acartia* sp. than it did in the large-size *Acartia* sp. (Figure 5.5). When given food, the small-size *Acartia* sp. showed resistance to mortality even at the highest temperature tested, 38 °C, a temperature that was not withstood by any of the other copepod

taxa (Figures 5.3 and 5.5). Hence, food supply appears to play a fundamental role in conferring resistance to warming for the smaller copepods, which can incorporate food faster and react to stress more rapidly (Alcaraz et al. 2014). Also, the production of astaxanthin, an important antioxidant, has been shown to increase with food supply (Holeton et al. 2009). These results are consistent with the metabolic theory of ecology (Brown et al. 2004), which predicts that the increasing in metabolic and developmental rates, including mortality, with increasing temperature is scaled to size, with smaller organisms exhibiting faster responses to increased temperature (Hall and Burns 2001; Lee et al. 2003; Brown et al. 2004; Alcaraz et al. 2014).

Candacia sp., *Ostracod* sp., and *Undinula* sp. (all without food), exhibited the lowest capacity to handle thermal stress, as their T_{opt} was only 30 °C (Table 5.4), a temperature below the *in situ* temperature at the time of sampling, suggesting these populations would be already stressed *in situ*. In contrast, the effect of food on *Undinula* sp., raised the optimal temperature to 32 °C (Table 5.4), indicating the important role, confirmed by experimental results, that food supply confers resistance, not only in terms of reducing mortality rate at temperatures close and above T_{opt} , but also by increasing the thermal scope of the species. This adds further evidence to the importance of an energy source in building resistance to thermal stress.

Interestingly, planktonic early life stages of crabs, such as zoea and megalopa, tested here, showed remarkable resistance to high temperature, being the only taxa showing significant survival at the warmest temperature, 38 °C (Figure 5.1).

Megalopa has also been shown to be more resistant to UV-B radiation, which is higher in oligotrophic seas (Tedetti and Sempéré 2006), than other common Central Red Sea zooplankton taxa (Al-Aidaros et al. 2015). Whereas the crab species could not be resolved, adult Red Sea crabs often inhabit mangrove ecosystems, where temperature can reach extreme values, requiring therefore, extreme resistance to heat stress, as observed for the planktonic crab stages tested here.

Marine organisms, including cold-water species, are often reported to grow in environments with maximum temperatures close to their thermal limits (Hofmann and Somero 1996; Feder and Hofmann 1999; Tomanek and Somero 1999; Thomas et al. 2012). The thermal limits for the most common Red Sea zooplankton groups range from 30 to 36 °C, with a modal value of 34 °C (Table 5.4), which corresponds with the annual maxima experienced in the Central Red Sea (Chaidez et al. 2017) where the zooplankton were sampled. This renders Red Sea zooplankton some of the most thermal resistant marine zooplankton yet reported (Gonzalez 1974; Clarke and Peck 1991; Ikeda et al. 2001; Zubakha and Usov 2004; Jiang et al. 2008; Alcaraz et al. 2013b; Hammock et al. 2016). Yet, the 6 °C range in T_{opt} across the species tested here, is of significance and may affect community composition and seasonal succession in the Red Sea, with species with low T_{opt} likely to be most abundant in winter and those with the highest T_{opt} likely to dominate in summer (Pörtner and Farrell 2008; Møller et al. 2012; Kjellerup et al. 2012). Stressors such as temperature and lowered pH, cause a greater proportion of organisms' energy budgets to be allocated to respiration, reducing the energy allocated to growth and reproduction, potentially affecting community composition (Pedersen et al. 2014).

However, beyond thermal control of seasonal community composition, marine heat waves will affect the Red Sea (Chaidez et al. 2017), and may cause catastrophic zooplankton mortality by bringing *in situ* temperatures to values above T_{opt} , even of the most thermally resistant species. Indeed, our results show that mortality rates increased greatly, on average 167 fold, when temperature exceeds T_{opt} .

The temperature performance curves for the zooplankton taxa tested here, follow the same pattern of two regimes as do the majority of ectotherms, with mortality gradually increasing until T_{opt} , and sharply increasing after T_{opt} (Freitas et al. 2007; Tewksbury et al. 2008; Tagliarolo and McQuaid 2015). The abrupt change marks a thermal threshold, which when reached, the organism or population goes into thermal collapse and it takes a much greater amount of energy to return to the previous stable state (Dell et al. 2011). Our study showed that food has a significant effect in combating thermal stress at high temperatures (Figure 5.5) and this was reflected in the activation energies, reducing the activation energy for $T < T_{opt}$ by 75 fold. However, the addition of food increased slightly, on average, the activation energy for $T > T_{opt}$ by 1.2 fold. This could indicate that the thermal thresholds are due to the effect of temperature alone, making the effect of $T > T_{opt}$ more pronounced because of the beneficial effect of a food source at lower temperatures. Some of the activation energies for $T > T_{opt}$ are comparable to other activation energies measuring the effect of temperature on respiration on copepods; these values are between 8.84 and 22.94 eV (Hirche 1987). Mass-corrected embryonic development for zooplankton was shown to have an activation energy of 0.12 eV by Gillooly et al. (2002), and a post-embryonic activation energy of 0.11 eV; and this is

most similar to the activation energy for $T < T_{opt}$ of the zoea crab larvae (0.12 ± 0.18 , this study).

Our results clearly show that food supply plays an important role in conferring thermal resistance to the animals, particularly at temperature near or in excess of T_{opt} . This is due to the high energy demands associated to increased temperature, such as increased respiration rates, and to mechanisms, such as DNA repair, protein folding and proteolysis, and protection from oxidative stress, reported to be involved in thermal resistance of zooplankton (Schoville et al. 2012; Lehette et al. 2016; Rahlff et al. 2017). However, the Red Sea is an ultraoligotrophic ecosystem, where food supply is very limited and, hence, zooplankton are expected to be generally food-limited, thereby rendering them more vulnerable to extreme temperatures and heat waves.

Our study delineates the thermal limits of zooplankton in the Central Red Sea when undergoing heat stress, with important implications for understanding the ecosystem of the Red Sea and its response to on-going warming, which is raising maximum seawater temperature in the Red Sea by $0.17 \text{ }^\circ\text{C decade}^{-1}$ (Chaidez et al. 2017). The impact of even slight warming ($0.90 \text{ }^\circ\text{C}$ increase in global SST, Edwards and Richardson 2004), on the marine pelagic community and environment is likely to be significant, particularly with the onset of more frequent heat waves (Meehl and Tebaldi 2004), also affecting the Red Sea (Chaidez et al. 2017), since organisms are adapted to grow near their T_{opt} and temperatures above T_{opt} lead to catastrophic mortality. Although zooplankton have the ability to enter diapause and migrate vertically to find cooler waters, they need to return to the photic layer to feed, and

cannot, therefore, entirely avoid warm waters by this strategy. We, therefore, conclude that zooplankton in the Central Red Sea are likely to already live at or close to their temperature optima in the summer. Past the thermal thresholds described in this study, physiological mechanisms may become impaired and reduce the chances of survival. We, therefore, conclude that Red Sea zooplankton are highly vulnerable to warming and extreme marine heat waves.

5.6. References

- Al-Aidaros AM, El-Sherbiny MMO, Satheesh S, Mantha G, Agusti S, Carreja B, Duarte CM (2015) Strong sensitivity of Red Sea zooplankton to UV-B radiation. *Estuaries and Coasts* 38:846-853
- Alcaraz M, Almeda R, Saiz E, Calbet A, Duarte CM, Agusti S, Santiago R, Alonso A (2013a) Effects of temperature on the metabolic stoichiometry of Arctic zooplankton. *Biogeosciences* 10:689-697
- Alcaraz M, Felipe J, Grote U, Arashkevich E, Nikishina A (2013b) Life in a warming ocean: thermal thresholds and metabolic balance of arctic zooplankton. *Journal of Plankton Research* 36:3-10
- Bethoux JP (1988) Red Sea geochemical budgets and exchanges with the Indian Ocean. *Marine Chemistry* 24:83-92
- Boyd PW, Rynearson TA, Armstrong EA, Fu F, Hayashi K, Hu Z, Hutchins DA, Kudela RM, Litchman E, Mulholland MR, Passow U, Strzepek RF, Whittaker KA, Yu E, Thomas MK (2013) Marine phytoplankton temperature versus growth responses from polar to tropical waters – outcome of a scientific community-wide study. *PLoS one* 8:e63091
- Brown JH, Gillooly JF, Allen AP, Savage VM, West GB (2004) Toward a metabolic theory of ecology. *Ecology* 85:1771-1789
- Calbet A (2001) Mesozooplankton grazing effect on primary production: a global comparative analysis in marine ecosystems. *Limnology and Oceanography* 46:1824-1830
- Chaidez V, Dreano D, Agusti S, Duarte CM, Hoteit I (2017) Decadal trends in Red Sea maximum surface temperature. *Scientific Reports* 7:8144

- Coyle KO, Pinchuk AI, Eisner LB, Napp JM (2008) Zooplankton species composition, abundance and biomass on the eastern Bering Sea shelf during summer: the potential role of water-column stability and nutrients in structuring the zooplankton community. *Deep Sea Research Part II: Topical Studies in Oceanography* 55:1775-1791
- Clarke A, Peck LS (1991) The physiology of polar marine zooplankton. *Polar Research* 10:355-370
- Dell AI, Pawar S, Savage VM (2011) Systematic variation in the temperature dependence of physiological and ecological traits. *PNAS* 108:10591-10596
- Edwards M, Richardson AJ (2004) Impact of climate change on marine pelagic phenology and trophic mismatch. *Nature* 430:881
- Feder ME, Hofmann GE (1999) Heat shock proteins, molecular chaperones, and the stress response: evolutionary and ecological physiology. *Annu. Rev. Physiol.* 61:243-282
- Fowler SW, Lawrence FS (1972) Sinking rates of euphausiid fecal pellets. *Limnology and Oceanography* 17:293-296
- Freitas V, Campos J, Fonds M, Van der Veer HW (2007) Potential impact of temperature change on epibenthic predator–bivalve prey interactions in temperate estuaries. *Journal of Thermal Biology* 32:328-340
- Gillooly JF, Brown JH, West GB, Savage VM, Charnov EL. (2001) Effects of size and temperature on metabolic rate. *Science* 293:2248-2251
- Gillooly JF, Charnov EL, West GB, Savage VM, Brown JH (2002) Effects of size and temperature on developmental time. *Nature* 417:70
- Gonzalez JG (1974) Critical thermal maxima and upper lethal temperatures for the calanoid copepods *Acartia tonsa* and *A. clausi*. *Marine Biology* 27:219-223
- Hall CJ, Burns CW (2001) Effects of salinity and temperature on survival and reproduction of *Boeckella hamate* (Copepoda: Calanoida) from a periodically brackish lake. *Journal of Plankton Research* 23:97-104
- Hammock BG, Lesmeister S, Flores I, Bradburd GS, Hammock FH, Teh SJ (2016) Low food availability narrows the tolerance of the copepod *Eurytemora affinis* to salinity, but not to temperature. *Estuaries and Coasts* 39:189-200
- Hirche HJ (1987) Temperature and plankton. *Marine Biology* 94:347-356

- Hofmann GE, Somero GN (1996) Interspecific variation in thermal denaturation of proteins in the congeneric mussels *Mytilus trossulus* and *M. galloprovincialis*: evidence from the heat-shock response and protein ubiquitination. *Marine Biology* 126: 65–75
- Holeton C, Lindell K, Holmborn T, Hogfors H., Gorokhova E (2009) Decreased astaxanthin at high feeding rates in the calanoid copepod *Acartia bifilosa*. *Journal of Plankton Research* 31:661-668
- Ikeda T (1985) Metabolic rates of epipelagic marine zooplankton as a function of body mass and temperature. *Marine Biology* 85:1-11
- Ikeda T, Kanno Y, Ozaki K, Shinada A (2001) Metabolic rates of epipelagic marine copepods as a function of body mass and temperature. *Marine Biology* 139:587-596
- Jiang Z, Zeng J, Chen Q, Huang Y, Xu X, Liao Y, Shou L, Liu J (2008) Tolerance of copepods to short-term thermal stress caused by coastal power stations. *Journal of Thermal Biology* 33:419-423
- Kjellerup S, Dünweber M, Swalethorp R, Nielsen TG, Møller EF, Markager S, Hansen BW (2012) Effects of a future warmer ocean on the coexisting copepods *Calanus finmarchicus* and *C. glacialis* in Disko Bay, western Greenland. *Marine Ecology Progress Series* 447:87-108
- Kürten B, Khomayis HS, Devassy R, Audritz S, Sommer U, Struck U, El-Sherbiny MM, Al-Aidaros AM (2015) Ecohydrographic constraints on biodiversity and distribution of phytoplankton and zooplankton in coral reefs of the Red Sea, Saudi Arabia. *Marine Ecology* 36:1195-1214
- Lee HW, Ban S, Ikeda T, Matsuishi T (2003) Effect of temperature on development, growth and reproduction in the marine copepod *Pseudocalanus newmani* at satiating food condition. *Journal of Plankton Research* 25:261-271
- Lee RF, Nevenzel JC, Paffenhöffer GA, Benson AA (1970) The metabolism of wax esters and other lipids by the marine copepod. *Calanus helgolandicus*. *J. Lipid Res.* 11:237–240
- Lehette P, Ting SM, Chew LL, Chong VC (2016) Respiration rates of the copepod *Pseudodiaptomus annandalei* in tropical waters: beyond the thermal optimum. *Journal of Plankton Research* 38:456-467
- Loosanoff VL (1958) Some aspects of behavior of oysters at different temperatures. *Biol. Bull.* 114:57–70
- Mauchline J (1998) *The biology of calanoid copepods*. Academic Press, San Diego

- Meehl GA, Tebaldi C (2004) More intense, more frequent, and longer lasting heat waves in the 21st century. *Science* 305:994-997
- Møller EF, Maar M, Jónasdóttir SH, Nielsen TG, Tönnesson K (2012) The effect of changes in temperature and food on the development of *Calanus finmarchicus* and *Calanus helgolandicus* populations. *Limnology and Oceanography* 57:211-220
- Müren U, Berglund J, Samuelsson K, Andersson A (2005) Potential effects of elevated sea-water temperature on pelagic food webs. *Hydrobiologia* 545:153–166
- Pedersen SA, Håkedal OJ, Salaberria I, Tagliati A, Gustavson LM, Jenssen BM, Olsen AJ, Altin D (2014) Multigenerational exposure to ocean acidification during food limitation reveals consequences for copepod scope for growth and vital rates. *Environmental Science & Technology* 48:12275-12284
- Planque B, Batten SD (2000) *Calanus finmarchicus* in the North Atlantic: the year of *Calanus* in the context of interdecadal change. *ICES J. Mar. Sci.* 57:1528–1535
- Poloczanska ES, Brown CJ, Sydeman WJ, Kiessling W, Shoeman DS, Moore PJ, Brander K, Bruno JF, Buckley LB, Burrows MT, Duarte CM, Halpern BS, Holding J, Kappel CV, O'Connor MI, Pandolfi JM, Parmesan C, Schwing F, Thompson SA, Richardson AJ (2014) Global imprint of climate change on marine life. *Nat Clim Chang* doi: 10.1038/nclimate1958
- Pörtner H (2001) Climate change and temperature-dependent biogeography: oxygen limitation of thermal tolerance in animals. *Naturwissenschaften* 88:137-146
- Pörtner HO, Farrell AP (2008) Physiology and climate change. *Science* 690-692
- Rahlff J, Peters J, Moyano M, Pless O, Claussen C, Peck MA (2017) Short-term molecular and physiological responses to heat stress in neritic copepods *Acartia tonsa* and *Eurytemora affinis*. *Comparative Biochemistry and Physiology Part A: Molecular & Integrative Physiology* 203:348-358
- Raitsos DE, Pradhan Y, Brewin RJW, Stenchikov G, Hoteit I (2013) Remote sensing the phytoplankton seasonal succession of the Red Sea. *PloS ONE* 8(6): e64909
- Rhein, M., S. R. Rintoul, S. Aoki, E. Campos, D. Chambers, R. A. Feely, S. Gulev, G. C. Johnson, S. A. Josey, A. Kostianoy, C. Mauritzen, D. Roemmich, L. D. Talley, and F. Wang (2013), Observations: ocean. In: *Climate Change 2013: the physical science basis. Contribution of Working Group I to the Fifth Assessment Report of the Intergovernmental Panel on Climate Change* (T. F. Stocker, D. Qin, G.-K. Plattner, M. Tignor, S. K. Allen, J. Boschung, A. Nauels, Y. Xia, V. Bex, and P. M.

Midgley, eds.), Cambridge University Press, Cambridge, United Kingdom and New York, NY, USA.

- Sawall Y, Al-Sofyani A, Banguera-Hinestroza E, Voolstra CR (2014) Spatio-temporal analyses of *Symbiodinium* physiology of the coral *Pocillopora verrucosa* along large-scale nutrient and temperature gradients in the Red Sea. *PloS one* 9
- Schoville SD, Barreto FS, Moy GW, Wolff A, Burton RS (2012) Investigating the molecular basis of local adaptation to thermal stress: population differences in gene expression across the transcriptome of the copepod *Tigriopus californicus*. *BMC Evolutionary Biology* 12:170
- Tagliarolo M, McQuaid CD (2015) Sub-lethal and sub-specific temperature effects are better predictors of mussel distribution than thermal tolerance. *Marine Ecology Progress Series* 535:145-159
- Tedetti M, Sempéré R (2006) Penetration of ultraviolet radiation in the marine environment. A review. *Photochemistry and Photobiology* 82:389-397
- Tewksbury JJ, Huey RB, Deutsch CA (2008) Putting the heat on tropical animals. *SCIENCE-NEW YORK THEN WASHINGTON-*, 320:1296
- Thomas MK, Kremer CT, Klausmeier CA, Litchman E (2012) A global pattern of thermal adaptation in marine phytoplankton. *Science* 338:1085-1088
- Tomanek L (2010) Variation in the heat shock response and its implication for predicting the effect of global climate change on species' biogeographical distribution ranges and metabolic costs. *Journal of Experimental Biology* 213:971-979
- Tomanek L, Somero GN (1999) Evolutionary and acclimation-induced variation in the heat-shock responses of congeneric marine snails (genus *Tegula*) from different thermal habitats: Implications for limits of thermotolerance and biogeography. *J. Exp. Biol.* 202:2925-2936
- Turner JT (2015) Zooplankton fecal pellets, marine snow, phytodetritus and the ocean's biological pump. *Progress in Oceanography* 130:205-248
- Turner JT, Ferrante JG (1979) Fecal pellets in aquatic ecosystems. *BioScience* 29:670-677
- Willett CS (2010) Potential fitness trade-offs for thermal tolerance in the intertidal copepod *Tigriopus californicus*. *Evolution*, 64:2521-2534
- Zubakha MA, Usov NV (2004) Optimum temperatures for common zooplankton species in the White Sea. *Russian Journal of Marine Biology* 30:293-297

6. SYNTHESIS

The Red Sea holds a unique position in the world ocean, as a young sea with a tropical ecosystem at higher latitude. The temperatures already observed in the Red Sea are on par with those predicted for other ocean basins as a consequence of climate change. There is much discussion surrounding the adaptability of life in the ocean with rising temperatures. The Red Sea offers a special glimpse into what that could look like, thus, it is imperative that research continue to be developed in this region.

This dissertation delineated basin-scale, decadal trends in sea surface maximum temperature and identified the rate of warming for the Red Sea, which hitherto was unknown. The Red Sea, already considered an extremely warm sea basin, is warming faster than the global average at $0.17\text{ }^{\circ}\text{C decade}^{-1}$ (Chaidez et al. 2017), compared to $0.11\text{ }^{\circ}\text{C decade}^{-1}$ (Rhein et al. 2013). This rate of warming may pose challenges to organisms already living close to their thermal limits across the Red Sea. This dissertation goes on to answer the question of what are the thermal limits of a keystone and ecosystem engineering plant species, *Avicennia marina*; as well as some of the most ubiquitous and important pelagic organisms, zooplankton.

According to the results of this dissertation, projected sea surface temperatures for the year 2050 in the Northern Red Sea will include temperature maxima between 28.5 and $30.9\text{ }^{\circ}\text{C}$. This is still within the thermal scope of the organisms tested here, although the Northern Red Sea is currently the northernmost boundary of *A. marina*'s range. By 2100, temperature maxima in the Northern Red Sea will be between 31.0 (in the two gulfs) and $32.4\text{ }^{\circ}\text{C}$ (northern portion). These temperatures

may cause mass mortality for *Candacia*, Ostracod, and *Undinula* spp. of zooplankton which exhibit a thermal threshold at 30 °C. In the Central Red Sea, sea surface maxima is due to increase from 0.0 to 0.3 °C decade⁻¹. By 2050, the Central Red Sea will experience annual temperature maxima within 30.5 to 32.4 °C, the same scenario as the Northern Red Sea in 2100, putting in danger the most vulnerable species of zooplankton. By 2100, the Central Red Sea will experience annual temperature maxima within 30.5 to 33.9 °C, placing added thermal stress on *A. marina* propagules and seedlings already near their thermal limits. These projected temperatures may also bring many of the common zooplankton species to thermal collapse as our experiments showed that they share a thermal threshold of 34 °C or lower; these species include *Acartia* spp., *Candacia* spp., *Centropages* spp., *Corycaeus* spp., Ostracod spp., *Tortanus* spp., *Undinula* spp., as well as Zoea crab larva.

As evidenced by this work, young *A. marina* mangroves are resilient to raised temperatures up to 4 °C above current values. This is significant, as plants are sessile organisms, and thus cannot escape their immediate thermal stress. This means they are a resilient species for the Red Sea. However, warming will have an effect on individual growth, productivity, and population densities as it was found that propagules kept at higher temperatures (+4 °C above current), produced shorter seedlings than those at mean and +2 °C above the mean. Already, *A. marina* in the Red Sea exhibits stunted growth compared to stands in other parts of the world (Mackey 1993; Almahasheer et al. 2016). We must also keep in mind that increased CO₂ and increased temperature may cause earlier flowering as evidenced

in terrestrial plants (Rusterholz and Erhardt 1998). Thus, *A. marina* may undergo phenological shifts in response to warming and climate change. Still, *Avicennia marina* will likely remain a keystone species for Saudi Arabia with a dense stronghold in the southern coast, which experiences the hottest air and surface water temperatures, but is also facing a slower warming trend than the rest of the basin (Chaidez et al. 2017).

In our zooplankton experiments, we resolved the thermal thresholds of the most common Red Sea zooplankton taxa, ranging from 30 to 36 °C. Of the taxa tested here, 34 °C was the modal temperature to be tolerated by large and small sized *Acartia* sp., *Centropages* sp., *Corycaeus* sp., *Tortanus* sp., and crab zoea, deeming 34 °C, an important thermal threshold in the Red Sea. The crab larvae at the zoea and megalopa stage showed the highest resistance to warming of all the groups tested. It is unknown what makes them so resilient, but it is clear they have adapted to extreme temperature. We know from other studies of crustaceans, that the thermal stress response occurs quickly (Madeira et al. 2016; Rahlff et al. 2016) but our experiments were able to capture the effects of prolonged heat stress which might occur in an environment where the organism would not be able to escape by vertical migration. Although organisms that must react quickly to thermal stress do so at a high energetic cost, under mild stress conditions, these organisms may be better adapted to cope with warming as has been seen with intertidal species (Madeira et al. 2012), as are adult crabs, which live in mangrove ecosystems. We showed that food confers a significant advantage against thermal stress, decreasing mortality rates at high temperatures for some taxa. For *Undinula* sp., the addition of food

raised its thermal threshold from 30 to 32 °C. This experiment provided valuable insight into the implications of warming on a key component of the Central Red Sea pelagic ecosystem, which is extremely warm and oligotrophic.

Tolerance windows are wider for tropical and temperate species than they are for polar ones (Peck and Conway 2000). It may be that in recent geological time, cold adaptation was the major challenge (Arntz et al. 1994) whereas now, in the Anthropocene, the upper limits of many species are being tested. While the present challenges are great, and we do not know the full capacity of species to adapt, the situation may not be dire as warm environments were likely the conditions in which many species first evolved under (Ivanov et al. 2000). Organisms and the communities they comprise are facing great changes and challenges due to ocean warming. The effects are multi-faceted and complex. Through this PhD dissertation, we have attempted to elucidate some of those effects. May the results presented here, combined with the understanding of the interaction between environment and life, allow us to be better poised to mitigate harmful effects, and adapt alongside the rest of the biosphere, now and into the future.

6.1. References

- Almahasheer H, Duarte CM, Irigoien X (2016) Nutrient limitation in Central Red Sea mangroves. *Frontiers in Marine Science* 3:271
- Arntz WE, Brey T, Gallardo VA (1994) Antarctic Zoobenthos. *Oceanography and Marine biology: an Annual Review* 32:241–304
- Boyd PW, Rynearson TA, Armstrong EA, Fu F, Hayashi K, Hu Z, Hutchins DA, Kudela RM, Litchman E, Mulholland MR, Passow U, Strzepak RF, Whittaker KA, Yu E, Thomas MK (2013) Marine phytoplankton temperature versus growth responses from polar to tropical waters – outcome of a scientific community-wide study. *PLoS one* 8:e63091

- Chaidez V, Dreano D, Agusti S, Duarte CM, Hoteit I (2017) Decadal trends in Red Sea maximum surface temperature. *Scientific Reports* 7:8144
- Ivanov KP (2000) Physiological blocking of the mechanism of cold death: theoretical and experimental considerations. *J. Therm. Biol.* 25:467–479
- Mackey AP (1993) Biomass of the mangrove *Avicennia marina* (Forsk.) Vierh. near Brisbane, south-eastern Queensland. *Marine and Freshwater Research* 44:721-725
- Madeira D, Narciso L, Cabral HN, Vinagre C, Diniz MS (2012) HSP70 production patterns in coastal and estuarine organisms facing increasing temperatures. *J Sea Res* 73:137-147
- Madeira D, Mendonca V, Vinagre C, Diniz MS (2016) Is the stress response affected by season? Clues from an in situ study with a key intertidal shrimp. *Marine Biology* 163:41
- Peck LS, Conway LZ (2000) The myth of metabolic cold adaptation: oxygen consumption in stenothermal Antarctic bivalves. In: Harper, E., Taylor, J.D., Crame, J.A. (Eds.), *Evolutionary Biology of the Bivalvia*, Vol. 177. Geological Society, Special Publications, London 441–450
- Rahlff J, Peters J, Moyano M, Pless O, Claussen C, Peck MA (2017) Short-term molecular and physiological responses to heat stress in neritic copepods *Acartia tonsa* and *Eurytemora affinis*. *Comparative Biochemistry and Physiology Part A: Molecular & Integrative Physiology* 203:348-358
- Rhein, M., S. R. Rintoul, S. Aoki, E. Campos, D. Chambers, R. A. Feely, S. Gulev, G. C. Johnson, S. A. Josey, A. Kostianoy, C. Mauritzen, D. Roemmich, L. D. Talley, and F. Wang (2013), Observations: ocean. In: *Climate Change 2013: the physical science basis. Contribution of Working Group I to the Fifth Assessment Report of the Intergovernmental Panel on Climate Change* (T. F. Stocker, D. Qin, G.-K. Plattner, M. Tignor, S. K. Allen, J. Boschung, A. Nauels, Y. Xia, V. Bex, and P. M. Midgley, eds.), Cambridge University Press, Cambridge, United Kingdom and New York, NY, USA.
- Rusterholz HP, Erhardt A (1998) Effects of elevated CO₂ on flowering phenology and nectar production of nectar plants important for butterflies of calcareous grasslands. *Oecologia* 113:341–349
- Thomas MK, Kremer CT, Klausmeier CA, Litchman E (2012) A global pattern of thermal adaptation in marine phytoplankton. *Science* 338:1085-1088